THE UNIVERSITY
of EDINBURGH

USING EMBRYONIC STEM CELL-DERIVED URETERIC BUDS FOR URETER ENGINEERING AND DEVELOPING METHODS TO CONNECT THEM TO HOST KIDNEYS IN CULTURE

May Sallam

THE UNIVERSITY *of* EDINBURGH

Edinburgh medical school

Biomedical sciences

A thesis submitted in fulfilment of the requirements for the degree of Doctor of Philosophy at the University of Edinburgh

2021

I declare that the work presented in this thesis has been composed entirely by me, except where stated otherwise in the text. The work has not been submitted for any other degree of professional qualification.

May Sallam

Abstract

Chronic renal disease is a global health care burden that has a high mortality rate. The only cure available is either life-long renal dialysis or to replace the damaged organ using human donor kidneys which have significant issues including availability and long-term rejection. Scientists have developed an increasing interest in producing lab-grown kidneys and hope that they can, one day, solve the organ transplantation problem. Recent techniques generate renal tissue but contain no ureter, which is required before engineered kidneys be of any use. In this thesis my aim was to engineer ES cell-derived ureters that could be connected to these kidney organoids. Mouse ES cells were differentiated into ureteric bud tissue using a stepwise protocol. ES cell-derived engineered ureteric buds (eUBs) were grafted into isolated fetal mouse kidneys in culture. The GFP-eUBs grafted into the cortex of embryonic kidneys showed branching and encouraged nephron formation. If placed in the peri-Wolffian mesenchyme, either attached to a kidney or independent, they showed no branching but made multilayer, uroplakin-positive urothelium and induced the mesenchyme to differentiate into a contractile smooth muscle. These eUBs formed collecting ducts with a ureter when grafted between the two kidney mesenchymes. Furthermore, the isolated ES cell-derived eUBs could be encouraged to connect to the host kidneys in culture using a simple mechanical technique (an incision in the wall of the host epithelium at the engraftment site). The results also show that connection is possible in older kidneys in culture, and those connected to ureters show rhythmic contractions. This work introduces new possibilities for renal regeneration and tissue engineering.

Lay Abstract

Chronic kidney disease is a serious health care problem worldwide. The only available treatment is either renal dialysis or kidney transplantation. There is a severe shortage in the numbers of available donors, which makes it difficult for patients to get a replacement organ and many of them die while waiting. It is necessary to find alternative treatment approaches using advances in biomedical research. Production of stem cell-derived kidney organoids (mini-organs) is one of the most recent promising techniques, but it is too early to use them clinically. One of the problems confronting these lab-grown organoids is the lack of a ureter, which is important for the kidney to excrete urine. The aim of this thesis was to produce stem cell derived ureters and find ways to connect them to kidneys. The work started by studying the influence of different mesenchymal tissues on the fate of these stem cell-derived structures using implantation techniques. The next phase of the work allowed the production of ureter-like structures that can contract, using the periureteric cells (cells adjacent to the ureter) of mouse kidneys and the engineered ureteric buds (eUBs). The final phase of the work allowed these structures to connect to the host kidneys, by introducing a cut into the epithelium of the host kidney tubules. Experiments using older kidneys showed successful connection, with the eUBs connected to ureters showing peristaltic-like contractions. This work lays a foundation for future use of these engineered structures in kidney regeneration and tissue engineering.

Acknowledgements

First and foremost, thanks to Allah for guiding me through this challenging journey.

Second, I would like to express my deep appreciation to my supervisor Professor Jamie Davies for his guidance, support and understanding. You are a wonderful mentor and I feel blessed to have worked with you.

I would like to thank my second supervisor Professor Lorna Marson and Chair of my thesis committee Professor Tom Gillingwater for their valuable advice and their willingness to give their time to listen and guide me.

I would like to thank all my colleagues in Jamie Davies' lab for their helpful comments and suggestions.

Many thanks to Anwar, Elva and Manuela for their constant support and valuable advice.

I would like to thank Professor Tung-Tien Sun (New York University) for providing the Uroplakin antibody, and Professor Ryuchi Nishinakamura (Kamamuto University) for the Hoxb7 cell line.

I wish to thank my husband Ayman and my children Basel, Hazem and Hamza for the enormous love and support they gave me. It would not be possible without you.

To my parents, I cannot thank you enough for the all the love and emotional support you gave me. You are the most amazing parents I could ever hope for.

Contents

List of figures

List of tables

List of Videos

List of abbreviations

ALK: ALK receptor tyrosine kinase

ASMA: Alpha smooth muscle actin

B cells: Basal cells of the urothelium

BMP4: Bone morphogenic protein 4

BSA: Bovine serum albumin

cKit: Tyrosine-protein kinase Kit

CM: Cap mesenchyme

DBA: Dolichos biflorus agglutinin

DMSO: Dimethyl sulfoxide

ES cell: embryonic stem cells

eUB: engineered ureteric bud

E: Embryonic day

Foxd1: Forkhead Box D1

Gata3: GATA Binding Protein 3

FGF9: Fibroblast growth factor 9

GFP: Green fluorescent protein

GDNF: Glial cell derived neurotrophic factor

Hoxb7: Homebox B7

I cells: Intermediate cells of the urothelium

iPSc: Induced pluripotent stem cells

iPWM: induced peri-Wolffian mesenchyme

iMM: induced metanephric mesenchyme (iNP,iSP)

Krt8/15: Keratin 8/15

KCM: Kidney culture medium

LHX1: LIM Homebox 1

MEM: Minimum Essential Medium Eagle

MET: Mesenchymal-to-epithelial transitions

MM: Metanephric mesenchyme

MYCD: Myocardin

LIF: Leukaemia inhibitory factor

OSR1: Odd-skipped related transcription factor 1

PTCH1: patched1

PAX 2/8: Paired box 2/8

PBS: Phosphate buffered saline

PFA: Paraformaldehyde

P cells: Progenitor cell of the urothelium

PWM: Peri-Wolffian mesenchyme

RET: Ret proto-oncogene

Robo2: Roundabout, Axon Guidance Receptor, Homolog 2

S cells: superficial cells of the urothelium

SEM: Standard error mean

SIX2: Sine oculis-related homeobox 2

Shh/SHH: Sonic the hedgehog

Slit1: Slit homolog 1 protein

SOX9: SRY-Box Transcription Factor 9

TSHZ: T-shirt zinc finger Homebox

UB: Ureteric bud

UPK: Uroplakin

WD: Wolffian duct

Wnt: Wingless-related integration site

1. Introduction Chapter

1.1 Overview

This chapter lays the foundation for the rest of the thesis. Here, I describe the detailed anatomy and embryonic development of both kidney and ureter as they share a developmental progenitor, the ureteric bud. It is crucial to understand the developmental mechanisms and the key growth factors underlying kidney and ureter development in vivo, in order to rebuild them in vitro.

It is known that the adult kidney with a ureter is structurally complex and the idea of producing it in vitro is challenging. For that, it is more realistic to reproduce the simpler form, the embryonic kidney (Bohnenpoll & Kispert, 2014) and let it grow. In 2017, Taguchi and Nishinakamura tackled the issue of reproducing an embryonic form of mouse kidney from ES cells, which greatly resembles the natural organ anatomically but with no ureter. The main aim of this thesis is to find a way to produce embryonic ureters from ES cells and to connect them to kidneys. The last part of this chapter focuses on the lab-built organs known as kidney organoids, and on the rapidly developing techniques used to produce them.

1. 2 Anatomy of Kidney and ureter

1.2.1 Similarities and differences between mouse and human kidney

Human and mouse kidneys are relatively similar regarding key growth factors and genes that control their development, but there are some significant differences in the anatomy, timing, and scale (Potter, 1972; Saxen,1987). In both mouse and human, the excretory system consists of bilateral bean-shaped kidneys, each connected to a ureter, which ends in a single bladder and urethra located in the midline. The functions of the excretory system

include control of blood pressure, osmoregulation, induction of red blood cells (RBCs) formation, calcium reabsorption, toxin excretion and metabolism.

The functioning element of the kidney is the nephron, which consists of glomerulus and tubules (Kriz & Koepsell, 1974). The nephron's structure is fairly similar in both species and formed of glomeruli, proximal convoluted tubules (PT), loop of Henle (LOH) and distal convoluted tubules (DT), but they vary in their number. In mice, up to 100,000 nephrons can be found per kidney, while around one million nephrons are formed in human kidney (Bertram, 2001). In humans, nephron formation is completed before birth (Rayan et al.,2018; Hinchliffe et al.,1991), while it continues two to three days after birth in mouse (Saxen,1987).

Anatomically, the human kidney consists of many conical lobes (pyramids) that end with papillae (where pyramids empty urine in minor calyces), while mouse kidney consists only of a single lobe that ends with one papilla. The multi-papillate human kidney contains from 7 to 9 papillae and takes more than 30 weeks to complete its development. The mouse uni-papillate kidney needs around two weeks to develop (Kriz, & Kaissling, 1992).

Human and mouse kidneys are retroperitoneal in position and they are surrounded by adipose tissue. Human kidneys are located in the area between T12 (thoracic vertebrae) to L3 (lumbar vertebrae), with the left kidney lying slightly higher than the right because of the presence of the liver in the right hypochondrium (Frimann, 1961).

Male kidneys are larger than female kidneys in both mice and humans and male rodents produce markedly concentrated urine with higher protein content than humans (Gamble et al.,1943). In both species, the blood vessels, nerves and lymphatics reach the kidney through the renal hilum which also contains renal pelvis and calyces (Kriz, & Kaissling, 1992). The colour of the human kidney is reddish-brown, and the surface is smooth but sometimes contains remnants of the fetal lobulations in the form of surface indentations (Fig. 1.1). Blood supply is similar in both species (Moffat, 1975).

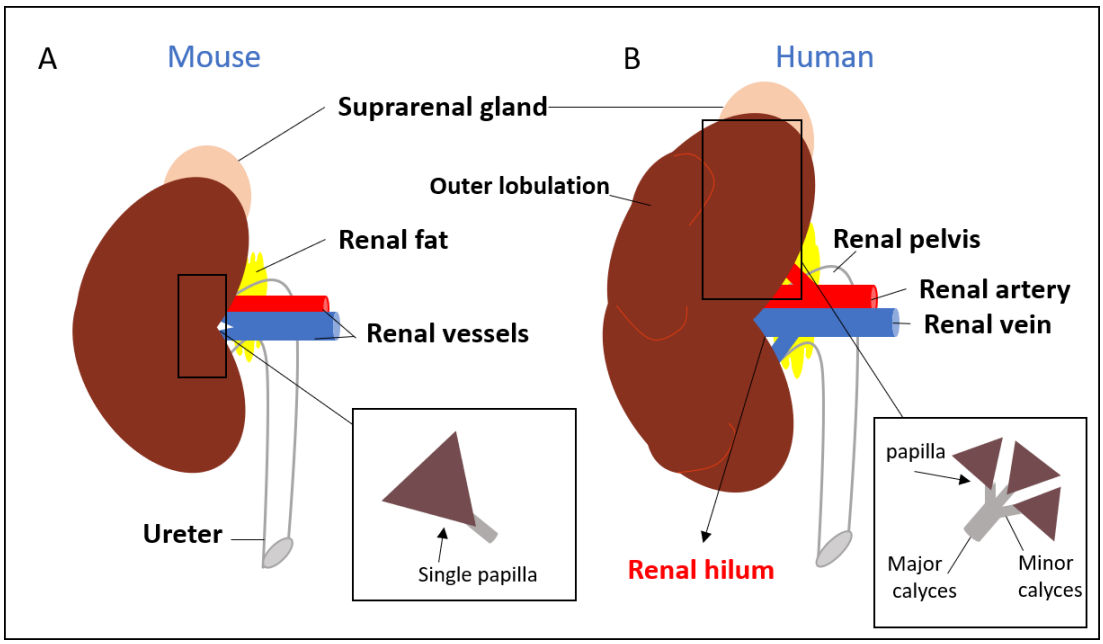

Figure 1.1 Gross anatomy of mouse and human kidneys (A) Mouse kidney. Small uni-papillate kidney with smooth outer surface. The hilum contains renal vessels and ureter. (B) Human kidney. Larger multi-papillate kidney with indented outer side.

1.2.2 Anatomy of the ureter

Ureters are tubular structures, three to four millimetres in diameter in humans, that extend from the kidneys to the bladder. Their function is to transfer urine from the renal pelvis to the urinary bladder to be stored and expelled (Narath,1951). Ureters start at the renal pelvis which lies posterior to the renal vein and artery in the hilum of the kidney (Pfeiffer, 1968). They run inferiorly in the abdomen crossing over the psoas major muscle and end in the trigone of the urinary bladder. In humans, each ureter has three bends along its length, which are common sites for stone obstruction, one lies at the pelvi-ureteric junction, one at the uretero-vesical junction and one at the level of the crossover of the common iliac artery (Fourman & Moffat, 1971).

The human ureter is surgically divided into three segments according to its blood supply, the upper segment supplied by the renal arteries, the common iliac arteries supply the middle part, and the lower part receives blood from the internal iliac artery. The innervation of the ureter is mainly sensory, carrying

pain sensation, and provided by the ureteric nerve plexus which derives from T12-L2 (Narath,1951).

1.3 Kidney development

The adult kidney is a sophisticated structure that contains at least 20 different cell types (Bohnenpoll & Kispert, 2014). The glomeruli of nephrons filter the blood to form urine under the effect of hydrostatic pressure allowing only small molecules to pass, while the larger blood components such as cells are retained. This filtrate passes through a series of tubules to recover useful components. For instance, sugar, amino acids and around 60% of electrolytes are retrieved in the proximal convoluted tubules, while water and some electrolytes are reabsorbed in loop of Henle, distal tubules and collecting ducts. The final filtrate passes from the collecting ducts to the renal pelvis, ureter and subsequently to the bladder (Kriz & Koepsell, 1974).

In mammals, kidneys develop from the intermediate mesoderm as three successive embryological pairs of kidneys which appear in cranial to caudal sequence, pronephros, mesonephros and metanephros (Redempta & Gibley 1966). The next sections will describe the process of kidney development; unless stated otherwise, all timings and gene abbreviations apply to mouse.

1.3.1 Gastrulation

To better understand the process of kidney development, it is sensible to start looking at the very early stages of embryonic development which ultimately lead to kidney formation-one of these key events is gastrulation. Gastrulation is defined as the specification of the embryonic disc into three germ layers, ectoderm, endoderm, and mesoderm. This stage is characterized by migration of a large subset of epiblasts ventrally through a furrow on the posterior caudal side of the embryo, called the primitive streak (Bellairs, 1986). Further, the mesoderm is subdivided into three regions according to their location relative to the neural tube. These regions are, from medial to lateral, the paraxial

mesoderm which forms the bony skeleton, extremities muscles and the skin dermis, the intermediate mesoderm which forms the kidneys, ureters and gonads, and the lateral plate mesoderm, which forms the heart, endothelia, body wall and the viscera (Saxen,1987).

1.3.2 Intermediate mesoderm development

Early in development, the expression of the transcription factor T box (TBXT) or Brachyury is elevated in the cells destined to the mesodermal fate, while low level expression present in cells of neural fate (Wilson and Beddington, 1997). At day E8-9 of embryonic development, expression of the transcription factors Pax2, Pax8, Lhx1 and Osr1 indicate differentiation towards the intermediate mesoderm (Marcotte et al., 2014).

One of the most important factors in specification of the mesoderm is bone morphogenic protein (BMP) signalling (Koster, 1991; Smith, 1997). High levels of BMP expression induce lateral plate mesoderm formation and low levels induce paraxial mesoderm and somite formation, while intermediate levels lead to intermediate mesoderm formation and expression of OSR1 and Pax2, early intermediate mesoderm (IM) factors (James and Schultheiss, 2005)**.** It is also known that Activin A is essential for expression of the IM markers (Willems & Leyns, 2008).

Factors including BMPs, GDFs and activin A, which are all members of TGFβ superfamily, perform an important role in development and disease (Schier, 2003). These factors signal via type I and II receptors serine/threonine kinases and Smad family second messengers. BMP signals via type I receptors Alk 3, 6 then through Smad 1,5 and 8, while Activin A operates through type I receptors Alk4, 5, 7 then Smad2,3 (Nishinakamura & Sakaguchi, 2014).

At earlier stages of renal development, Pax2 and Pax8 expression help the specification of the intermediate mesoderm into nephric duct committed cells. Another key factor at this stage which induces further specification and helps

the extension of nephric duct is gata3 (Grote et al., 2006). Lhx1 expression is important for the survival and further extension of the Wolffian duct to fuse with the cloaca (Kreidberg, 1996).

1.3.3 Stages of kidney development

1.3.3.1 Pronephros

The pronephroi develop and function in lower vertebrates such as Xenopus embryos and fish larva and are responsible for regulation of salt and water reabsorption and blood pH (Agarwal & John, 1988). In Amniotes, the pronephros is simple transitory structure, even though its function is not evident, its formation is important for the development of the subsequent renal stages. Pronephroi form at the level of the 5th to the 8th somite at day E8 in mouse (Bouchard et al., 2000), and around day 20-21 post-coitum in humans (Woolf et al. 2003).

The pronephros consists of a nephrotome containing a cavity called a nephrocoel which opens directly in the intra-embryonic coelom (Fig. 1.2). The nephrotome wall gives rise to epithelial tubules which open in a duct called pronephric duct (Fig. 1.2). The glomus is the filtration unit of the pronephros- it is a vascularized structure that filters directly into the coelom. The pronephric duct, the future Wolffian duct, terminates in the cloaca and the number of tubules vary between species (Vize et al., 2003). It expresses similar genes to those expressed in the later renal stages such as Pax2, WT1, Gata3, Lim1, Six1 (Grote et al., 2006).

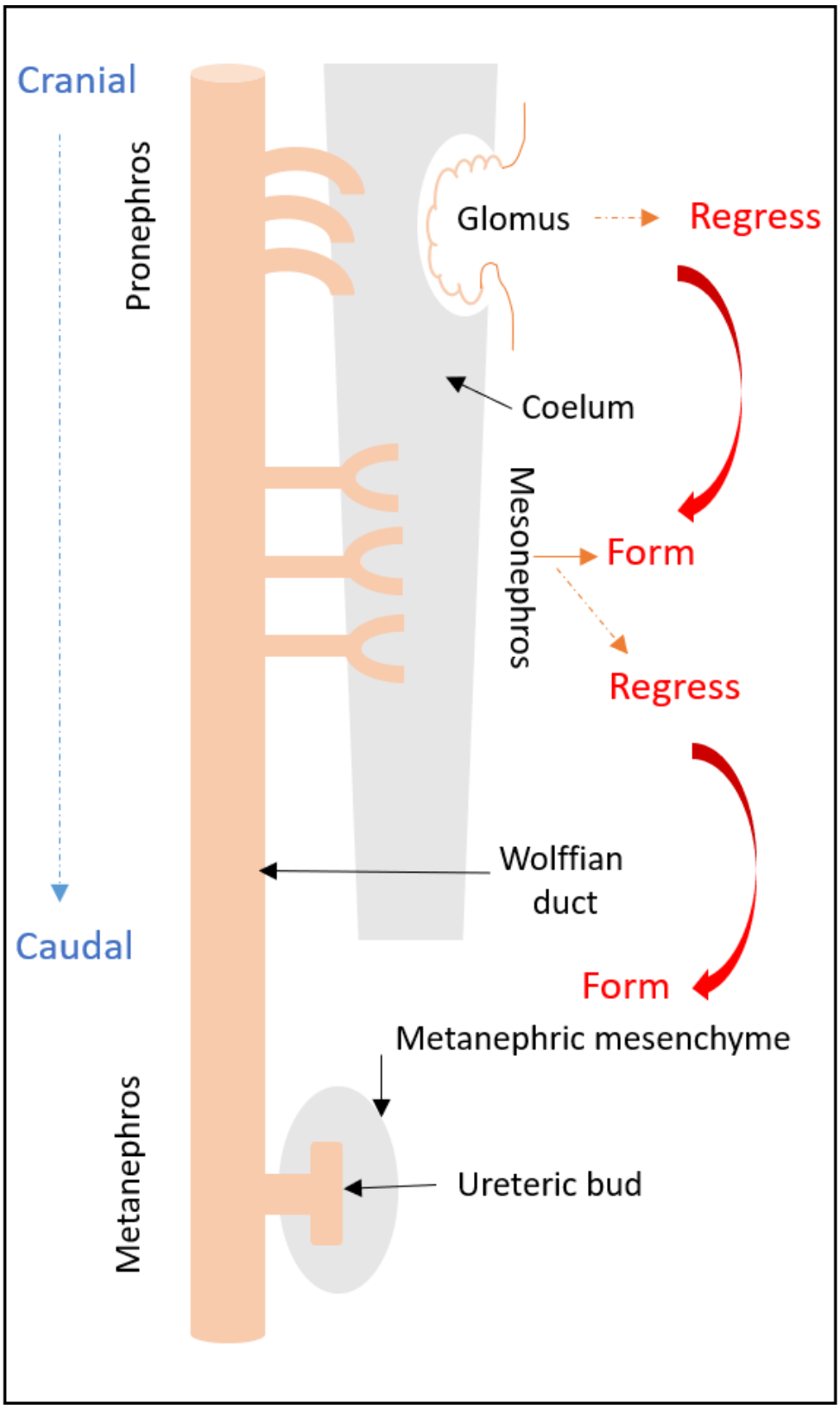

Figure 1.2 Stages of mammalian kidney development. Image showing successive development of embryonic kidney stages pronephros, mesonephros and metanephros. Image modified from Mortiz et al., 2008.

1.3.3.2 Mesonephros

The mesonephros is the second kidney to develop and lies caudal to the pronephros. It starts at the level of 10th to 17th somite at day E9 in mice (Sainio & Ahokas, 2003) and 25 days post-coitum in humans (Ludwig and Landmann, 2005). The mesenchyme of the nephrogenic cord aggregates and undergoes MET (mesenchymal-epithelial transition) in order to form the renal vesicles (Sainio & Ahokas, 2003). Subsequently, these vesicles further elongate and form simple nephrons that connect directly to the WD. The mesonephros consists of about 18 tubules in mice (Vetter and Gibley, 1966), and around 40 tubules in humans, which work transiently to excrete urine (Ludwig and Landmann 2005). The mesonephros and Wolffian duct start to degenerate with the onset of the metanephric development. They regress in females, and their remnants are called epoophoron and paroophoron, while they persist in males to form the testicular efferent tubules (epididymis, vas deferens and ejaculatory duct). Mesonephroi express some genetic markers that are also involved in the metanephric development such as Pax2, Osr1, Six1 and Wt1 (Carroll et al. 2005).

1.3.3.3 Metanephros

In mammals, the metanephros is the permanent functioning form of the kidney, which starts developing at day E10 in mice and around 30 days post coitum in humans (Woolf et al., 2003). The caudal end of the mesonephric Wolffian duct is induced to form a projecting epithelial tubule known as the ureteric bud (UB). The UB elongates and its proximal end enters a mass of mesenchyme called the metanephric mesenchyme (MM). Once invasion occurs, a series of reciprocal interactions between the ureteric bud (UB) and the metanephric mesenchyme (MM) takes place (Saxen and Sariola, 1987). The MM stimulates the growth and branching of the proximal part of the UB to form collecting ducts, calyces and renal pelvis, while the UB induces the survival and differentiation of the MM to form nephrons. The distal part of the UB which remains outside the MM forms the future ureter (Saxen and Sariola, 1987).

1.3.4 Development of metanephric mesenchyme (MM)

The metanephric mesenchyme comprises two main cell populations, Six2+ cells and Foxd1+ cells (Oliver et al., 1995). Studies have showed that Six2+ cells are the progenitors of nephrons, while the Foxd1+ are stromal cell progenitors (Kobayashi et al., 2008). Two factors are known to influence nephron formation: signals from the ureteric bud and Foxd1+ stromal cells (Guillaume et al., 2009). Failure of UB formation leads to kidney agenesis, while defects in the Foxd1 cells lead to reduced sized kidneys with increased population of undifferentiated cells (Das et al., 2013).

1.3.4.1 Nephron formation

In metanephric development, formation of the cap mesenchyme (CM) is the earliest step in nephron formation and starts by the mesenchymal cells condensation around the UB tips. The CM is formed of a layer of cells that encloses the tips of the ramifying ureteric bud and is distinct from the uninduced surrounding mesenchyme (Schmidt-Ott et al., 2007). These cells characteristically express Pax2, Eya1, Six2, Wt1, Sall1 as well as GDNF and BMP7. Their function is to provide cells for nephron differentiation. Survival of these cells depends on the expression of multiple factors including members of Wnt, FGF and BMP families (Schmidt-Ott et al., 2007). It is also believed that BMP7 plays a role in sustaining the undifferentiated state of the cap mesenchyme cells in order to maintain their survival (Dudley et al., 1999).

Further, under the effect of wnt9b expression by the UB, these mesenchymal caps form pre-tubular aggregates (PTA) (Sariola, 2002). These PTAs express Wnt4 which induces mesenchymal to epithelial transition and leads to renal vesicles formation, which subsequently develop into comma-shaped then S-shaped bodies. Later, those S-shaped bodies develop into mature nephrons containing Bowman's capsule at its proximal end, proximal convoluted tubules, and loop of Henle at the middle part, while the distal part forms the distal convoluted tubules which become connected to the collecting duct tree (Kloth et al., 1994).

1.3.4.2 Formation of renal stroma

Renal stromal cells express the transcription factor Foxd1 and are located peripheral to the cap mesenchyme (Hatini et al., 1996). Later in development, they arrange themselves around the branches of the ureteric bud and nephrons to form kidney interstitium (Alcorn et al., 1999). Both cortical and medullary stromal cells provide structural support to the surrounding collecting ducts and nephrons and are important in regulating UB branching and nephron differentiation (Cullen- McEwen et al., 2005).

Two important factors are produced in stromal cells in the renal cortex: the transcription factor Foxd1 and the RA synthesizing enzyme retinaldehyde dehydrogenase-2 (Batourina et al., 2001). It is believed that the Foxd1 gene plays a vital role in differentiation of nephrons and branching of the UB. RA is an important signalling molecule connected to the cortical stromal cells. Tissue distribution of RA is highly influenced by RA-synthesizing enzymes (Napoli 1999; Duester 2001). Retinaldehyde dehydrogenase-2 (Raldh2), secreted by the cortical stromal cells, is important for RA synthesis and action (Niederreither et al., 1996).

Studies have indicated that retinoic acid signalling is important for UB branching, as it influences the UB tips' expression of the GDNF receptor, Ret. Whilst Ret is essential for the UB to grow and branch, it is also important for stromal cell patterning (Schuchardt et al., 1996). This occurs via reciprocal signalling between the cortical stroma and the UB (Batourina et al., 2001). Cortical stroma expresses RA-dependant signals to stimulate the UB branching, while UB produces Ret-dependant signals which control branching and cortical stromal patterning (Das et al., 2013).

1.3.4.3 Development of the ureteric bud (UB)

The development of the ureteric bud depends on the development of the Wolffian duct (WD) as its precursor. Pax2, Pax8 and Lim1 are important factors

for successful Wolffian duct development, and failure of this process results in failure in kidney development (Dressler et al., 1990).

The earliest detectable step of metanephric kidney development is the emergence of the UB from the WD, which is strictly controlled by the surrounding mesenchyme to allow only one bud formation and block any ectopic budding. To ensure this, the interaction between two major TGF- β superfamily pathways is required, the BMP4 and the GDNF pathways. Stimulation of UB budding is influenced by GDNF which can be detected in the metanephric mesenchyme close to the site of UB emergence from the WD (Hellmich et al., 1996). The Wolffian duct expresses GDNF receptor Ret and the co-receptor Gfrα1, and Ret expression becomes confined to the UB tips after the first UB branching. Mice deficient in GDNF or its receptors show renal agenesis (Sainio et al., 1997).

The ectopic UB budding from the WD is prohibited by the BMP4 expression from the surrounding mesenchyme (Costantini and Shakya, 2006). At the site of the UB emergence, the MM expresses gremlin1, which is a potent inhibitor of BMP4 (Fig. 1.3) to allow the formation of the UB in the desired location (Costantini and Shakya, 2006). The BMP4 expression can also be detected in the mesenchyme surrounding the unbranched ureteric stalk where gremlin expression is absent, which suggests the role of BMP4 in blocking the budding and the role of gremlin in inducing it (Miyazaki et al., 2000).

The formation of the UB is stimulated by the activation of ERK (extracellular signal-regulated kinase), PLC (phospholipase C) and PI3K (phosphatidylinositol 3-kinase) pathways and inhibited by the activation of SMAD pathway. Activin A is a factor expressed by the nephric duct and works through the SMAD activation to prevent UB budding (Woolf & Davies, 2013). Collectively, the TGFβ superfamily members BMP4 and Activin inhibit UB emergence by binding to ALKs (Activin receptor-like kinases) and consequent activation of SMAD pathway (Michos et al., 2007).

GDNF and FGFs interact with the receptors Ret and FGFR2 on the nephric duct epithelium, and activate PI3K, ERK and PLC pathways to induce ureteric bud formation (Eswarakumar et al., 2005; Weering and Bos,1998). Factors influencing Ret receptor expression include the nephric duct expression of GATA3 and β-catenin (Grote et al., 2008; Michos, 2009) as well as RA synthesis by the stromal cells (Rosselot et al., 2010).

Prevention of ectopic UB budding is also influenced by the expression of the cytoplasmic protein sprouty1 (Basson et al., 2005), the signalling between ROBO2 and SLIT1 (Grieshammer et al., 2004) as well as the expression of FOXC1, to prevent the extension of GDNF effect within the intermediate mesoderm (Kume et al., 2000).

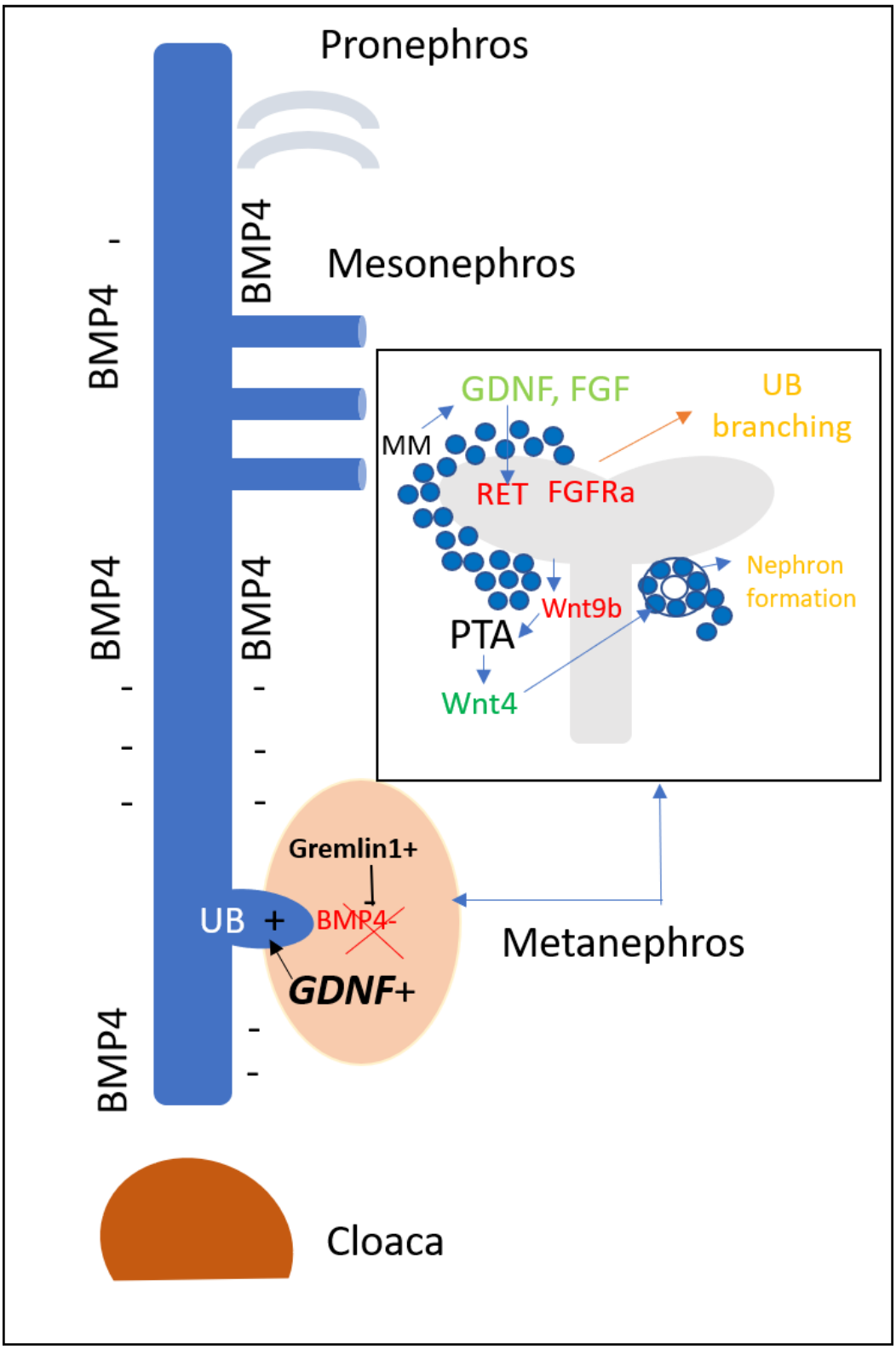

Figure 1.3 Factors affecting UB budding from the WD. The small box shows reciprocal signalling between the MM and the UB. Image modified from Woolf & Davies, 2013.

1.4 Ureter development

The mammalian ureter is simpler in structure than kidneys and comprises a tube that transports urine unidirectionally from renal pelvis to the bladder (Crelin, 1978). It is formed of two major tissue precursors (Fig. 1.4), the ureteric epithelium, and the surrounding mesenchyme (Trowe et al., 2012). The mesenchyme differentiates into an external fibroelastic layer called tunica adventitia, an internal lamina propria, and a smooth muscle layer in between, while the epithelium forms a multilayer specialized urothelium (Bohnenpoll et al., 2017).

1.4.1 Development of the ureteric mesenchyme

In mice, the Wolffian duct (WD) reaches the urogenital sinus (the primordium of the bladder and urethra) at day E9. The caudal part of the WD starts budding at E10, forming the UB. At E11, the proximal part of the UB (the part nearest its tips: kidney uses a definition of proximal and distal opposite to most glandular organs) extends within and interacts with the metanephric mesenchyme to branch and form a collecting duct network, while the distal part of the UB outside the MM remains unbranched and differentiates into ureter (Chisht et al., 2014). Mutual stimulating signals also occur between the distal UB and the surrounding mesenchyme, resulting in urothelial differentiation and smooth muscle formation (Schedl et al., 2007).

Using lineage tracing, it has been reported that mesenchyme surrounding the distal and proximal parts of the developing UB have different origins. While the MM originates from the posterior IM, the mesenchymal cells surrounding the distal ureter are derived from an undifferentiated cell population in the most caudal part of the embryo called tailbud (Brenner et al., 2007). Cell migration is important to establish this mesenchyme around the distal UB. The tailbud-derived mesenchyme expresses high levels of BMP4 which is important for ureteric differentiation and smooth muscle development (Miyazaki et al., 2003; Airik et al., 2006).

The mesenchyme that envelops the distal part of the ureteric bud expresses the transcription factor TBX18, which is necessary for mesenchymal proliferation and formation of smooth muscle (Airik et al., 2006). The peri-ureteric mesenchyme remains undifferentiated from E11.5 to E15.5. At E16.5 the mesenchyme starts to differentiate to form 3 layers. The first layer is the stromal cell layer which lies between the urothelium and the smooth muscle layer and it is responsible for the elasticity of the ureteric tube. The second layer is the smooth muscle which is arranged in longitudinal and transverse directions. The outermost, loosely attached cells form the adventitial layer (Airik and Kispert, 2007).

1.4.1.1 Development of the urothelium

Urothelium is a distinctive type of epithelium that covers the luminal side of the ureter and bladder and acts as a barrier to prevent urine from being reabsorbed. In mouse, it is formed of a single cuboidal cell layer of basal cells separated from the lamina propria by a basement membrane, one or two layers of intermediate cells that resemble basal cells in size and shape, and an apical layer of superficial squamous cells (umbrella cells) that express uroplakin UPK (Velardo 1981; Yu et al., 1990). All cells of the urothelium derive from a common Pax2+Shh+ cell population in the ureteric bud stalk (Bohnenpoll et al., 2017).

Previous studies on the bladder urothelium revealed that the urothelial cell layers can be distinguished using three immunological markers: cytokeratin 5 (KRT5), the transcription factor P63 (ΔNP63) and the UPK (Bohnenpoll et al., 2017). Basal layer cells express Krt5+ and NP63+, intermediate cells express weak UPK+ and NP63+ but are KRT5-; of all the molecules mentioned in this paragraph, superficial cells express only UPK (Shin et al., 2011). The first marker to appear is p63 at E14.5 while both the superficial and basal cell markers can be detected from E15.5 and E16.5, respectively. This suggests

that the intermediate cells might be the main precursor of both basal and superficial cells (Bohnenpoll et al., 2017).

Krt15 is a transcript that can be found in cornea (Figueira et al., 2007), oesophagus (Leube et al.,1988), uterine cervix (Smedts et al.,1993), and the epidermis of the skin (Whitbread and Powell, 1998; Garza et al., 2011). In the ureters of wild type mice, occasional basal cells co-expressing Np63 and Krt15 can be detected and P63 expression in urothelium is needed for Krt15 expression (Tai et al., 2013).

In urothelial development, it was believed that basal cells were the source of both the intermediate and superficial cells (Shin et al., 2011). In 2013, Ghandhi and colleagues proposed the presence of a transient cell population called progenitor P-cells which they claimed to be the source of both intermediate and superficial cells, while intermediate cells are the superficial cell progenitors in adult ureter regeneration (Fig. 1.5). The origin of the basal cells is still unidentified (Ghandi et al., 2013).

Retinoids are strong inducers of urothelial differentiation (Mauney et al., 2010). Defects in RA signalling result in failure of the P-cell formation and subsequently loss of both intermediate and superficial cell layers in embryo, and defective regeneration in adult ureter after injury (Ghandi et al., 2013). Other studies have shown that some basal urothelial cells have stem cell properties and can regenerate any cell type in the urothelium after injury. When injury occurs, shh expression in basal cells increases, leading to increased Wnt signalling from the stromal cells resulting in proliferation of both cell types (Shin et al., 2011).

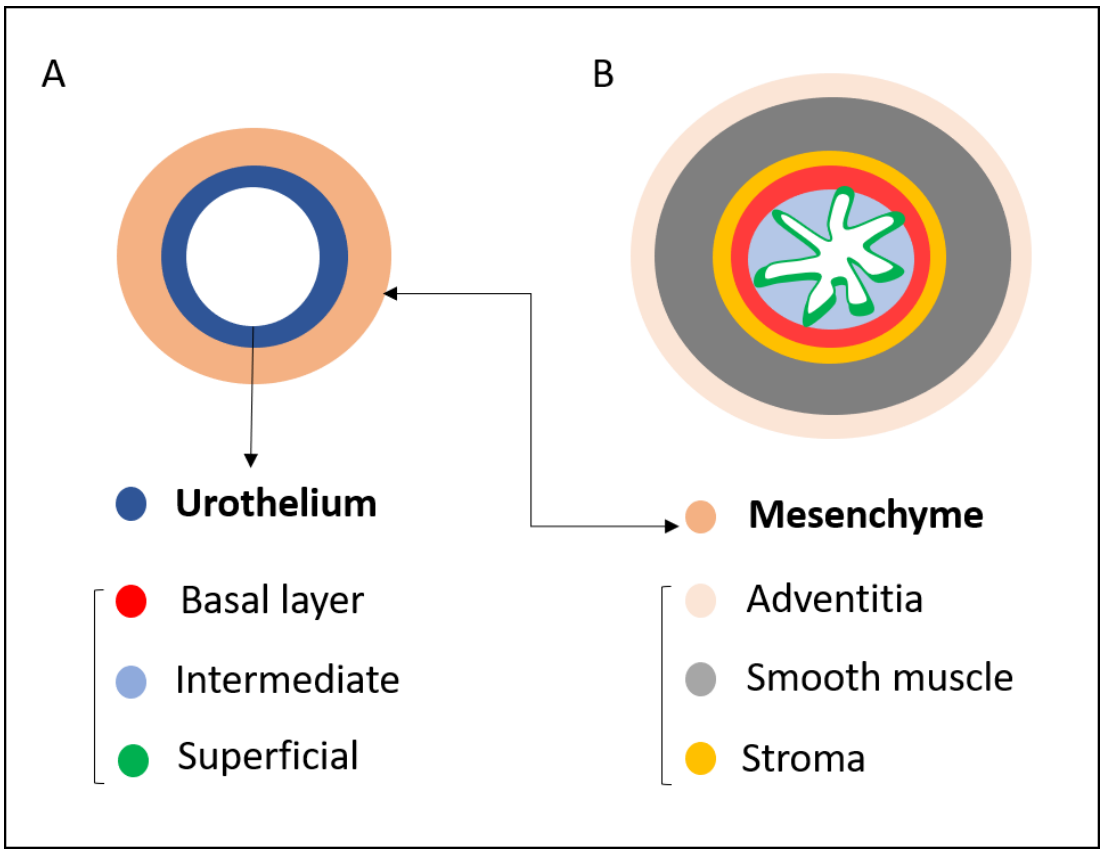

Figure 1.4 Structure of embryonic and adult ureters. (A) Early developing ureter consists of two layers, mesenchyme and urothelium. (B) Mature ureter contains outer adventitia, inner lamina propria, and smooth muscle layer and a multilayer urothelium contains basal, intermediate, and superficial cell layer.

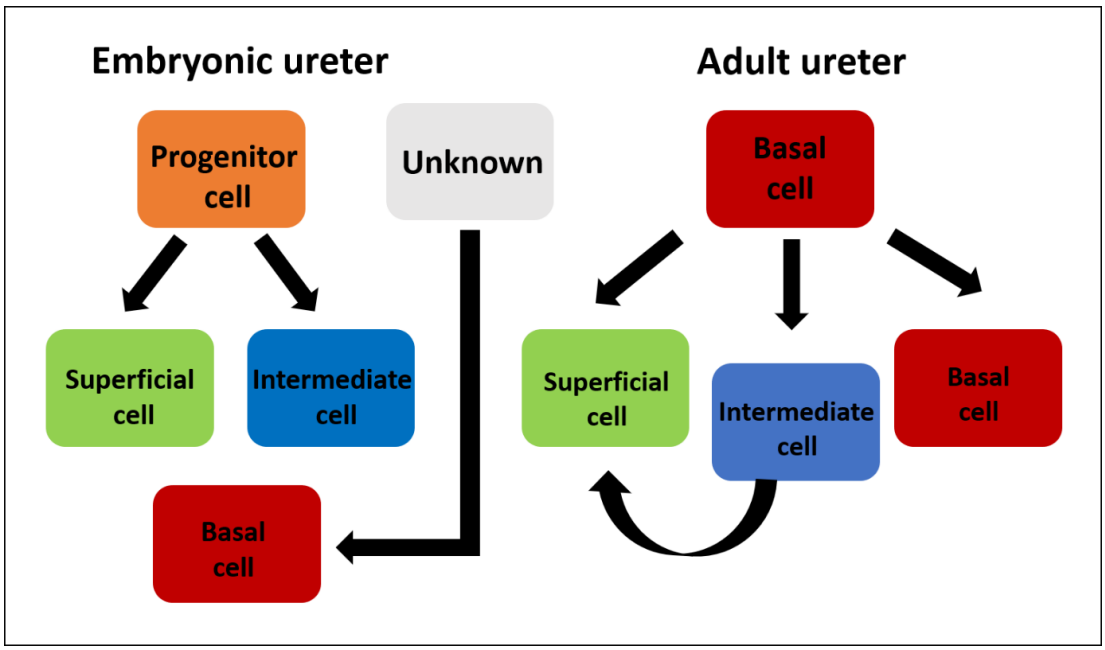

Figure 1.5 Possible origins of different urothelial cell types in embryonic and adult ureters.

1.4.1.2 Uroplakins

The urothelium of the lower urinary tract is constantly exposed to urine as it passes through. While urine contains toxic substances, the urothelium is structurally adapted to protect the underlying tissue from the harmful effect of these toxins (Hicks, 1965). It is characterized by the presence of a group of urothelial-specific-integral-membrane proteins called UPKs which can be found as plaques in the luminal side and as fusiform vesicles in the cytoplasm of the superficial cells (Wu et al., 2009). These vesicles act as a reservoir to maintain the UPK barrier, as well as playing a role in adjusting the surface area during urothelial contraction or extension (Lewis & Moura, 1982; Hichs, 1965). UPK covers the luminal surface of the renal pelvis, ureter, bladder, and urethra (Hicks 1995; Porter and Bonneville,1963). It is also called asymmetric unit membranes (AUMs) and does not exist in any other type of epithelium (Yu et al., 1990).

UPK is considered a substantial differentiation marker of urothelium which plays a key role in its structure and function (Pauli et al., 1983; Hicks, 1975). It consists of 4 major proteins which are known as UPK Ia, I b, II and III (Yu et al., 1990; Yu et al., 1994). UPKIII is characterized by the presence of a cytoplasmic tail which is believed to have a role in binding UPK plaques to the underlying cytoskeleton (Wu et al., 1993). Disorganization of the UPK plaques with loss of the water-tight property can be seen in the urothelium of mice deficient in UPK3a or UPK2 (Jenkins and Woolf, 2007; Wu et al., 2009). BMP4 and TBx18 expression are important for the expression of UPK in mouse ureters (Wu et al., 2009; Brenner et al., 2007). UPK expression in UB branches can be induced by application of BMP4 to kidneys in culture, which suggests that these branches can be induced to differentiate towards urothelium (Brenner et al., 2007; Mills et al., 2017).

1.4.2 Ureteric smooth muscle development

The interaction that occurs between the epithelium of the ureteric stalk and the surrounding mesenchyme is important for the development of both urothelium and smooth muscle (Lye et al., 2010). The mesenchyme expresses PTCH1 receptors which interact with SHH, a growth factor produced by the UB epithelium, to stimulate the mesenchymal proliferation (Yu et al., 2002). Simultaneously, the mesenchyme expresses BMP4 which stimulates urothelial differentiation and induces the mesenchyme itself to differentiate into smooth muscle (Brenner et al., 2007).

This occurs due to activation of the SMAD pathway and upregulation of the transcription factor TSHZ3. TSHZ3 is important for the activation of MYCOD expression, a transcriptional activator, which is responsible for upregulating the expression of actin and myosin within ureteric smooth muscle cells (Fig. 1.5) (Caubit et al., 2008). Mutations in SHH result in perturbed expression of BMP4 in the peri-Wolffian mesenchyme, which leads to formation of an abnormally thin layer of smooth muscle (Lye et al., 2010). Sox9 expression in

the peri-ureteric mesenchyme is also important for ureteric smooth muscle development (Airik et al., 2010).

At E16.5, ureters become completely enveloped by a smooth muscle layer formed of bundles of contractile filaments strongly expressing smooth muscle alpha actin (Santicioli and Maggi, 2000). Within a short time, these muscles develop unidirectional peristaltic contractions starting from the renal pelvis and propagating distally (Golenhofen and Hannappel, 1973).

1.4.2.1 Ureteric muscle contraction and function

The function of the kidney is the filtration of blood at the glomerulus to eliminate toxins and waste products by producing urine. The excess fluid and solutes are then transferred to the bladder by peristaltic movement of the smooth muscle of the ureter (Barbuti and DiFrancesco, 2008; Biel et al., 2009). The contractile electrical activity is initiated at the renal pelvis under the influence of pacemaker cells (Bohnenpoll & Kispert, 2014).

Defective ureteric peristalsis is a common congenital anomaly, associated with a wide range of renal pathologies such as urinary tract obstructions, kidney damage due to reflux and persistent infections (Chevalier and Peters, 2003; Becker & Baum, 2006).

In vitro-isolated-ureters have the ability to generate peristaltic contractions independently, suggesting the presence of more than one pacemaker cell population (Caubit et al., 2008).

1.4.2.2 Pacemakers

The primary pacemaker cells are a population of atypical spindle-shaped smooth muscle cells, which express the receptor tyrosine kinase Kit. Kit - positive-cells were detected in the proximal part of mouse ureter (Pezzone et al., 2003) and in human ureter (Metzger et al., 2004). In mouse, Kit expression

is upregulated in ureteric cells by day E15.5, before the onset of the peristaltic contractions (David et al., 2005). In vitro-cultured E11.5 ureters develop peristaltic contractions after 7 days in culture, and ureters cultured in the presence of anti-Kit antibodies fail to develop contractions (David et al., 2005). Immunohistochemical analysis revealed that the atypical smooth muscle cells of the pacemaker have weak act2 expression, short cellular processes, fewer contractile filaments, and the filaments they have are arranged in loosely packed bundles (Gosling and Dixon, 1971; Lang et al., 2001). The distribution of these cells coincides with the detected electrical activity (Constantinou et al., 1978).

The renal pelvis expresses the hyperpolarization-activated cation channel HCN3 which is believed to be responsible for induction of peristaltic contractions in vivo and can also be detected in the pacemaker cells in the heart and autorhythmic cells in the brain (Hurtado et al., 2010). Blocking this channel causes loss of electrical activity at the PUJ and disturbance in smooth muscle contraction (Hurtado et al., 2010). SHH Expression is important for the expression of both HCN3 and KIT, and mutations in SHH lead to perturbation of the SM contractions (Cain et al.,2011). Additionally, angiotensin and calcineurin are found to be important factors in the ureteric pacemaker cells development (Bohnenpoll & Kispert, 2014).

Sensory nerves and prostaglandins are believed to control the pacemaker activity in the proximal portion of the ureter (Weiss et al., 2006). The sensory axons in the ureter contain Calcitonin gene-related peptide (CGRP) which is proposed to influence the pacemaker cells in the ureter (Maggi and Giulani, 1991). Other factors influencing the smooth muscle contractility are the presence of adrenergic and cholinergic receptors (Cain et al., 2011).

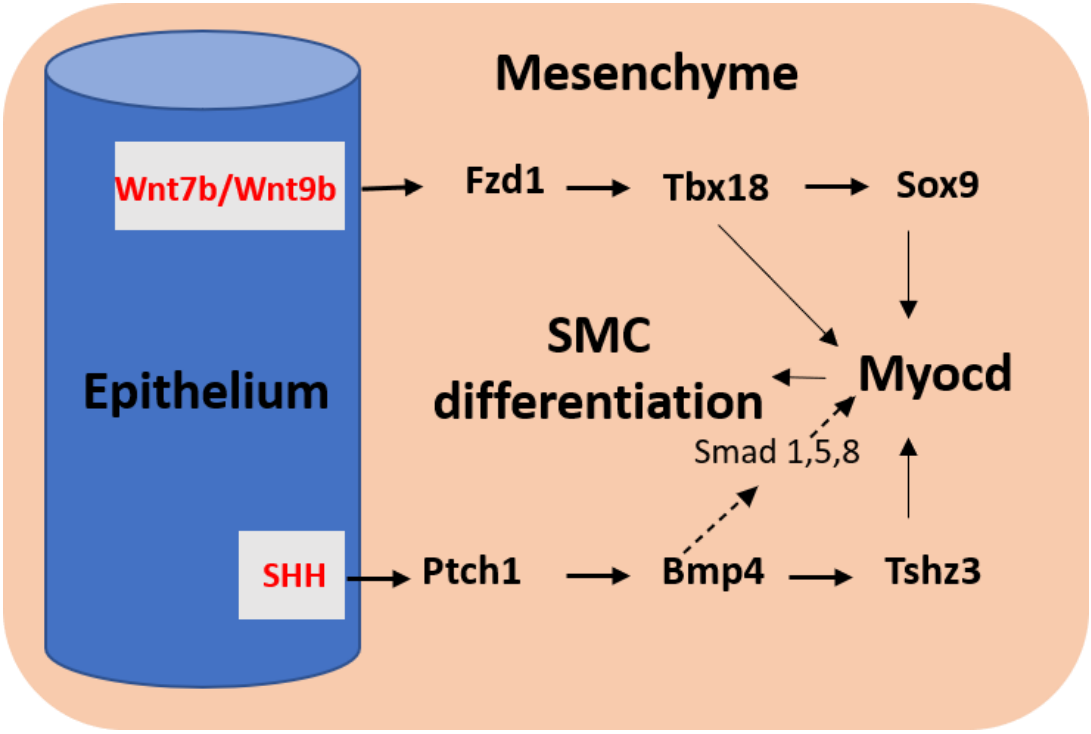

Figure 1.6 Role of SHH and Wnt in the regulation of the growth and differentiation of urothelium. Image is modified from Bohnenpoll & Kispert, 2014.

1.5 Development of renal vasculature

Blood supply is essential for the survival of transplanted engineered structures in vivo. Recent findings suggest that blood supply helps the maturation and function of stem cell-derived organoids (Homan et al., 2019). For that reason, understanding the process of vascularization is important for the future success of engineered ureters.

The metanephric mesenchyme consists of two main cell populations, the nephron progenitors NPs, and the stromal progenitors SPs. While the nephron progenitors go through a process called mesenchymal to epithelial transition (MET) in order to form nephrons, stromal cells migrate internally to form renal supporting tissue. Studies have showed that stromal cells differentiate into vascular smooth muscle cells (SMCs), pericytes and fibroblasts (Lopez and Gomez, 2011; Dressler, 2006). Additional studies have showed that endothelial progenitors (Sequeira-Lopez et al., 2015) and tissue macrophages

(Rae et al., 2007) can be detected in the stroma of early metanephros. Lineage tracing experiments of Foxd1, an early stromal marker, have reported that the perivascular endothelial cells including renin-secreting cells are derived from cortical stroma (Kobayashi et al., 2014). It is also believed that the TBx18-expressing mesenchymal cells contribute to the formation of muscular coat around the ureter as well as medullary stroma (Bohnenpoll et al., 2013). Expression of Tbx18 can be detected in stromal cell-derived vascular SM cells, glomerular mesangial cells and pericytes (Xu et al., 2014).

1.6 Kidney organoids

Renal failure is a major health problem that causes suffering and premature death (Steenkamp et al., 2011). Patients with chronic renal failure require frequent haemodialysis as a life-saving procedure and kidney transplantation is the only cure at least for some time, approximately 10-15 years, before the organ gets rejected by the patient's immune system. Developing alternative strategies to regenerate or replace damaged kidney tissues is urgently needed (Little., 2019).

The main functions of the kidney are to eliminate toxins from the blood, control blood pressure, pH and electrolyte balance, and the retention of valuable compounds such as glucose and amino acids (Takasatu et al., 2014). Renal failure is a common condition, and many factors can contribute to its high prevalence including congenital abnormalities, renal toxic medications, infections, and chronic diseases such as diabetes and hypertension. After injury, the adult kidney has a limited ability to self-regenerate (Humphreys et al., 2008) and nephrogenesis occurs only during development in humans, consequently nephron loss is permanent. Congenital or acquired defects in functioning nephrons are the main cause of kidney failure (Humphreys et al., 2008).

The adult kidney is complex in structure and relatively large to be constructed directly, therefore it is more realistic to engineer immature simpler forms and

allow them to mature in vivo via transplantation into a living host, or in vitro using advanced culture techniques (Davies & Chang, 2014).

New advances in stem cell biology have raised expectations to find new therapeutic strategies to treat patients with chronic kidney disease (Morizane et al., 2017). Recent studies have identified the key signals important for kidney development and used that knowledge to recapitulate renal developmental stages in vitro using stem cells (Taguchi & Nishinakamura, 2017).

Organoids are defined as 3D structures that form in culture plates in vitro and resemble, to a certain extent, the natural organ structurally and functionally (Morizane & Bonventre, 2017). Organoids can be classified according to their cell sources into two main categories, primary tissue-derived organoids and stem cell-derived organoids (Fatehullah et al., 2016). I think a third category can be added to this classification, which is hybrid organoids that are formed by mixing cells from primary tissue with other stem cells.

1.6.1 Embryonic tissue-derived kidney organoids

An early study about self-organization of murine renal progenitor cells by Grobstein et al.,1952 showed that it is possible to form kidney structures in vitro by recombining intact UB with MM (Grobestein et al.,1952). The formation of kidney organoids from single cell suspension of dissociated embryonic kidneys was not possible as the dissociation triggers cell apoptosis. In 2010, Unbekandt and colleagues reported that pharmacological inhibition of Rho-associated protein kinase (ROCK) blocks the dissociation-induced cell death (apoptosis) in embryonic renal tissue, and therefore renal structures can grow (Unbekandt et al., 2010). These organoids were the first to be made of renogenic stem cells derived from enzymatically dissociated kidney rudiments and expressed markers similar to the natural CD/ nephrons. However, the Unbekandt organoids were anatomically disorganized, containing multiple

islands of UB epithelial cells that organized themselves and grew into multiple small branching trees surrounded by immature nephrons. In 2011, Ganeva and colleagues introduced a modification to the Unbekandt organoids using serial reaggregations to achieve a more realistic anatomical organization. A single UB epithelial spheroid was isolated from Unbekandt cultures and recombined with fresh MM. This has led to formation of renal organoids with a single collecting duct that ramifies symmetrically and organizes nephron formation around itself, but with no ureter. By applying asymmetric cues of BMP4 signals to one branch of the CD in Ganeva organoids, a single unbranched UPK-expressing urothelial tube was formed (Mills et al., 2017).

1.6.2 Pluripotent stem cells and kidney organoids

Pluripotent stem cells are characterized by infinite capability for self-renewal and the ability to produce all cell types in the human body. They normally exist transiently in the early blastocyst stage of the human embryo (Martin 1981; Evans & Kaufman, 1981). This indefinite growing ability as well as pluripotency have made them a great tool for studying development, disease pathogenesis, drug screening and possibly formation of replacement tissues to treat patients with incurable diseases such as spinal cord injuries (Thomson et al., 1998). However, the utilization of human embryos as a source for these cells has yielded enormous ethical debates that have led to restrictions over the applications of these cells.

Induced pluripotent stem cells (iPSC) are adult reprogrammed cells that have been manipulated to restore their pluripotency using the transfection of 4 genes Oct3/4, Sox2, Klf4 and c-Myc (Takahashi and Yamanaka, 2006). These cells resemble embryonic stem cells in morphology, propagation, genetic profile as well as the ability to form teratomas. Additionally, mouse iPS cells can create adult chimeras, when transplanted into blastocysts (Wernig et al., 2007). It is feasible to produce patient-derived pluripotent stem cells which is important for effective stem cell application into clinical practice.

Embryonic stem cells (ES) and iPS cells represent an important advance towards formation of in vitro organoids. Several research groups worked to find ways to differentiate these cells towards the renal fate. In 2014, Taguchi and colleagues developed a stepwise method for in vitro differentiation of kidney organoids from ES and iPS cells, that produces mainly nephron progenitors (NPs). They reported that both MM and UB have distinct developmental origins: although both derive from the IM, the UB develops from the anterior IM, while the MM derives from the posterior IM. Other groups have published protocols for inducing nephron progenitors from human ESCs and iPSCs (Mea et al., 2013; Little et al., 2018; Morizane & Bonventre, 2017). Takasato and colleagues have reported the differentiation of human kidney organoids using a simple protocol carried over 3-4 weeks (Takasato et al., 2014). In 2015, Morizane and colleagues have developed a similar protocol, that required a shorter duration. More recently, Przepiorski et al. described a method for organoid formation using a bioreactor that was relatively simple and low-cost (Przepiorski et al., 2018). Although these protocols were different, they shared common features: lack of the formation of ureteric bud tissue and the organoids were formed mainly of nephron progenitors. An exception to this is the Takasato protocol, which generated cells that express some UB markers. These cells however, failed to show branching or maintain nephrogenic niches (Naganuma & Nishinakamura, 2019).

In 2017, Taguchi and Nishinakamura developed a protocol for differentiation of UB cells from mESCs and hiPSCs. This protocol was established independently of their previous protocol for nephron progenitor induction, based on their in vivo analysis. When mixing mESCs-derived iUB with iNPs in the presence of ex-fetu stromal cells, they developed organoids that showed higher-order anatomical organization, with a single collecting duct tree connected to nephrons. However, neither protocols produced stromal cells from the pluripotent progenitors, which is why ex-fetu stromal cells were needed as it is thought they are required for effective renal organoid development. While the Taguchi organoids derived from human cells have failed to maintain nephrogenic niches, probably due to the lack of stromal cells,

Takasato reported the induction of stromal-like cells (Takasato et al., 2015), and Morizane showed that stromal cell proliferation occurs in organoids treated with IL-1b (Morizane et al., 2015).

1.6.3 Generation of a single ureteric exit

All the currently existing models of renal organoids share one common problem, which is lack of a ureter that extends outside the organoid. This makes them unsuitable for transplantation as it hinders their excretory function and will lead to failure of the graft due to hydronephrosis (Naganuma & Nishinakamura, 2019).

1.7 Aims and approaches

In this thesis, I address the problem of the missing ureter by exploring methods to engineer ureter tissue from ES cells. It is now well established that mesenchymal signals play an important role in determining the fate of the UB epithelium either into collecting duct or urothelium. However, this plasticity has never been tested on UBs derived from ES cells. My starting hypothesis was that the presence of this plasticity might be a way to achieve my aim to engineer ureters from ES cells in vitro.

The aims of this work can be summarized as:

1. Reproducing the Taguchi and Nishinakamura protocol to differentiate mESCs into UB-like structures and to further characterize the nature of these ES cell-derived epithelial structures.
2. Investigating the ability of ES cell-derived UBs to take different fates - either CDs or ureters - according to signals from surrounding mesenchyme. This was done using series of grafting experiments in

different parts of the embryonic kidney rudiments either into metanephric mesenchyme or peri-Wolffian mesenchyme.

3. Engineering ureter-like structures using ES cell-derived UBs and peri-ureteric mesenchyme.
4. Finding ways to connect these engineered structures to different parts of the collecting duct system of foetal kidneys.

Chapter 2. Materials and Methods

2.1 Animals

Pregnant CD1 mice were sacrificed at day E11.5, and this was done by trained UK Home Office license holders (BRR, Hugh Robson building, University of Edinburgh) according to methods registered under schedule one of the UK Animals (Scientific Procedures). After 11 days from finding the plug, the uterine horn was dissected out and moved to a 10 cm petri-dish containing minimal essential media (MEM). Using flame-sterilized blade and forceps, embryos were extracted from the uterine horn, then decapitated using 25-gauge hypodermic needles. A cut was made between the hind-limb and fore-limb and the tail was removed. The caudal parts of the embryos were transferred to a new petri-dish containing fresh MEM and a midline incision was made to cut the embryo into two halves along the developing spinal cord. The metanephric kidney was identified and extracted. Dissection to obtain the metanephric kidney including the ureter and the adjacent Wolffian duct and peri-ureteric mesenchyme, or just isolated mesenchyme, was performed according to the experiment.

2.2 Culture and maintenance of mESCs

2.2.1 Cell lines

The Hoxb7-GFP mESC line was obtained as a gift from Prof. Ryuchi Nishinakamura (Kamamuto University). The E14 mESC line was obtained from Prof. John Mason's Lab.

2.2.2 Thawing of cells

A cryopreservation vial containing1x10^6 cells was first placed in a water bath and shaken gently to thaw its frozen content. The contents of the vial were then transferred to a tube contains 10 ml of warm mESC media and centrifuged for 5 minutes. The supernatant was discarded, and cells were resuspended in a fresh 2 ml of mESC media containing 1000 units/ml Leukaemia inhibitory factor (LIF). Plates were incubated at temperature 37 °C with 5% CO_2. The replacement of the culture medium with fresh medium containing LIF was performed daily.

2.2.3 Coating plates with Gelatine

0.1% gelatine in PBS was left to warm up to room temperature prior to use. In a stem cell culture hood and under sterile conditions, 1.5 ml of the pre-warmed gelatine was added to each well of a 6-well plate suitable for cell culture. The plates were left with lids on for at least 30 minutes at room temperature inside the hood. After that, the gelatine solution was aspirated and discarded and the media containing cells were added immediately to avoid the gelatine film drying.

2.2.4 mESCs culture media

Cells were cultured in Glasgow minimal essential media GMEM (Sigma G5154) fortified with 10% fetal bovine serum FBS, MEM-NEAA (1x, Gibco), sodium pyruvate (1 mM, Gibco), GlutaMAX (1x, Gibco), β-mercaptoethanol

(0.1 mM, Gibco), and leukaemia inhibitory factor (LIF, 1 U/µl, Santa Cruz sc-4989).

2.2.5 Maintenance and Passaging of mESCs

After two to three days, after which the cells had achieved 70-80% confluence, the old media were discarded, and cells were washed with sterile PBS and incubated in 1 ml Accutase (Gibco) for 3 minutes. Cells were detached from culture plate by gentle pipetting and transferred to a tube containing 4 ml fresh mESC media. Cells were centrifuged for 5 minutes and the supernatant was discarded. Cells were suspended in new media containing LIF and plated on a gelatinized plate in a ratio 1:10.

2.2.6 Cryopreservation of mESCs

Cells were passaged as described before and suspended in fresh mESC media containing 10% DMSO at a density of $1x10^6$ cells/ml. They were then transferred to cryopreservation tubes, 1 ml/vial, which were kept on ice and stored in -80°C for 24 hours before being stored in liquid nitrogen.

2.3 eUB differentiation

2.3.1 Ureteric bud differentiation from mESCs using Taguchi protocol

The Hoxb7-GFP mouse ES cell line was kindly provided by Professor Ryuichi Nishinakamura's laboratory, Kumamato University, Japan. The E14 cells were kindly provided by professor John Mason's laboratory. Cells were maintained in mESC culture media, as described before.

First, cells were dissociated from the culture plates using 1 ml/well Accutase (Gibco), then re-aggregated at around 2,000 cells/well in 96-well, U-bottomed, low binding plates (Greiner 650970) and cultured for 48hrs to form embryonic bodies (EBs) in basal media consists of 75% Iscove's modified Dulbecco's medium (Gibco 12440-046) and 25% Ham's F12 (Gibco 11765-054), with 0.5 × N2 supplement (Gibco 17502-048), 0.5 × B27 (Gibco 12587-010), 0.5 × penicillin/streptomycin, 0.05% BSA (Sigma), 2 mM L-glutamine (Life Technologies), 0.5 mM ascorbic acid (Sigma), and 450μM 1-thioglycerol (Sigma). After 48h, the basal medium was replaced by a fresh media contained 10 ng/ml human Activin A (R&D 338-AC) as step number 1. After 24hrs of step 1, the medium was replaced with medium contained 0.3 ng/ml human BMP4 (R&D 314-BP) and 10 μM CHIR99021 (TOCRIS 4423) as step number 2. After 36 hrs of step 2, the medium was replaced with basal medium contained 0.1 μM retinoic acid (RA; Sigma R-2625), 100 ng/ml human FGF9 (R&D 273-F9), and 10 μM SB431542 (TOCRIS 1614) as step 3. After 24 hrs of step 3, the medium was replaced with media containing 0.1 μM RA, 100 ng/ml human FGF9, and 5 μM CHIR99021 in step 4. After 24 hrs of step 4, medium was replaced with medium contained 10μM Y27632 (Stem Cell Technologies 72302), 0.1 μM RA, 1 μM CHIR99021, 5 ng/ml human FGF9, and 10% growth factor reduced Matrigel (Corning 354230) as step 5. After 24 hrs of step 5, media replaced by fresh medium contained 0.1 μM RA, 3μM CHIR99021, 5 ng/ml human FGF9, 1ng/ml GDNF (R&D 212-GD) and 10% growth factor reduced Matrigel (Corning 354230) as step 6. After 24 hrs of step 6, media was changed with the same medium in step6 with 2ng/ml GDNF (R&D 212-

GD) and without FGF9 as step 7. After 24hrs of step 7, the cell spheroids developed abundant ES cell-derived UB-like structures, which I refer to, in this thesis, as engineered UBs (eUBs) (Fig. 2.1).

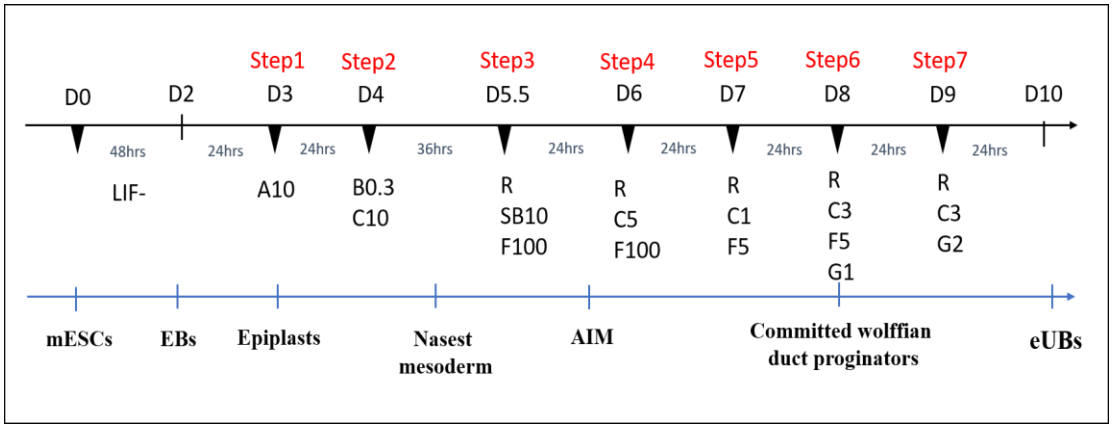

Figure 2.1 Schematic illustration of the steps of Taguchi protocol for eUB differentiation.

2.3.2 Characterization of the mESCs derived eUBs

Characterization was done by testing the ability of the engineered UBs to generate branching tree-like structures in 3D gel and by immunofluorescence analysis of several UB markers and UB tip and stalk markers (RET, Sox9 and binding of fluorescein-Dolicous Biflourus Agglutinin).

For RET staining, day 10 spheroids were fixed with 4%PFA, dissected and individual eUBs were isolated, cleaned from the surrounding Matrigel, and washed with PBS. The dissected eUBs were incubated with primary antibody solution containing 5% PSA in PBS and 1:50 anti-RET (Santa Cruz SC-167) for 2 hours at room temperature. The excess primary antibody was washed away with PBS three times, 5 minutes each. After washing, the eUBs were incubated with the secondary antibody solution containing 5% BSA in PBS and

1:100 of DAR 594 (Invitrogen 21207) for 2 hours at room temperature, and later washed 3 times/15 min each. Finally, imaging was carried out using a Zeiss epifluorescence microscope. Staining with DBA and for Sox9 was performed using the methods described later in this chapter.

2.3.3 Isolation and Culture of UBs and eUBs in 3D Matrigel

The isolated E11.5 kidneys were collected and incubated for 3-5 minutes in 1x trypsin EDTA at room temperature. To stop the enzymatic reaction, the kidneys were transferred to a new dish containing Kidney culture media (KCM; MEM, 10% FBS and 1% Penicillin/streptomycin). The metanephric mesenchyme (MM) was dissected out carefully and removed from the UBs, which were dissected to isolate single tips. The mESC-derived spheroids were collected in a 60 mm petri dish and the radiating eUB tubules were dissected one by one using fine needles. Both UBs and eUBs were suspended independently in 20% Matrigel in DMEM/F12 (Thermofisher,12634010) medium, supplemented with 10% FBS, 0.1 µM RA, 100 ng/ml human Rspondin1 (R&D 4645-RS), 1ng/ml human GDNF (R&D 212-GD), and 100 ng/ml mouse FGF1 (Pepro Tech 450-33A) in a low-binding -U bottom- 96 well plate, one per well. A serum free medium has also been used which consists of DMEM/F12, 1x N2 supplement (Gibco 17502-048), 1x B27 without vit A (Gibco 12587-010), 1mM nicotinamide (Sigma) and 1x antibiotic antimycotic (Gibco 15240-096).

2.4 eUBs Grafting into cultured kidney rudiments

Kidneys were dissected and isolated from CD1 mouse embryos at day E11.5. Kidney rudiments were cultured on 24 mm, 0.4 µm-pore membranes (Transwells, Corning 3450) , air fluid interface, in kidney culture medium (KCM) containing Minimum Eagle's Medium (MEM; Sigma M5650) enriched with 10% fetal bovine serum (FBS) and 1 % penicillin/streptomycin. The mESC-derived eUBs were manually dissected from day 10 spheroids using sharp tungsten needles, and implanted into different nephrogenic areas, the metanephric mesenchyme (Fig. 2.2), the peri-Wolffian mesenchyme (Fig. 2.3) or in between the two (Fig. 2.4). Grafting was performed to E11.5 fetal mouse kidneys in culture as mentioned above, after making a hole in the mesenchyme with the needle away from the epithelium. The grafted kidneys were cultured for 5 days for the MM grafts and 9 days for the PWM grafts in KCM, medium change was carried out every 48hrs.

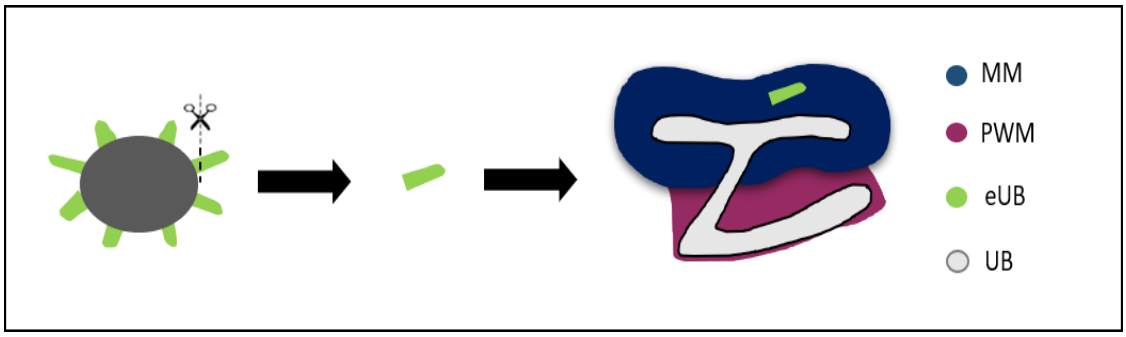

Figure 2.2 Illustration showing the steps of engineered ureteric bud (eUB) grafting into the metanephric mesenchyme (MM) of a host kidney.

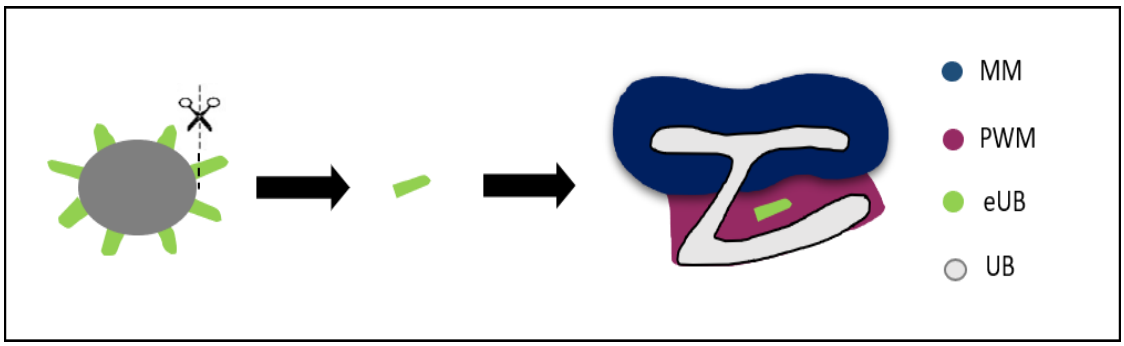

Figure 2.3 Illustration showing the steps of eUB grafting in the periwolffian mesenchyme (PWM) of a host kidney.

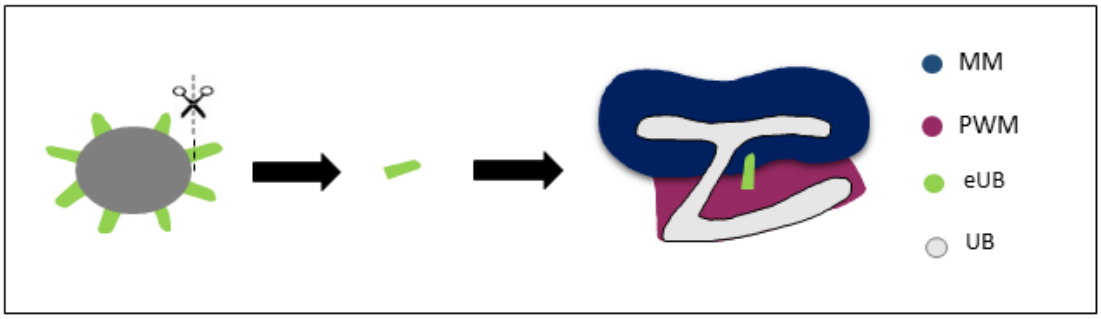

Figure 2.4 Illustration showing the steps of eUB grafting in between the MM and the PWM of a host kidney.

2.5 eUBs connection to host kidneys in culture

To test the ability of the mESC-derived eUBs to connect to either CD /or ureter of an E11.5 kidney, a single cut was made into either one branch of the 'T' inside an E11.5 host kidney in culture (Fig. 2.5), or into the shaft of the UB stalk of a fetal E11.5 kidney rudiment (Fig. 2.6), using a sharp Tungsten needles. Then an eUB (at which one end had been cut as a result of its isolation from its parent spheroids) was grafted in contact with the site of the cut in the natural collecting duct or ureteric bud stalk. Grafted kidneys were cultured in KCM on 24mm Transwell inserts, and incubated at 37°C, in 5% CO_2. For connection to older kidneys, E11.5 kidneys were cultured on

Transwells for 9 days, and E13.5 kidneys were cultured for 4 days, before grafting took place.

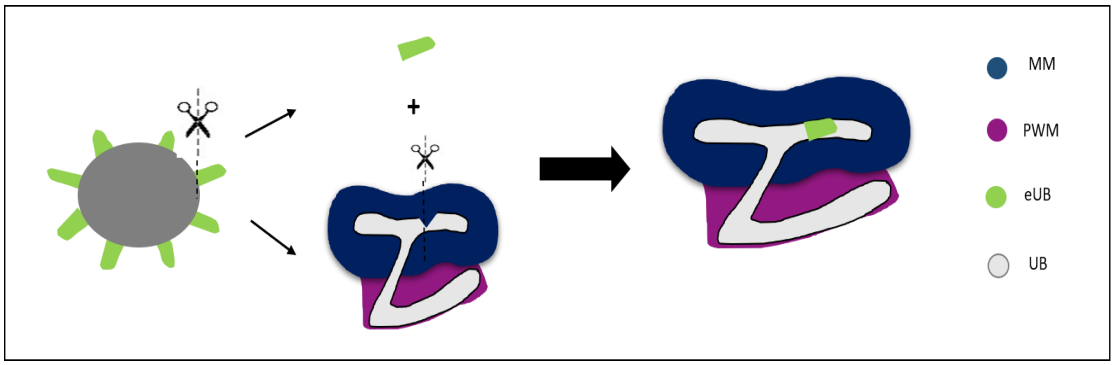

Figure 2.5 Illustration showing the steps of eUB connection to the CDs.

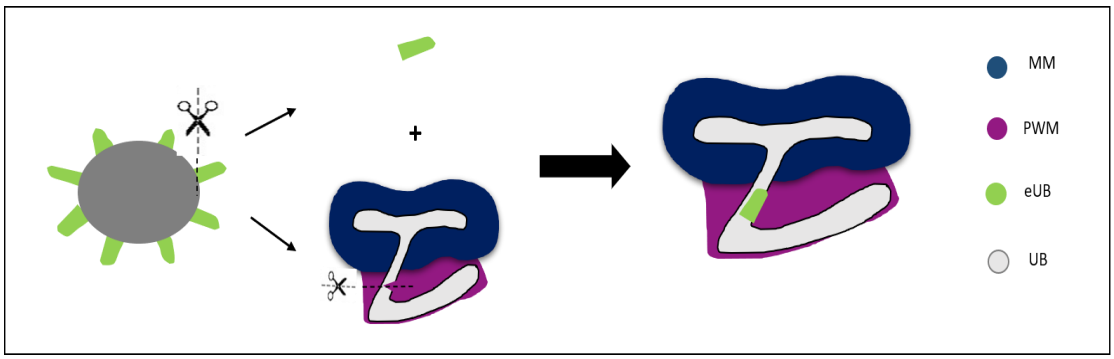

Figure 2.6 Illustration showing the steps of eUB connection to the ureter.

2.6 Combination of eUB with PWM or MM

Before mesenchymal isolation, kidneys were incubated in 1x trypsin/ EDTA (Sigma T4174), for 2 min at 37°C, then KCM was added to stop the enzymatic reaction. The peri-Wolffian mesenchyme was isolated manually using sharp Tungsten needles. The isolated mesenchyme was collected in a 500 µl Eppendorf, and cells were dispersed by gentle pipetting. Around 150,000 cells were resuspended in 150-200 µl KCM and centrifuged (3 min at 3000 g), in

order to obtain a cell pellet. Pellets were transferred to low binding-U bottom-96 well plates, one pellet/well. The eUBs were isolated from day 10 spheroids as mentioned before and transferred to the mesenchymal cell pellets 1 eUB/well and incubated at 37°C and 5% CO_2. After 24hrs, the eUB and the mesenchyme had generated a compact spheroid, which was transferred a 24 mm, 0.4 µm-pore Transwell membrane (Corning 3450) containing 1.5 ml KCM. The same described method was used to combine the isolated (MM) with eUBs, and the formed spheroids were cultured for 5 days in kidney culture media, with 50 µl KCM containing 10% Matrigel on top.

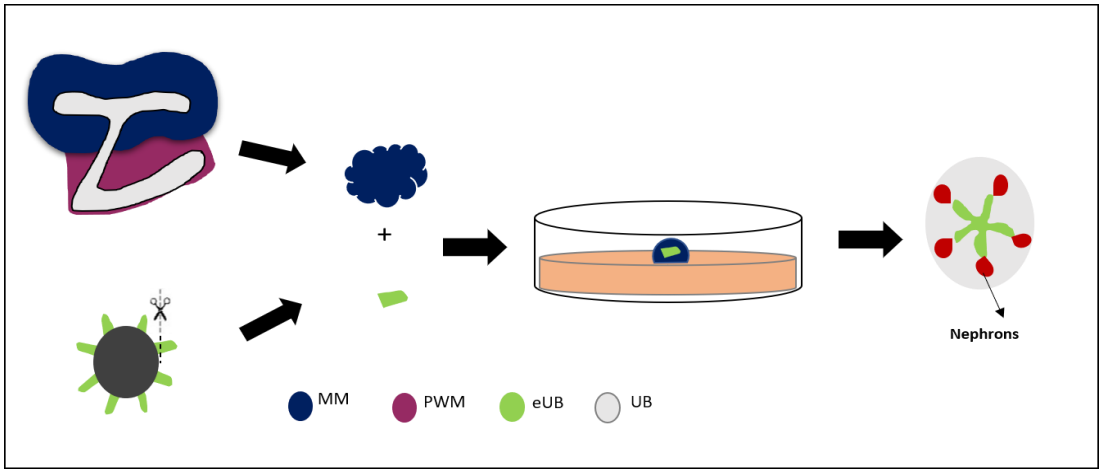

Figure 2.7 Illustration showing the steps of eUB combination with MM cells.

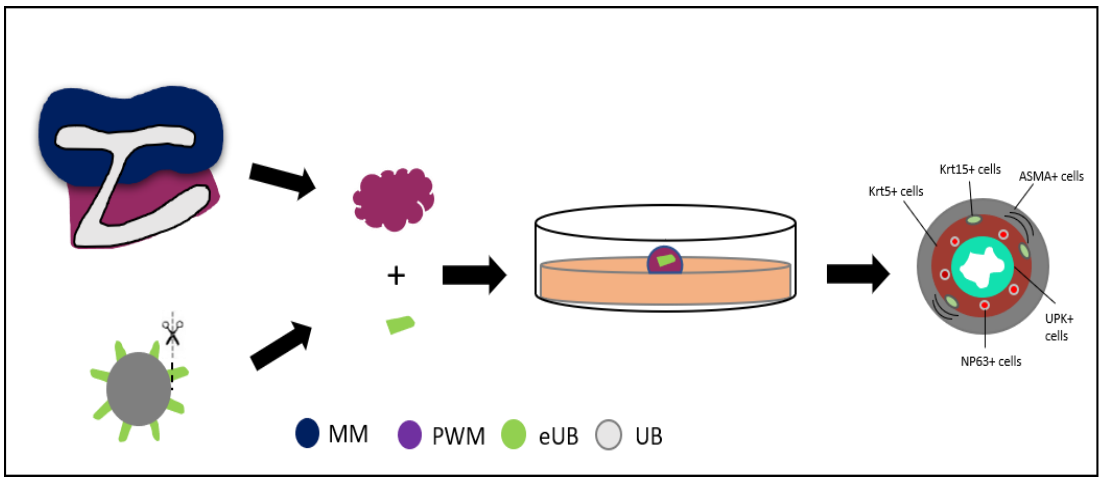

Figure 2.8 Illustration showing the steps of eUB combination with PWM cells.

2.7 Immunofluorescence

Sample fixation was performed using cold methanol which was stored in -20°C, and samples were left to warm up in room temperature for 30 mins. Then, samples were washed twice with phosphate buffer saline (PBS) and blocking was performed using a staining buffer, consisting of 5 % bovine serum albumin (BSA) in PBS, overnight at 4 °C. After blocking, samples were washed with PBS and the primary antibodies diluted in staining buffer were added to samples and left overnight at 4 °C. The excess primary antibody was washed (3 x 5 min PBS), and the secondary antibodies solutions were added to the samples and incubated for 24 hrs at 4 °C. Finally, the secondary antibodies were washed (3 x 15 min PBS), then samples were placed on a glass slide in a box drawn using a PAP pen (Z377821; Sigma) and mounted with Vectashield (H-1000; Vector Laboratories).

For PKC, NP63 and Sox9 staining, 4% PFA was used to fix the samples for 30 minutes in room temperature. Blocking and permeabilization were

performed using 5% BSA contains 0.2% Triton X-100 (sigma) for 24 hrs in 4°C. The same blocking buffer was used to prepare the primary antibody solution (Table 1).

2.8 Histological tissue sections

Sample fixation was performed as outlined before and wax-infused samples were prepared by placing the tissue in a wax processor (Sakura VIP E300), and tissue blocks were then embedded in paraffin. Using a Leica RM2245 microtome, 6 µm tissue sections were obtained. Sections were then floated in a warm water bath and mounted on + charged slides (Superfrost plus; Thermo Fisher) and left to dry in a 37 ºC oven for 24hrs. Dewaxing of the samples was carried out by placing them in xylene for 30 mins. Then they were rehydrated in gradually decreasing ethanol concentrations (100%, 90%, 70%, 5 mins each), and then put under running tap water. For antigen retrieval, samples were submerged in sodium citrate buffer (10 mM Sodium citrate, 0.05% Tween 20, pH 6.0) in a microwavable vessel and microwaved for 3 x 5 mins.

For immunofluorescence staining, slides were placed in a suitable container filled with blocking buffer (5% BSA in PBS) and placed on a rocking shaker for 1 hr. They were then left to dry by standing them on tissue paper for 2 minutes. 200 µl of the primary antibody solution (antibody in 5 % BSA in PBS) was prepared and added to the tissue on the slides. To ensure that the tissue on the slide was completely covered with the antibody, a square was drawn

around the tissue using fluid blocking PAP pen (Z377821; Sigma). Slides were placed on a suitable humified container and incubated in 4°C overnight.

The unbound primary antibody was eliminated by placing the slides in a container filled with PBS on a rocking shaker for 30 minutes, with the PBS changed three times.

The secondary antibody solution containing 5%BSA in PBS was added to the slides, 200 µl per slide. The slides were incubated in a suitable slide container overnight in 4°C. The secondary antibody was washed by submerging the slides in PBS on a rocking shaker for 30 minutes. Slides were mounted by Vectashield mounting fluid (H-1000; Vector) and coverslips (631-0142; VWR) were placed before imaging.

2.9 Imaging

Imaging was carried out using a Zeiss Axiovert epifluorescence microscope (Axiovision software), and Ziess LSM800 confocal microscope. Bright field and GFP images were taken on Leica upright dissection microscope (MSV269). Live imaging was carried out using Nikon A1R FLIM confocal microscope. Image and video preparation was performed using image j.

2.10 Statistics

For the categorical data (feature Yes/No), Calculation of 95% confidence intervals was performed using the formula $t= \pm 1.96 [\sqrt{} (p (1 - p)/n)] + 1/2n$, where t is the 95% CI, P is the positive proportion, and n is the total number of samples examined (Bremer& Doerge, 2010).

Table 1 Antibody list

Antibody	Host Species	Supplier & catalogue number	Working dilution
Alpha-smooth muscle (FITC)	Mouse	Sigma 3777	1/100
Alpha-smooth muscle actin	Goat	Novus nb300-978	1/100
Calbindin D28k	Mouse	Sigma C9848	1/100
E-cadherin	Mouse	BD biosciences 610182	1/100
GATA3	Goat	R&D AF2605	1/100
Jagged 1	Goat	R&D AF599	1/100
Krt5	Rabbit	Abcam ab24647	1/100
Krt8	Rat	DSBH repository TROMA-1 (concentrate)	1/100
Krt15	Rabbit	Abcam Ab52816	1/100
Pax2	Rabbit	Biolegend PRB-276P-200	1/100
Uroplakin	Rabbit	Gift from Tung-Tien Sun, New York University	1/500
Uroplakin III	Goat	Santa Cruz sc15180	1/100
WT1	Rabbit	Abcam ab89901	1/100

Fluoricin Dolicous Bifluorus	Conjugated	Vector FL-1031	1/50
Sox9	Rabbit	Sigma AB5535	1/100
NP63	Rat	Biolegend 699501	1/100
RET	Rabbit	Santacruz SC-167	1/50
Six2	Mouse	Santacruz Sc377193	1/100
Podocalyxin	Goat	AF1556 (R&D)	1/100
Anti-PCK zeta	Rabbit	Abcam ab59364	1/100
Anti-Rabbit 594	Donkey	Invitrogen 21207	1/100
Anti-Rabbit 488	Donkey	Invitrogen 21206	1/100
Anti-Rabbit 647	Donkey	Invitrogen A-31573	1/100
Anti-Goat 488	Donkey	Invitrogen A-11055	1/100
Anti-Goat 594	Donkey	Invitrogen A-11058	1/100
Anti-Goat 647	Donkey	Invitrogen A-21447	1/100
Anti-mouse 488	Donkey	Invitrogen 21202	1/100
Anti-mouse 594	Donkey	Invitrogen 21203	1/100

Anti-Rat 594	Chicken	Invitrogen A-21471	1/100
Anti-Rat 488	Donkey	Abcam Ab150153	1/100

Table 2 Media and reagents

LIF	Santacruz cat# sc4989
Y27632	Stem Cell Technologies cat# 72302
h-BMP4	R&D cat#314-BP-010
h-FGF9	R&D cat# 273-F9-025
SB341542	TOCRIS cat#1614
CHIR99021	Tochris cat#4423
Retinoic acid	Sigma cat#R-2625
h-GDNF	R&D cat# 212-GD-010
R-Spondin1	R&D cat# 4645-RS
mFGF 1	Peprotech cat# 450-33A-50
Activin A	R&D cat#338-AC-010
N2 supplement	Gibco cat#17502-048
B-27 without vit A (x50)	Gibco cat#12587-010
Na pyruvate-100mM	Gibco#11360-039
MEM NEAA (100x)	Gibco#11140-035
2- mercaptoethanol-50mM	Gibco#31350-010
Glutamax-100x	Gibco#35050-061
DPBS (1x)	Gibco#14190-094
MEM	Sigma# M5650

GMEM	Sigma# G5154
IMDM [+ L-glutamine, + HEPS]	Gibco#12440-046
F12 (1x) [+ L-glutamine]	Gibco#11765-054
BSA (7.5%)	Gibco# 15260-037
Advanced DMEM/F12 (1x) [+ NEAA, + Na pyruvate]	Gibco#12634-010
FBS	Cat# FCS-SA, Batch# 71133
Hyclone Serum	Fisher scientific SV30160.03
TrypLE Express	Gibco cat#12604-021

Chapter 3. Differentiation of mESCs into ureteric buds

3.1 Introduction

It is well known that the cellular component of the metanephric kidney includes three main progenitor cell types: the ureteric bud cells, the nephron progenitors and the stromal progenitors which together form the metanephric mesenchyme (Saxen and Sariola, 1987).

Recently, several research groups have published protocols aimed at differentiating stem cells into renal progenitor lineages (Taguchi et al., 2014; Takasato et al., 2015; Morizane et al., 2015). In 2015, Takasato and colleagues reported the development of multiple kidney cell types simultaneously using one protocol. They showed cells expressing UB markers and others expressing NPs, stromal and even endothelial cell markers. However, their UB cells failed to show branching or support a progenitor niche, suggesting that these cells may be functionally immature (Taguchi & Nishinakamura, 2017). Another group (Xia et al., 2013) have reported the selective induction of UB, NPs, and stromal progenitors but the UB did not

show branching or NP induction capacity. Lately, Taguchi and Nishinakamura have developed a new approach aimed at producing kidney organoids that show anatomical and physiological competence. Using advanced microarray techniques and working backwards through developmental stages to study the genetic molecular details of mouse metanephric development, they generated a detailed protocol to produce UB-like structures that resemble, to some extent, the natural UB structurally and functionally (Taguchi and Nishinakamura, 2017).

Early in development, the intermediate mesoderm undergoes anterior posterior patterning that determines the cells' fate either into UB or NPs. The UB cells differentiate from the T+ immature mesoderm, 1 day earlier than the nephron progenitors which differentiate into posterior intermediate mesoderm at E9.5 (Taguchi et al., 2014). Accordingly, Taguchi and colleagues succeeded in obtaining both UB and NPs separately, by shortening or prolongation of the epiblasts high Wnt exposure time respectively (Taguchi & Nishinakamura, 2017).

The Taguchi protocol to induce the UB from mESCs depends on the primitive streak induction, then the intermediate mesoderm using activin A, BMP4 and CHIR (Wnt agonist). As previously described, Taguchi and colleagues in 2014 found that the NP cells originate from the posterior intermediate mesoderm (PIM), while the UB cells derive from the anterior intermediate mesoderm (AIM). They suggested that the anterior intermediate mesoderm cells, the source of UB cells, differentiate from the T+ immature mesoderm earlier than the posterior intermediate mesoderm which remain in T+ immature state longer, and commit to the NP fate later in development. Based on that, shortening of the high Wnt exposure time to 1.5 days in the UB protocol instead of 2.5 days helped the anterior intermediate mesoderm specification.

The small molecule SB431542 is a selective inhibitor of the Alk4/5/7 pathway that supresses the phosphorylation of smad2. Suppression of smad2/3 using SB431542 induces the anterior intermediate mesodermal markers (Schier, 2003). Also, the addition of retinoic acid and high FGF9 helps further

specification of the anterior intermediate mesoderm and formation of committed Wolffian duct progenitors. Subsequent utilization of GDNF and the rho kinase inhibitor (Y27632) at the last three steps of the differentiation protocol help the maturation of the committed Wolffian duct progenitors to form presumptive ureteric bud-like structures (Taguchi & Nishinakamura, 2017).

In metanephric kidney development, the UB go through iterative branching in order to form the collecting duct tree. The ES cell-derived UBs resulting from the Taguchi protocol, unlike those from any other protocol, showed extensive branching abilities both in 3-dimensional gel culture and in combination with metanephric mesenchymal as well as induction of nephron differentiation. Based on that, I decided to use this protocol for the purpose of my project.

The aim of this chapter is to reproduce the Taguchi protocol to differentiate mESCs into ureteric bud-like structures. This work includes characterization of these structures by assessing their ability to form branching trees in 3D gel supplemented with branch-inducing factors. It also includes testing the expression of UB markers including markers specific for UB tips and stalks, using immunofluorescence staining. The ES cell-derived ureteric bud-like structures will be referred to, in this chapter and the following chapters, as engineered UB (eUB).

3.2 Results

3.2.1 Engineering of ureteric bud-like structures from mESCs

To reproduce the Taguchi protocol for UB differentiation, the mESCs were maintained, for a few days, on gelatine coated dishes using mESC maintenance media. After reaching 80-90% confluence, cells were dissociated and passaged using Accutase then counted, and suspended in the basal differentiation media as described in detail in chapter 2.

To start the differentiation, around 2000 cells/well were used, optimized from the Taguchi protocol (which used 1000 cells/well), for easier handling and

visibility of the EBs during media change. Cells were inserted into 96 well low-adherent U-bottom plates and incubated for 48hrs to allow cell aggregation and formation of embryoid bodies (Fig. 3.1).

The Taguchi protocol is a seven-step protocol carried out over 10 days. By 2 days from the start of the protocol, Hoxb7-GFP mESCs had formed embryoid bodies (Fig. 3.2A); these showed no Hoxb7-GFP fluorescence (Fig. 3.2B) as expected, which indicated that cells were not yet differentiated.

Step 1 of the differentiation protocol began 48 hrs after seeding the cells in the U-bottom low adherent plates by treating the embryoid bodies that had formed in the plates with Activin A for 24hrs followed by CHIR and BMP4 treatment as step 2, in order to induce primitive streak, then the intermediate mesoderm fate.

According to the Taguchi & Nishinakamura protocol, the time window for the induction of the anterior intermediate mesoderm needs to be limited strictly to 36hrs of CHIR treatment. Based on that, step 3 media containing RA, FGF9 and SB431542 were added after 36hrs-this combination was designed to suppress the Smad 2/3 pathway. After 24 hrs, cells were treated with media containing RA, FGF9 and CHIR as step 4 to help further specification of the anterior intermediate mesoderm and formation of committed Wolffian duct progenitors. After step 4, the spheroids were dissociated and FACS sorting was done to isolate the CXCr4+, C-Kit+ cell population as in the Taguchi protocol.

The cell sorting step required large number of spheroids to compensate for the cell loss that occurs in the sorting process. Avoiding this step did not affect the eUB formation at the end of the protocol (12 differentiation runs were performed, 12 spheroids each: a total 144 spheroids all showed numerous eUB projections). Subsequently, moving from step 4 to step 5 was performed directly without FACS. The last three steps of the differentiation protocol help the maturation of the committed Wolffian duct progenitors to form ureteric bud-like structures aided by the addition of Matrigel. First, a combination of RA,

FGF9, CHIR and Y27632 was used for cell treatment in step 5. After 24 hrs GDNF was added to the same combination and media was changed as step 6. Finally, a combination of RA, GDNF and CHIR was added to the cells as step 7 for 24hrs (Fig. 3.1).

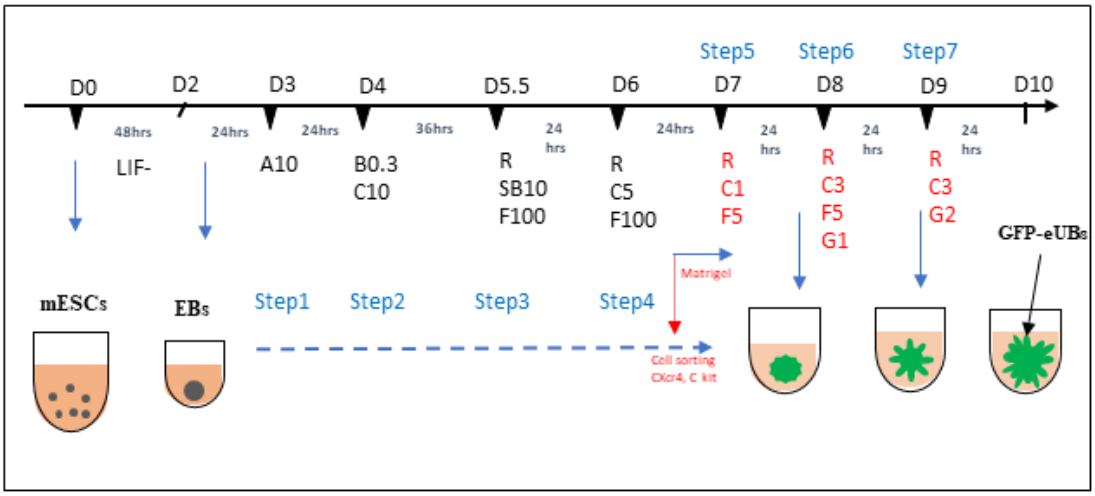

Figure 3.1 Diagrammatic illustration of the steps of eUB formation. The upper panel shows timings of the cell's treatment using the Taguchi protocol. The lower panel shows the steps of the eUB formation.

By day 10 of the protocol, the cell aggregates had developed numerous epithelial projections (Fig. 3.2C), many of which branched. These projections resembled the early ureteric bud in shape, and expressed the UB marker, Hoxb7-GFP (Fig. 3.2D) which is the first sign of successful UB differentiation. Hoxb7 is one of the Hox gene family that is strongly expressed in the kidneys and specifically in the ureteric bud and its derivatives throughout development (Brunskill et al., 2008).

To characterize these projecting epithelial structures, the expression of several immunological UB markers was assessed using immunofluorescence staining. The ES cell-derived eUBs showed positive staining for UB markers that were expressed in the natural UB, such as Cytokeratin 8, Calbindin D_{28k}, (Bouchard et al. 2002) the UB epithelial markers Pan-cytokeratin, and E-cadherin (Sakurai et al.,1997 ; Georgas et al., 2009), Pax2, a common IM marker that

can be detected in Wolffian duct progenitors (Torres et al., 1995; Brophy et al., 2001), and GATA3, which can be detected in the nephric duct and its derivatives (Grote et al., 2006), 3/3 samples were tested, suggesting successful differentiation towards the UB fate (Fig. 3.3).

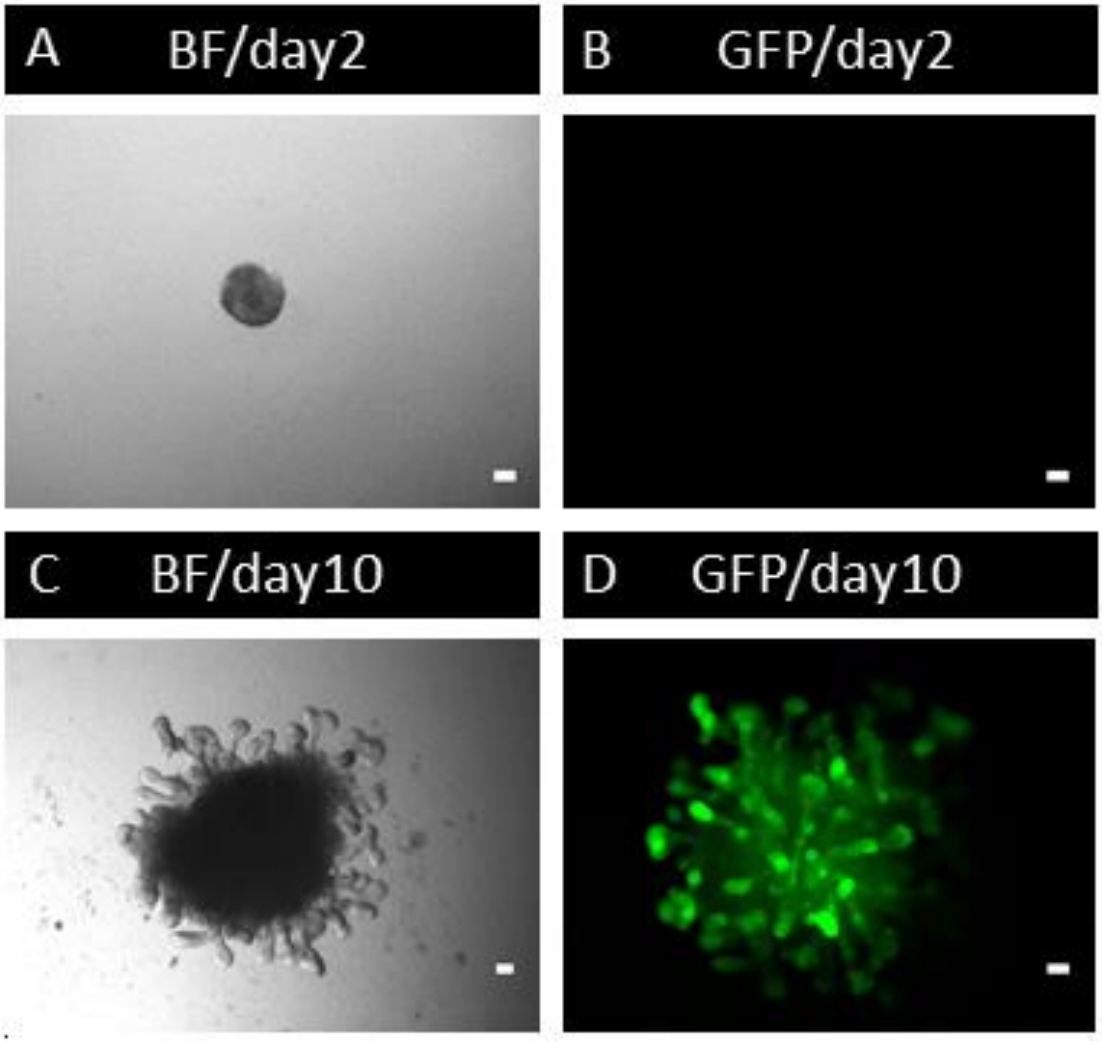

Figure 3.2 Embryoid bodies and GFP-eUBs. (A) Bright field image showing an embryoid body (EB), on day 2 of the Hoxb7-GFP mESC differentiation. (B) it expresses no GFP after 48hrs of the start of the protocol. (C) Bright field image of stem cell aggregates 10 days after induction of differentiation, showing UB-like projections, and (D) expressing the UB marker Hoxb7-GFP. Scale bar=100µm.

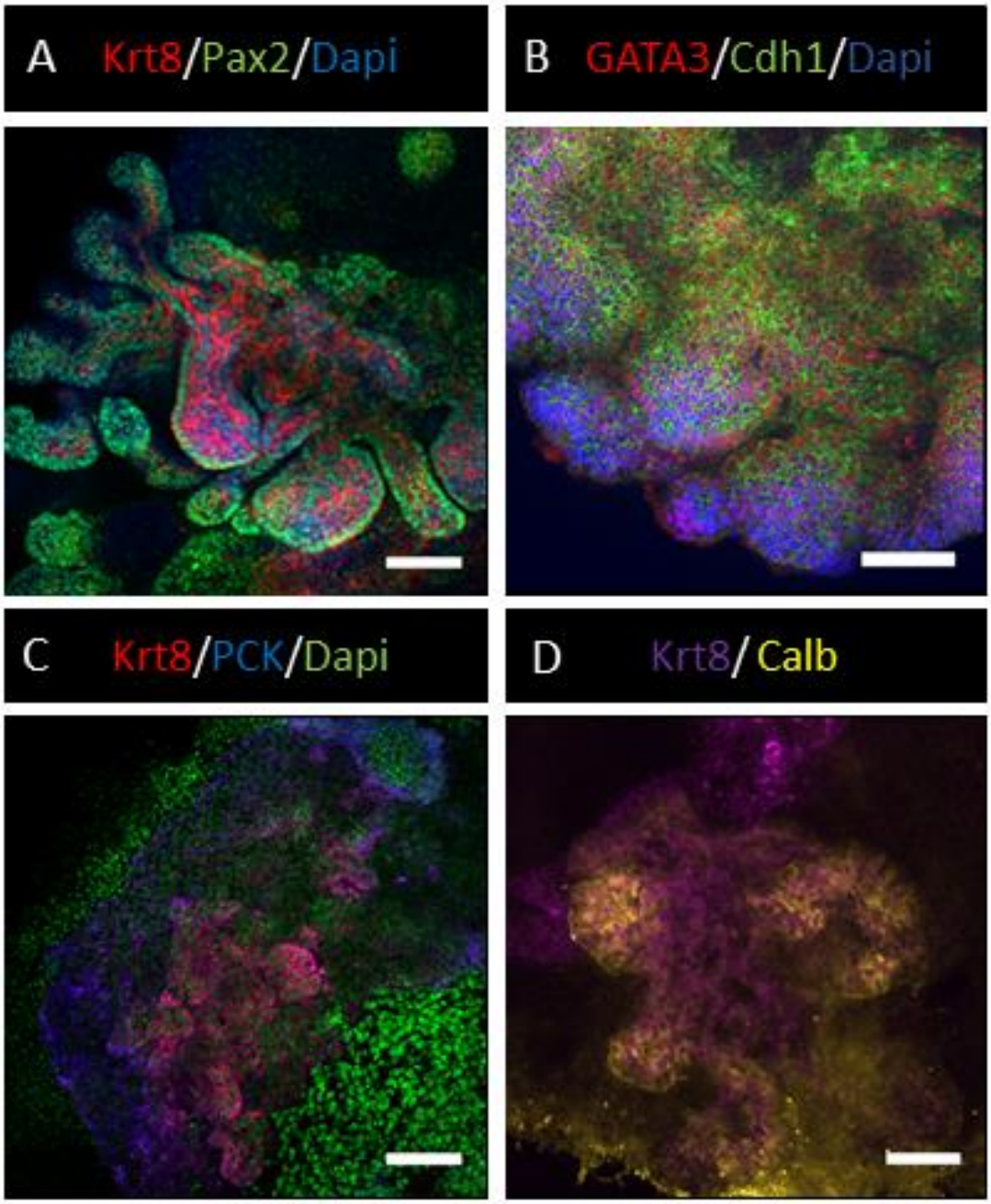

Figure 3.3 ES cell-derived eUBs express various UB markers. (A-D) Immunofluorescence images of day 10 spheroids stained for several UB markers, ES cell derived eUB structures exhibited positive staining of the UB markers: keratin 8 (Krt8), GATA3, pan-cytokeratin (PCK), E-cadherin (Cdh1), Calbindin and Pax2. Scale bar = 100μm.

3.2.2 The ES cell-derived eUBs branch in 3D gel

Branching morphogenesis is a crucial event in mammalian kidney development as well as in other organs that develop epithelial networks, such as prostate, pancreas and salivary glands. In mid-gestation mouse embryos, the UB invades the MM, and undergoes several rounds of branching, approximately 10-11 rounds to generate more than 1600 branches (Cebrian et al., 2004).

Qiao and colleagues have reported that the natural UB epithelium, which forms the collecting duct system and the upper part of the urinary tract, can undergo iterative radial branching in vitro, when cultured in appropriate 3D extracellular matrix, in absence of any mesenchymal cells (Qiao et al., 1999). This suggests that the branching property is inherent in the UB epithelium. This branching depends on the interaction between the epithelium and the surrounding environment either by the presence of mesenchymal cells or by imitating the signals derived from these cells in vitro.

The question here is, does the ES cell derived eUB have the same branching capability? To test this, Hoxb7-GFP mESCs derived eUBs were dissected from day 10 spheroids as described in detail in chapter 2. These eUBs were cultured one-by-one in three-dimensional Matrigel (Fig. 3.4A), supplemented with ramogenic factors; R-spondin, GDNF, retinoic acid and FGF1 (Taguchi and Nishinakamura, 2017). The eUBs isolated from day 10 spheroids were showing expression of UB marker Hoxb7-GFP (Fig. 3.4B).

These isolated epithelial projections (eUBs) underwent radial branching morphogenesis (3 replicates each contained 4 eUBs all showing branching; Fig. 3.4C, E, G). Their expression of Hoxb7-GFP was maintained in these branching structures after 7 days of culture in branch-inducing gel culture (Fig. 3.4D, F, H), suggesting that these eUBs retain the ureteric bud character.

Collectively, ES cell-derived eUBs showed features comparable to the natural UB including expression of UB markers as well as the branching morphogenesis capability.

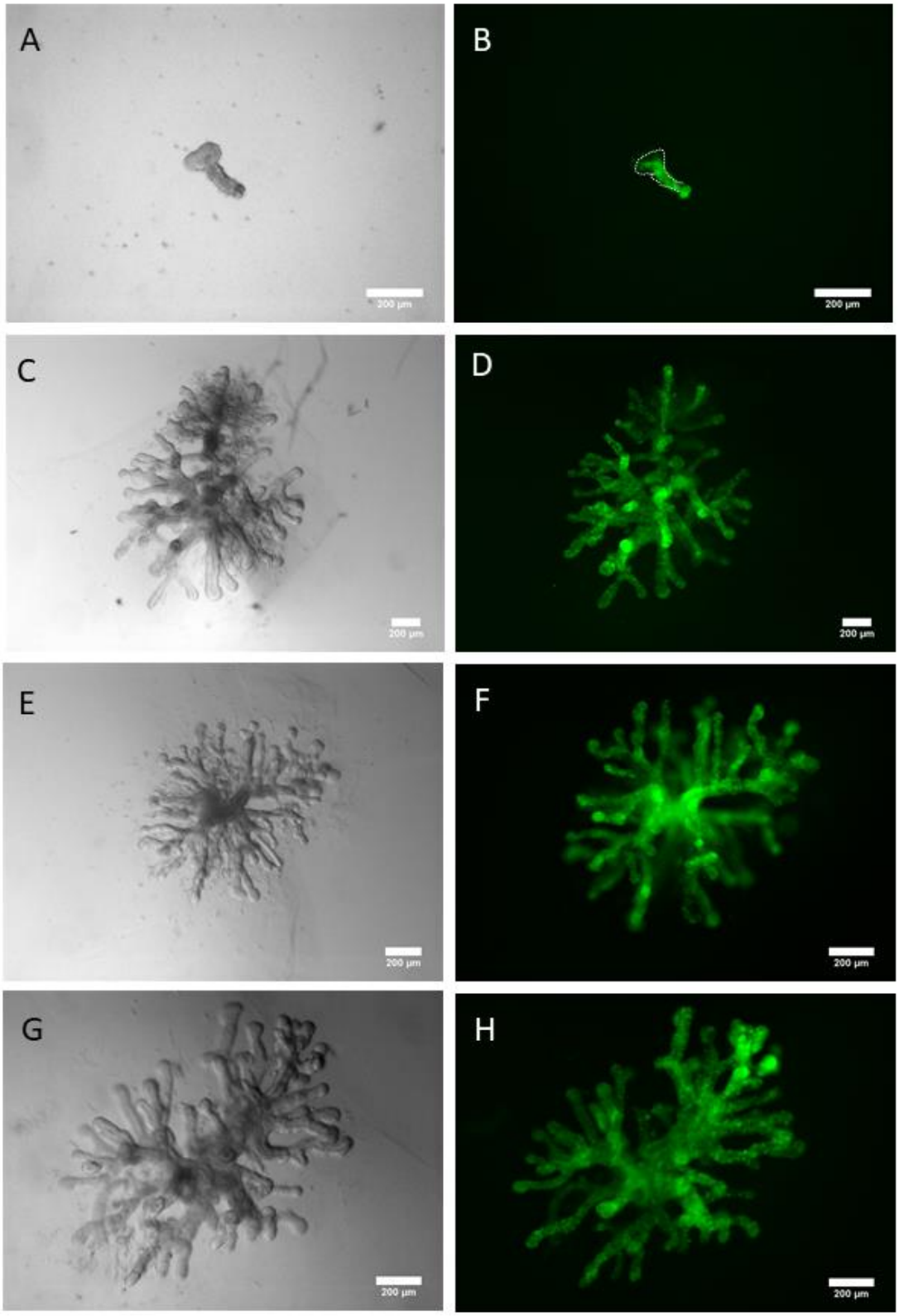

Figure 3.4 GFP-eUBs produce branching trees in 3D gel culture. (A) Bright field image of a single eUB isolated from day 10 spheroids, day 0. (B) GFP image of A showing HoxB7-GFP expression. (C, E, G) The eUB branch and form tree-like

structure after 7 days of culture in 3D gel supplemented with branching mixture. (D, F, H) Showing the corresponding C,E,G continue to express Hoxb7-GFP. Scale bar=200μm.

3.2.3 ES cell-derived eUBs express ureteric bud tip markers but not the stalk marker

It is well established that the UB epithelium is formed of two parts; tip and stalk, each of them having its specific markers. Tips are the active branching ends of the UB which lie in the MM, while the stalk is the elongated part of the UB that lies outside the MM (Kispert et al., 1996). To characterize the eUB epithelium and whether it expresses tip markers, stalk markers or both, I tested their expression.

Earlier work has shown that expression of the transcription factor Sox9 can be detected in two places in the developing mouse kidney, the UB tips and the peri-ureteric mesenchyme (Reginensi et al., 2011). Although a strong expression of Sox9 in UB tips was maintained throughout the developmental stages, only a transient expression could be detected in the mesenchyme that surrounds the distal ureteric stalk around E12.5 (Kent et al., 1996; Airik et al., 2010). Thus, I decided to use Sox9 as a marker for UB tips.

The eUBs were stained for the tip marker Sox9 and showed positive expression along the whole structure, slightly stronger at the tips by eye, in 6/6 samples were tested (100%, $CI^{95\%}$±8.3%; Fig. 3.5B, E).

Metanephric development starts with the UB that rises from the caudal part of the WD and invades the MM. The UB induces the differentiation of MM into nephrons and the MM signals back to induce UB branching and elongation. This interaction depends mainly on GDNF signalling via its receptor tyrosine kinase Ret and the co-receptor GFR-a. (Yu et al., 2004; Lechner and Dressler, 1997). Disruption of RET signalling can cause some forms of CAKUT such as multicystic kidneys, kidney hypoplasia, kidney agenesis, and faulty ureteral maturation (Enomoto et al., 2001; Schuchardt et al., 1994; Batourina et al.,

2002). Based on that, I considered using Ret as another tip marker because it is actively expressed in cells of the UB tips which interact with the GDNF signalling from the MM to induce UB branching.

The eUBs were dissected and stained for the GDNF receptor RET (5/5 samples were tested, showing positive expression,100%, $CI^{95\%}$±10%; Fig.3.6 A-C). Co expression of both Ret and sox9 along the whole length of the eUB strongly suggests the tip nature of these epithelial structures-however testing for stalk markers was necessary as the next step in the characterization.

Previous studies have showed that Dolichos Biflorus Agglutinin (DBA) is a ureteric bud marker that binds to all parts of the UB epithelium except the active branching tips that exhibit Sox9 and wnt11 expression (Michael et al., 2007). Thus, I decided to use the DBA stain to test expression of the stalk marker in eUBs.

Staining with the stalk marker Fluorescein Dolichos Biflorus Agglutinin could not be detected (0/3 samples, 0%, $CI^{95\%}$±17%), with no evidence of differentiation to stalk (Fig. 3.5 C, F). Fig. 3.5G shows a metanephric kidney rudiment which has been cultured for few days and stained at the same time with DBA as a positive stain control. The figure shows the DBA stain is exhibited by the collecting ducts indicating the effectiveness of the stain. Taken together, these experiments show the eUB to have the character of UB tips not UB stalk.

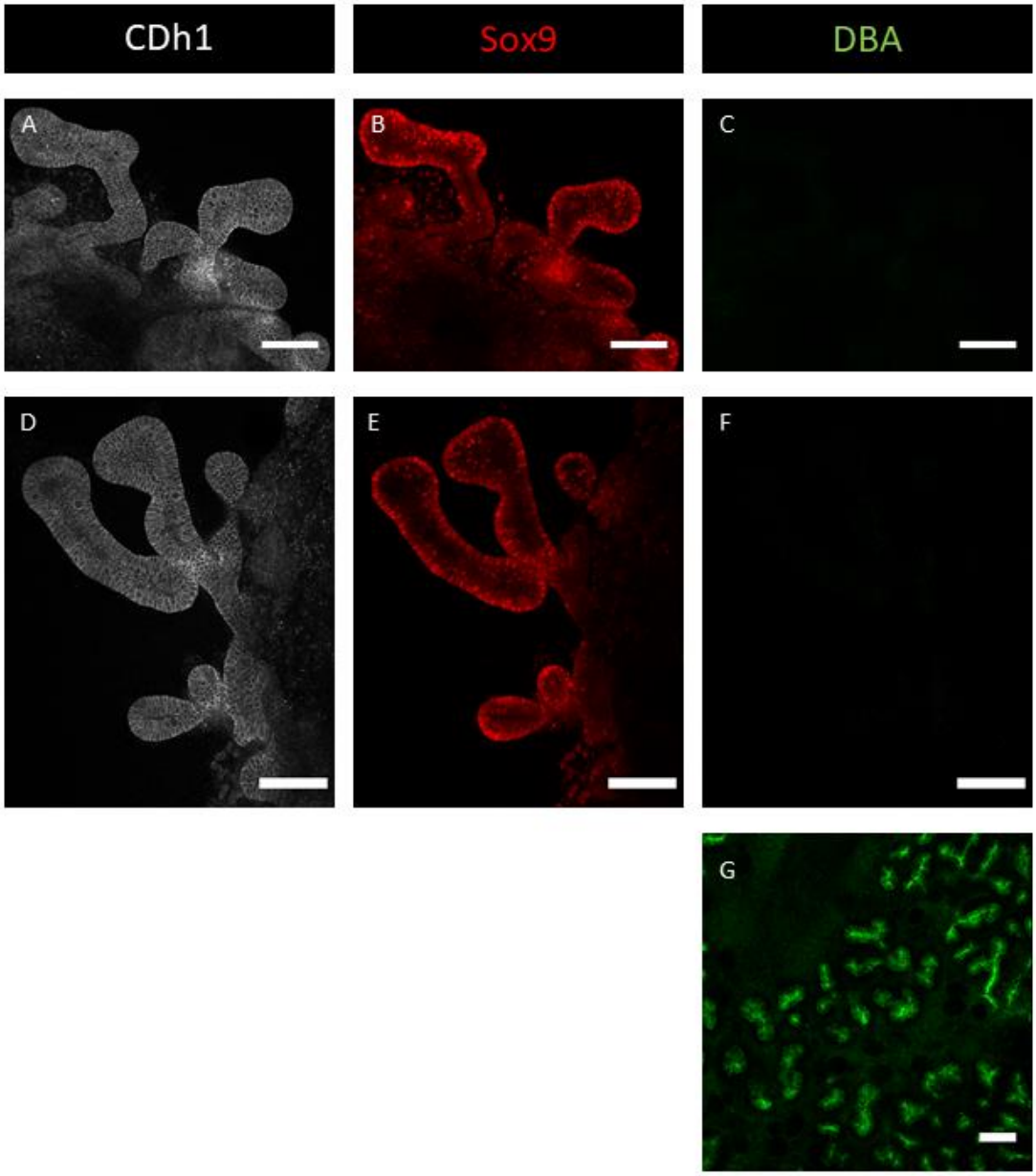

Figure 3.5 eUBs express the tip marker Sox9 but not the stalk marker DBA. (A-F) Show day 10 eUBs stained for CDH1 in (A, D), Sox9 in (B, E) and show positive expression of both markers, while binding to the stalk marker DBA in (C, F) could not be detected. (G) Is a cultured embryonic kidney stained with DBA as a positive staining control. Scale bar=100µm.

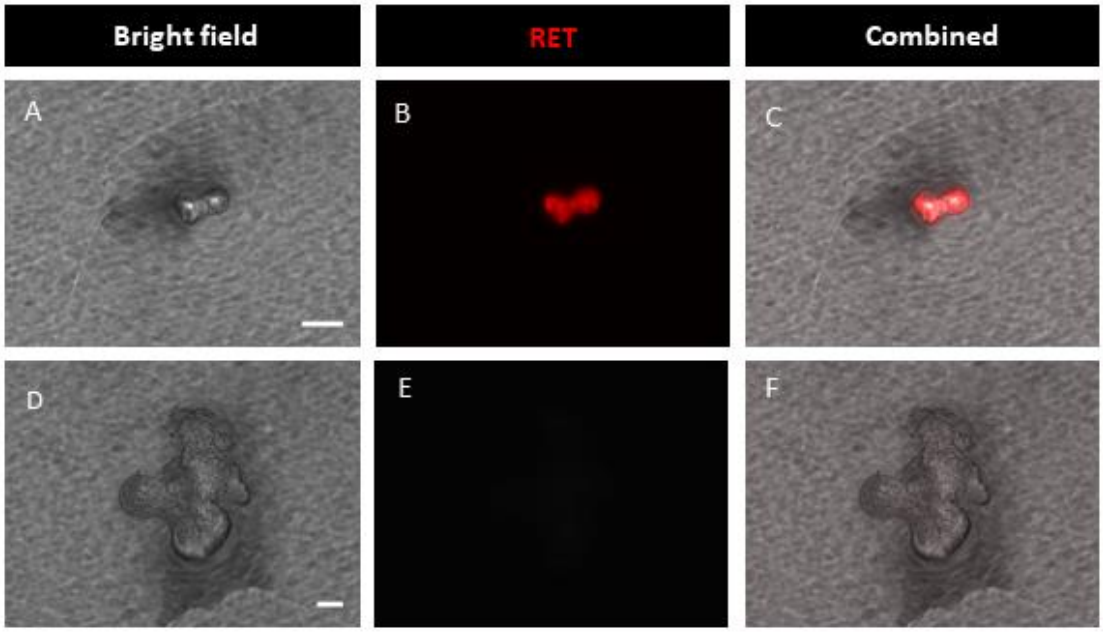

Figure 3.6 ES cell-derived eUBs express the tip marker RET. (A-C) Show bright field and immunofluorescence images of an eUB stained for the tip marker RET showing positive expression. (D-F) are the corresponding secondary-only control. Scale bar=100µm.

3.3 Discussion

The aim of this chapter was to replicate the Taguchi protocol for the differentiation of mESCs into ureteric buds, and the results match those published by Taguchi and Nishinakamura 2017, confirming that this protocol can be reproduced.

The mESC-derived UB-like structures, the eUBs, showed features comparable to those of natural UB, in the form of expression of UB markers as well as undergoing repetitive branching morphogenesis when cultured in 3D gel culture supplemented with branching media. The eUBs strongly expressed tip markers Ret and Sox9, but did not bind the stalk-specific lectin, DBA.

According to the work performed by Clifford Grobstein, it was believed that direct cell-cell contact between the epithelium and the mesenchyme is essential for branching morphogenesis in most epithelial structures. However, Qiao et al., 1999 reported the ability of the UB to branch independently and form a tree-like structure in absence of direct contact with the metanephric mesenchyme, using in vitro 3D culture system supplemented with a mixture of growth factors and conditioned media derived from an immortalized cell line of early metanephric mesenchyme cells. This has indicated that the branching property is inherent to the UB itself and depends on its interaction with the surrounding environmental signals.

Taguchi and Nishinakamura, 2017 have reported that mESC-derived eUBs have a branching capability equivalent to the natural UB, using a branching mixture that contains definitive factors with no need for cell line derived conditioned media. The mixture they used contained GDNF, R-spondin 1 (Wnt modulator), FGF1 and retinoic acid.

Studies have shown that retinoic acid signalling is essential for maintaining the expression of Ret cells at the UB tip, which is important to induce branching (Batourina et al., 2001; Mendelsohn et al., 1999). GDNF, which is expressed by the condensing metanephric mesenchyme around the UB, also plays a vital role in the process of UB branching, most likely because it stimulates the cells

that characterize the UB tip to proliferate (Costantini and Shakya, 2006). UB branching is initiated by the formation of GDNF-Ret complexes where GDNF binds to UB tips that express the tyrosine kinase receptor Ret (Schuchardt et al., 1994). Also, Canonical Wnt signalling is known to be involved in the UB branching via the β-catenin pathway (Maretto et al., 2003). Additionally, some studies have shown that adding FGFs to kidney cultures in vitro enhances the ureteric bud growth and branching (Qiao et al., 1999).

Here, I have used the same published sequence of branch-inducing factors created by Taguchi and Nishinakamura, 2017 via a modification of a previously published method (Rosines et al., 2007). Unsurprisingly, the mESC-derived eUBs showed extensive branching in 3D gel after 7 days in culture, as the mixture contains most of the factors known to induce branching in vivo. It is also noticeable that the eUB branching in 3-dimensional gel was taking a radial shape, apparently because the branch inducing gel surrounded the eUB from all directions. This resembles the branching pattern described by Rosines et al., 2007.

It has been shown in previous reports that the ability to branch is not only confined to the epithelial parts expressing tip markers, but similarly the stalk can undergo branching if cultured in an environment that recapitulates the MM signals, either by direct contact with MM or in 3D gel supplemented with branching factors (Sweeney et al., 2008; Mills et al., 2017). For that reason, further characterization of the eUBs was needed to determine the nature of their epithelium either toward tip or stalk.

Dolichos biflorus agglutinin (DBA) is a well-known collecting duct marker for developing kidneys in some mammalian species including mouse embryos (Micheal et al., 2007). It is an α-N-acetyl-galactosamine-binding lectin (Imberty et al., 1994). While DBA strongly stains the shafts of branching CDs, it does not stain the tips of these branches (Micheal et al., 2007). The tips of actively growing collecting duct branches are characterized by expression of the tip markers Sox9, Ret and Wnt11 (Kent et al., 1996; Kispert et al., 1996). The results I describe in this chapter are consistent with these previous studies.

The mESC-derived eUBs show strong expression of Sox9 and Ret transcription factors along the whole length of the structure, but there was no evidence of expression of the stalk marker DBA, which suggests that the epithelial nature of these structures is more towards the growing tips at least at this developmental time point.

Chapter 4. Engineering ureter-like structures from mESC-derived eUBs

Data presented in this chapter has been published in ***Sallam et al., 2020***

4.1 Introduction

Production of the basic type of renal organoid, from a cell suspension, began in 2010 with the formation of the first renal organoids. These organoids were made of mouse ex-fetu renogenic stem cells using disaggregation-reaggregation technique (Unbekandt & Davies, 2010).

These organoids produced foetal kidney structures that were realistic at small scales, producing numerous independent collecting duct treelets with nephrons forming nearby. However, they lacked the large-scale organization of real foetal and adult kidneys where only one collecting duct tree exists (Ganeva et al., 2011). A series of improvements to the technique, most of which consisted of ways to generate large-scale order by breaking the symmetry of the formed tissues, had improved the realism of these organoids. Steps included organizing the organoid around one central collecting duct tree (Ganeva et al., 2011) using serial reaggregations. This was done by isolating one ureteric bud-type epithelial tubule from the Unbekandt culture and recombining it with fresh MM, in order to form organoids with a single branching collecting duct. Following this, the group developed techniques to improve the maturation of these organoids to have cortex and medulla, and loop of Henle (LoH), using the Sebinger culture technique (Davies & Chang, 2014). The next problem to be tackled was construction of a ureter.

Previous studies have shown that the type of mesenchyme controls the identity of the underlying epithelium by sending signals that guide epithelial differentiation (Sweeney et al., 2008; Bohnenpoll and Kispert, 2014). The MM induces UB epithelium to branch and form collecting ducts, while the Tbx18+ peri-ureteric mesenchyme promotes urothelial differentiation (Airik et al., 2006). This indicates that each mesenchyme has its unique signalling molecules that drive epithelial differentiation towards different fates (Brenner-

Anantharam et al., 2007). One of these essential factors is BMP4, which is abundantly expressed in the peri-Wolffian mesenchyme (Miyazaki et al., 2003; Dunn et al., 1997). It has been reported that the BMP4 plays a key role in urothelial differentiation as described in detail in chapter 1. Administration of BMP4 to cultured kidneys causes reduced branching and induces the collecting duct to express the urothelial specific marker UPK, which indicates the role of BMP4 in reprogramming the CD epithelium towards urothelium (Bohnenpoll and Kispert, 2014). Based on that, Mills and colleagues in 2017 reported that the local application of BMP4, using BMP4-loaded beads, to one side of the early branched collecting ducts in the Ganeva organoid promotes the duct to elongate, stop branching and to express UPK, which indicates its urothelial differentiation. This broke the symmetry of these organoids and gave them a morphology more like that of the normal kidneys, with one branched collecting duct tree connected to a single urothelial exit tube. Nephrons in these organoids showed some physiological functions (Lawrence et al., 2015). They could also acquire vasculature when implanted in the subcapsular area of adult rat hosts (Xinaris et al., 2012).

All the work described above was done using renogenic stem cells obtained from mid-term mouse foetuses and was therefore rather far removed from any human application.

In parallel, however, several research groups were publishing protocols to allow the production of renal organoids utilizing mouse and human ES and iPS cells (Taguchi et al., 2014; Takasato et al., 2015; Morizane et al., 2015;). These organoids have tissues that are realistic models for immature kidneys, and they can connect with host blood systems when implanted under the renal capsule of adult mice (Van de berg et al., 2018). Similar to the 2010 ex-fetu mouse organoids described earlier, these ES cell-derived organoids lacked high-order anatomical organization.

In 2017, Taguchi and Nishinakamura partly addressed this issue by generating an anatomically structured organoid derived in part from stem cells (ureteric bud and nephron progenitor cells) and in part from ex-fetu mouse kidneys

(stromal progenitor cells). The organization was comparable to that described by Ganeva in 2011, in that it was organized around one collecting duct tree, but without a pelvis or ureter to conduct urine away. Clearly, a ureter is required if engineered kidney rudiments are to be useful clinically.

This chapter focuses on addressing the question of how to generate a ureter, using the Taguchi and Nishinakamura, (2017) differentiation method along with kidney culture and grafting techniques used by Mills et al., 2017. Engineered ureteric buds (eUBs) were combined with different fetal mesenchymes with or without host kidney to examine their plasticity. This allowed the generation of ureter-like structures that mimic the micro-anatomy of the fetal ureter by forming multiple epithelial cell layers and a smooth muscle cell layer capable of producing spontaneous contractions. These results might be a step forward toward improving the current organoid model by adding the ureter.

4.2 Results

4.2.1 eUBs can differentiate into collecting duct-like epithelia when transplanted into the MM of a host kidney

Building on previous work (Sweeney et al., 2008; Michos et al., 2007; Bohnenpoll et al., 2013), Mills and colleagues reported that the fate of natural UBs, to produce either collecting duct epithelium or ureter epithelium, is controlled by the mesenchymal cells that surrounds it. This was demonstrated by grafting natural ureteric bud into different sites of ex-fetu nephrogenic regions in organ culture; these explanted ‘nephrogenic regions’ consisted of the metanephros, its own ureter, a length of the Wolffian duct and the peri-Wolffian mesenchyme that surrounded it. When engrafted in the metanephric mesenchyme of the metanephric part of a ‘nephrogenic region’, a natural ureteric bud grew and branched in a manner similar to a natural collecting duct tree, as previously shown by Sweeney and colleagues. When engrafted in the

peri-Wolffian mesenchyme, a natural ureteric bud became a non-branching duct that expressed the ureteric marker, Uroplakin (UPK) (Mills et al., 2017).

I aimed to test the hypothesis that ES cell-derived eUBs demonstrate the same capacity, using grafting experiments. Before grafting could be attempted, it was necessary to find a GFP reporting cell line to allow the graft and host cells to be distinguished and to allow any morphological changes to be observed, after some time in culture.

In 1999, Srinivas and colleagues generated a strain of transgenic mice that expresses GFP under control of the Hoxb7 promoter in their ureteric buds to facilitate the visualization of living kidneys in culture. Hoxb7 is one of 13 Hox genes that can be detected in the ureteric bud-its expression is confined to the UB and its derivatives throughout the developmental stages (Brunskill et al., 2008). The fluorescent protein is expressed in all the ureteric bud branches during development, and later in adult kidney epithelium.

The Hoxb7-GFP mESCs line was generated using the blastocyst stage of Hoxb7-GFP mice embryos (Taguchi & Nishinakamura, 2017). Cells were obtained from Professor Nishinakamura's lab and were thawed and cultured according to the methods described in (Taguchi & Nishinakamura, 2017).

The Hoxb7-GFP eUBs were dissected from day 10 spheroids of the differentiation protocol as described in detail in chapter 2. Day 10 spiky spheroids were transferred from the U-bottom plates to a petri-dish where the eUBs were dissected manually using sharp needles. E11.5 embryos were dissected, and kidneys were extracted and incubated in KCM for 30 min in 37° C and 5% CO_2 to allow them to recover, as embryos were preserved in cold PBS buffer. The Wolffian duct was not removed, to preserve the area of peri-Wolffian mesenchyme for grafting.

The GFP-eUBs were then grafted into the metanephric mesenchyme of fetal kidney in organ culture. This was done using the grafting technique described in Mills et al., 2017, but by grafting eUBs instead of UBs, as shown in Fig. 4.1A.

After grafting, the location of the eUB graft within the host kidney mesenchyme was detected by GFP-fluorescence using a Leica inverted microscope and morphological changes were visualized and imaged after 5 days of culture using the same method.

The eUBs that were implanted in the metanephric mesenchyme (Fig. 4.1B) grew and branched to produce structures that were typical of the immature collecting ducts (Fig. 4.1C). These structures maintained the expression of the UB marker Hoxb7-GFP and induced a nephrogenic response in the host MM after 5 days in culture (10/10 samples branched, 100%, CI95% ± 5%).

The branched eUBs as well as the host kidney collecting duct expressed the epithelial marker Krt8 and their tips became surrounded by Six2-positive cells, typical of cap mesenchyme (Georgas et al., 2009) that surrounds tips of natural growing collecting duct in embryonic kidneys (3/3 samples tested 100%, CI95% ± 17%; Fig. 4.1D'). Early-stage nephrons, expressing the markers WT1 and Jagged 1, formed near the grafted eUBs (8/8 samples tested 100%, CI95% ± 6%; Fig4. 2B, B'). Eventually, they connected to them as shown in (Fig. 4.2D) where staining with the apical marker PKC shows that the lumen of the graft is continuous with the surrounding nephrons.

In most examples of these grafts into metanephric mesenchyme, there was no evidence of expression of the ureter marker UPK in the graft (Fig. 4.1D, D''), although the host ureter did express it, so acted as a positive staining control for the immunofluorescence. One out of six grafts examined did show weak UPK expression, but this was in a disfigured kidney with no ureter and apparently had a disorganized mesenchyme (Fig. 4.3 A, B). Across the experiments, UPK expression rate was 17% ($CI_{95\%}$ ± 39%).

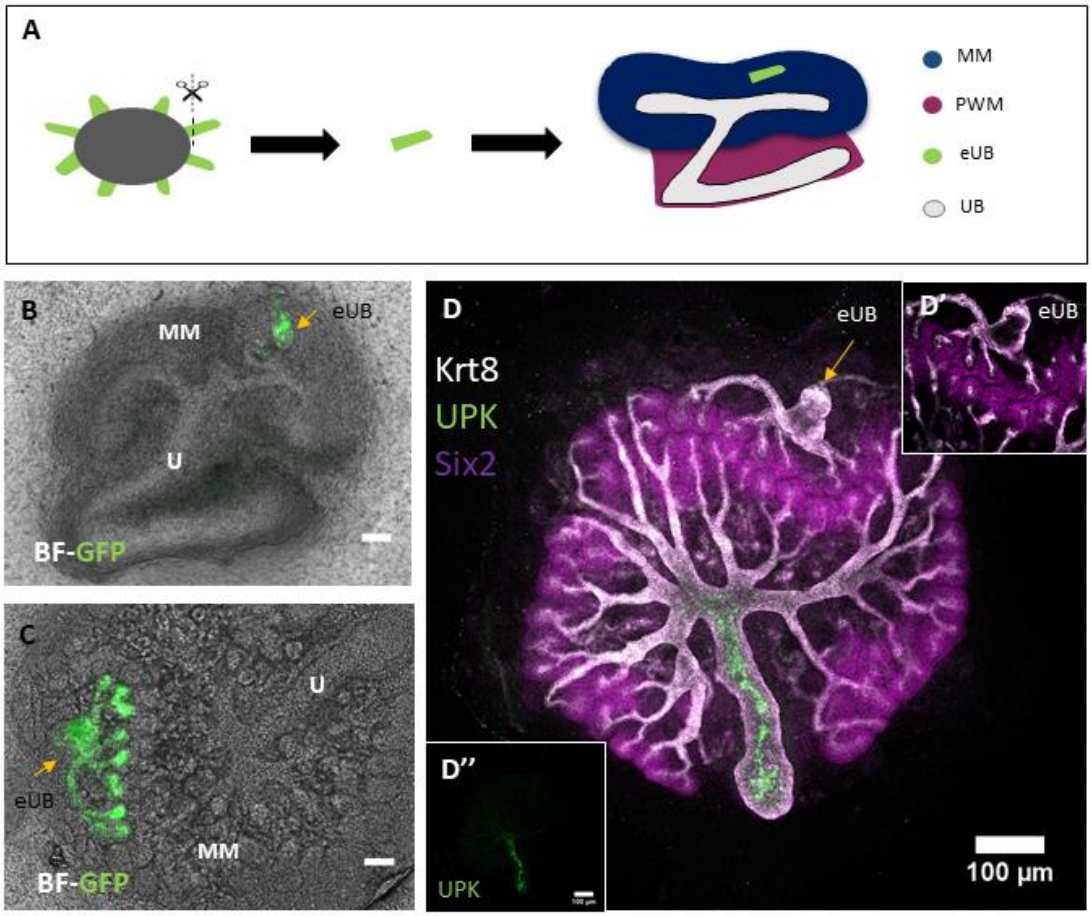

Figure 4.1 eUBs branched and induced nephrogenesis in MM of host kidneys in culture. (A) Illustration shows eUB grafting in MM. (B) Bright-field image with GFP channel showing GFP-eUB grafted into the host kidney MM at (B) day 0 of grafting, and (C) after culture for 5 days. (D) Immunofluorescence stain of C, shows the eUB placed in the MM, marked with an arrow (the image is rotated 90º because it was captured on a different microscope); (D') magnified image of D showing nephron progenitor cells expressing SIX2+ surround the eUB tips, as those of the host UB branches. (D'') separate UPK channel of D, shows the expression of UPK in the host ureter but no expression in the eUB graft. (eUB; engineered UB, U; natural ureter, MM; metanephric mesenchyme,). Scale bar=100µm.

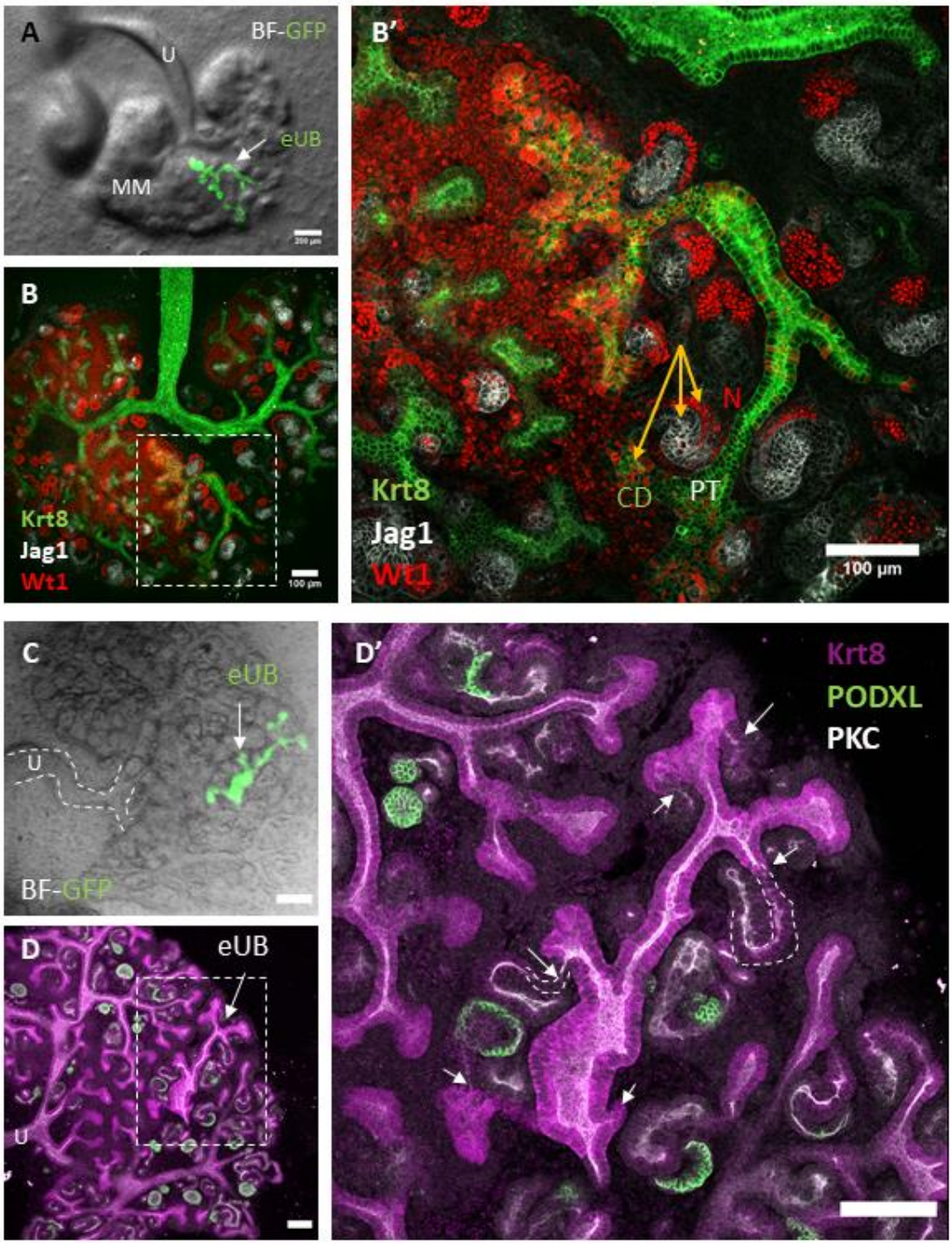

Figure 4.2 eUBs induced differentiation of MM into nephrons and connected to them. (A) Bright-field image with GFP channel indicating the location of the grafted GFP-eUB in the host MM (arrow). (B) Immunofluorescence image of A showing the grafted eUB, expressing the epithelial marker Krt8, branched and induced WT1+, Jag1+ expressing immature nephrons. (B') A high magnification of the area marked with a box in B (C) Bright field image with GFP channel showing another eUB placed in the MM. (D) Immunofluorescence stain of C.(D') Magnification of the boxed area in D, showing the eUB stained for krt8 and the luminal marker PKC connected

(arrows) to the surrounding nephrons expressing the nephron marker PODXL. CD; collecting duct, PT; proximal tubules. N; Nephrons. Scale bar 100µm.

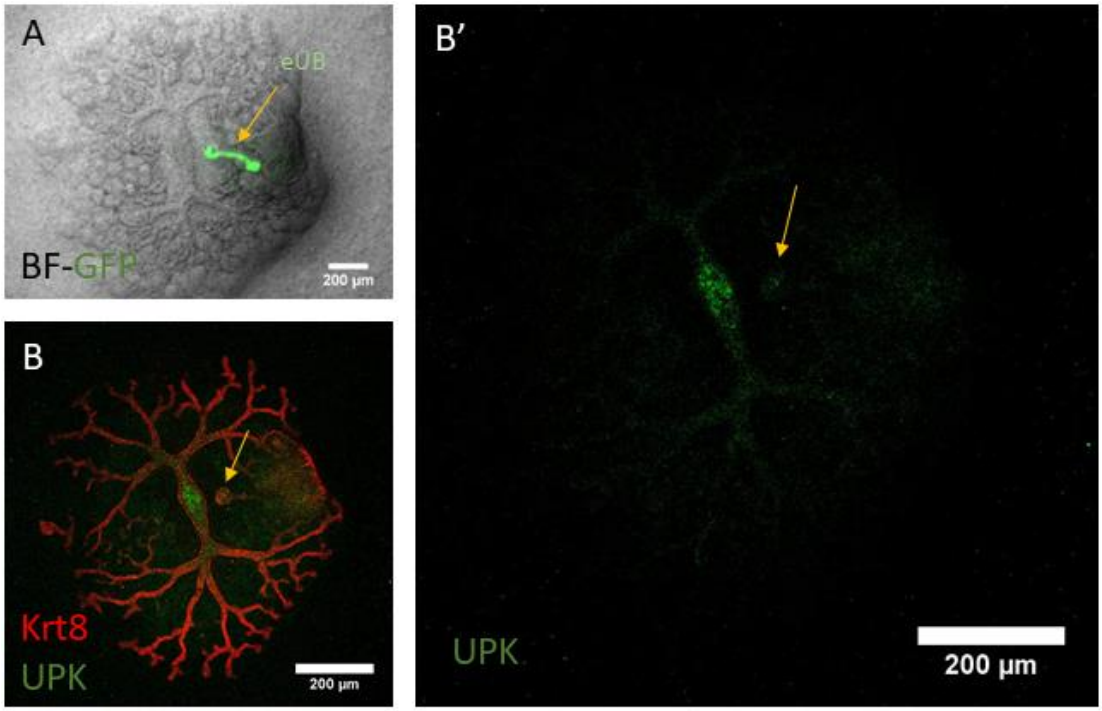

Figure 4.3. One out of six eUB grafts expressed week UPK in a deformed kidney with no ureter. (A) Bright-field image with GFP channel showing the location of grafted GFP-eUB (arrow). (B) Immunofluorescence image of A showing the eUB graft expressing week UPK (arrow), and UPK expression in a nearby duct of an odd-shaped kidney with no ureter. (B') Individual UPK channel for clarity, arrow points to the graft.

4.2.2 eUBs combined with isolated metanephric mesenchyme

Combining eUBs with pure metanephric mesenchyme that had been isolated from E11.5 kidneys is illustrated in Fig. 4.4A. In an old study of self-organization properties of kidney tissues, Clifford Grobstein isolated the tips of UBs from E11.5 kidneys where all the surrounding mesenchyme was removed. Further, he recombined these bare UBs with freshly isolated metanephric mesenchyme. The UB tips branched to form tree-like structures, and induced nephron differentiation (Grobstein et al.,1953). This suggested that these mesenchymal cells were able to organize themselves and interact with the UB after dissociation.

In the previous section, I showed that the mESC-derived eUBs were able to differentiate into collecting ducts that showed branching and encouraged nephron differentiation, when grafted into the MM of host kidney. In this respect, they were similar to the natural UB. Is the MM mesenchyme alone sufficient to induce eUBs differentiation into CDs, or are other paracrine signals from the host kidney also required? To test this, I set some recombination cultures where the eUBs combined with MM in absence of a host kidney.

The combination of eUBs and MM cells resulted in eUBs branching and apparently induced nephrogenic response while maintaining a Hoxb7-GFP expression (Fig. 4.4B). Immunofluorescence analysis of these combination tissues showed that the branching collecting duct-like structures expressed the epithelial marker Krt8 and induced the differentiation of nephron progenitors within the mesenchyme into maturing nephrons expressing the podocyte marker WT1 (Georgas et al., 2009) and the proximal tubular marker Jag1 (Fig. 4.4C); this was seen in 3/3 examples tested (100%, CI95% ± 17%). This indicated that eUBs were capable of interacting with the metanephric mesenchyme to form branching trees and induce nephron differentiation in absence of a host kidney, comparable to the natural ureteric bud in the Grobstein model.

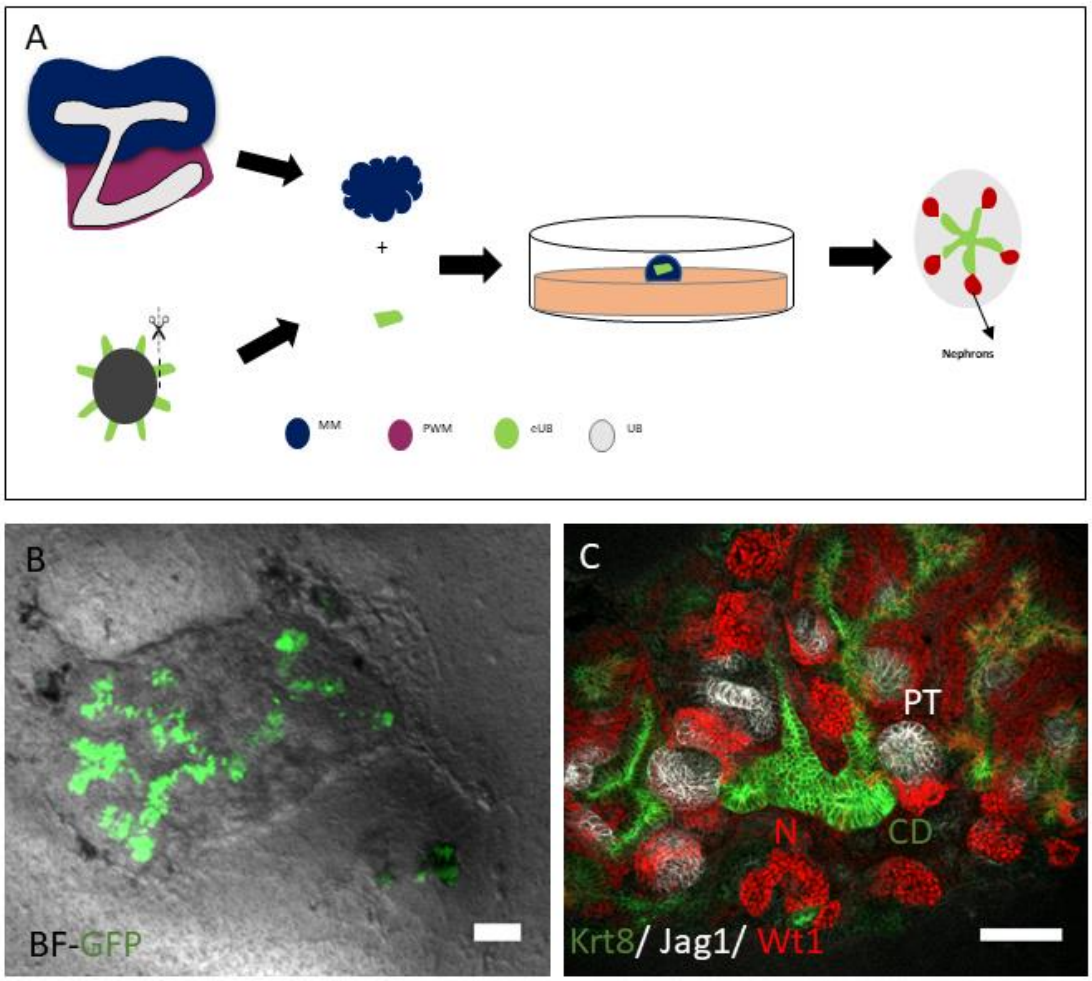

Figure 4.4 eUBs branched and induced nephrons when combined with isolated MM. (A) Illustration shows the process of eUB combination with MM cells. (B) Bright-field image with GFP channel showing the combination tissue of eUB with MM, the GFP-eUB is showing branching and apparent nephrogenic reaction. (C) Immunofluorescence stain of B shows the branching of eUB epithelium marked by the expression of Krt8, and condensation of nephrons marked with the expression WT1+ and Jag1+ cells that surround and connect to the eUB branches. Scale bar =100µm.

4.2.3 eUBs differentiate into urothelium when transplanted into the PWM of a host kidney

Metanephric kidney formation starts at E10, with the emergence of the UB from the caudal part of the WD. The UB is the main origin of both CDs and ureter. At E11, the proximal part of the UB extends into the MM and mutual interaction occurs between the two (see chapter1 for details) which results in formation of the CD tree with nephrons (Schedl et al., 2007). The part that remains outside the MM (the presumptive ureter) becomes surrounded by specialized TBx18+ mesenchymal cells. The interaction between the two results in the formation of a specialized multilayer urothelium surrounded by a functioning smooth muscle layer (Trowe et al., 2012).

As described in the previous section, the GFP-eUBs differentiate into collecting duct-like structures when combined with MM with or without a host kidney. Those eUB-derived collecting ducts are comparable with other components of the natural CDs in forming branching trees that connect to nephrons. What will happen if these eUBs were grafted into PWM instead? Will they differentiate into urothelium? To investigate this, I set some grafting cultures where eUBs were isolated from day 10 spheroids and grafted into the peri-Wolffian mesenchyme of host E11.5 kidneys.

When the eUBs were grafted in the peri-Wolffian mesenchyme of a host kidney (Fig. 4.5 A, B), they did not show branching or nephron induction (Fig. 4.5C). Instead, they showed robust UPK expression, a characteristic urothelial marker (Fig. 4.5 D, D') in 12/12 examples tested (100%; $CI_{95\%}$ ± 4%). In addition to expressing UPK, eUBs implanted into the peri-Wolffian mesenchyme acquired a layer of smooth muscle cells, which could be visualized using an antibody against smooth muscle actin (Fig. 4.5D). This suggests that the fate of the ES cell-derived eUBs is highly influenced by the surrounding mesenchyme like the natural ureteric bud.

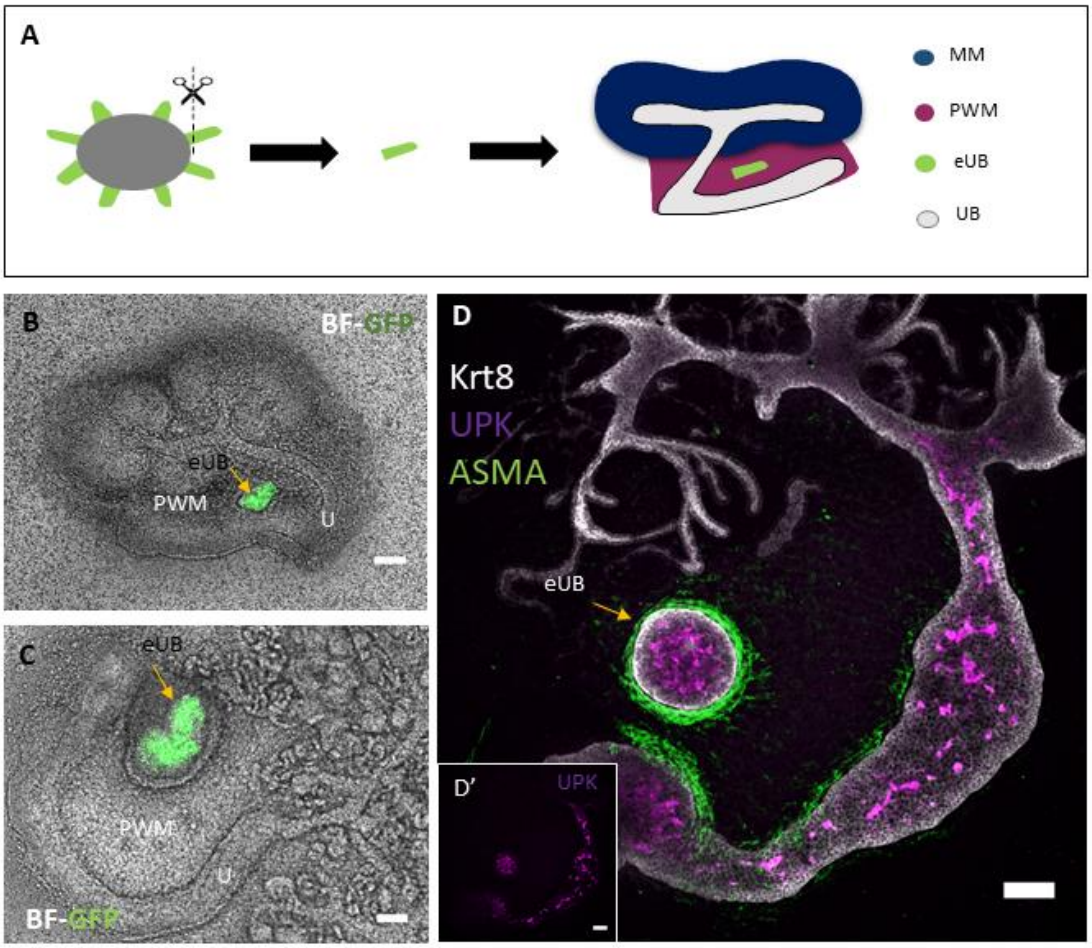

Figure 4.5 Formation of ureter-like structures when eUBs were grafted into the PWM of a host kidney. (A) Illustration shows the grafting steps (B) Bright-field image with GFP channel indicating the location of the implanted GFP-eUB in the host PWM, just after grafting, and (C) on day 7 of culture. (D) Immunofluorescence image of the implanted eUB expressing the urothelial marker UPK, and the epithelial marker KRT8, and surrounded by a layer expressing smooth-muscle actin (ASMA) (D') an individual UPK channel, shows the expression of UPK in both the graft and the host ureter. PWM; Peri-Wolffian mesenchyme, U; ureter. Scale bar =100µm.

4.2.4 eUBs grafted into the PWM show contractile activity

The smooth muscle coat enveloping the ureter and the renal pelvis is responsible for peristaltic contractions which are unidirectional contractions initiated at the renal pelvis, and propagate downwards (Gosling, 1970). The function of these peristaltic waves is to move urine from the kidney to the urinary bladder. The smooth muscle coat of the ureter consists of inner stroma, muscle layer and outer adventitia which contains blood vessels and nerves (Hicks, 1965).

It is known that the in vitro-cultured ureters develop peristaltic contractions after 7 days in culture (Caubit et al., 2008). As I showed in the previous section, eUBs grafted in the PWM develop a layer of smooth muscle cells that surrounds the graft and can be detected by staining for SMA. Are these structures able to develop contractile activity similar to the natural ureter? To assess that, these grafted eUBs were observed for 7 days in culture using a Leica inverted microscope and videos were recorded using a confocal microscope.

After 7 days of culture, eUBs grafted in the PWM of E11.5 kidney rudiments had formed ureter-like structures that started to display spontaneous contractions. These contractions increased in frequency and amplitude with more time in culture (particularly on day 9)- samples were filmed under time-lapse (3/3 examples examined; 100%, CI95% ± 17%; video 4.1). To analyse the relation between the graft contractions and those of the host ureter, the recorded videos were thoroughly examined and the times of the minimal diameter (contraction peaks) of both the host and the graft were separately recorded.

Fig. 4.6 shows the times of each individual contraction. In the host kidney ureter, the average period of contraction in eight intervals between nine contractions in the recorded video was 12s (SEM 0.8s). While the average period of the graft in seven intervals between eight contractions was 15s (SEM 0.6) which is a little slower. No evident relationship could be detected between

the timings as the contraction of the graft sometimes preceded and sometimes followed the contraction of the host kidney ureter. Analysis was performed by Prof. Jamie Davies.

No peristaltic movements were seen in the eUBs grafted into the metanephric mesenchyme, while the host ureteric contractions were clearly observed and worked as a positive control (0/3 samples tested and recorded using time lapse,0%, $CI^{95\%} \pm 17\%$, video 4.2).

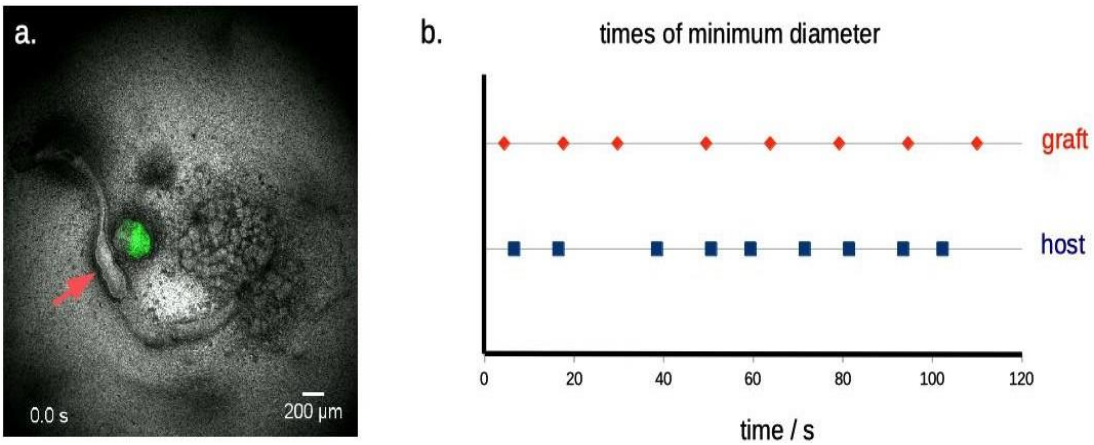

Figure 4.6 Contractions of the grafted eUB vs the natural ureter. (A) shows a starting frame of the video recording (video 4.1); the graft is detectable by the GFP fluorescence in its ES-derived urothelial tissues, and the arrow indicates the place at which contractions in the nearby natural ureter were timed (they passed this point as waves from kidney to distal ureter). (B) shows the timings at which contractions occurred, illustrated as dots on the same time scale. Timings for the host were 6.6, 16.5, 38.5, 50.6, 59.4, 71.5, 81.4, 93.5 and 102.3s, and for the graft, 4.4, 17.6, 29.7, 49.5, 63.8, 79.2, 94.6 and 110s**. *(Analysis performed by Prof. Jamie Davies for a jointly authored paper).***

4.2.5 eUBs combined with PWM cells in the absence of kidney

In ureteric development, studies have reported reciprocal communications between the epithelium of the ureteric stalk and the adjoining mesenchyme (reviewed in Woolf and Davies, 2013). The ureteric epithelium expresses SHH, which is essential for the expression of the BMP4 signalling from the PWM mesenchyme (Bohnenpoll et al., 2017). The mesenchyme expression of BMP4 induces urothelial differentiation (Jenkins and Woolf, 2007), as well as its own differentiation into smooth muscle with the aid of epithelial signals (Wang and Olson, 2004; Caubit et al., 2008). It is also reported that this urothelium to mesenchymal interaction includes expression of Wnt7B and/or WNT9B, beta catenin-mediated Wnt signalling molecules, from the stalk epithelium (Trowe et al., 2012). Additionally, it is reported that retinoic acid signalling is essential for the balanced differentiation of both urothelium and smooth muscles .(Bohnenpoll et al., 2017).

The results of the grafting experiments described above showed that eUBs can differentiate into contractile, UPK-expressing ureter-like structure when cultured in the environment of the peri-Wolffian mesenchyme. The experiments did not make clear, though, whether the peri-Wolffian mesenchyme alone was sufficient to induce this, or whether influences from the nearby kidney were also necessary. To test this, I combined ES cell-derived eUBs with isolated fetal peri-Wolffian mesenchyme, with no other tissues.

The ureter is made up of two main components: a multilayer urothelium and a smooth muscle coat. Its function is to transfer urine, which contains potentially harmful products, therefore the luminal side of the ureter is adapted to this by a specialized water-resistant layer expressing the UPK protein, which is characteristic for urothelial cells (Yu et al., 1994; Wu et al., 1990) (see chapter 1 for details). When eUBs were dissected and recombined with isolated peri-Wolffian mesenchyme cells from mouse embryos as showed in Fig. 4.7A, the eUBs remained unbranched and maintained GFP expression, driven by the

Hoxb7 promoter (Fig. 4.7B). Immunofluorescence staining of the combined tissues showed strong UPK expression in the adluminal space (Fig. 4.7C). Furthermore, a smooth muscle actin-expressing layer formed around these epithelia and could be detected by staining against the SMA (3/3 cases examined, 100%, CI95% ± 17%; Fig. 4.7C). These ureter-like structures showed spontaneous rhythmic contractions after 7 days in culture (video 4.3).

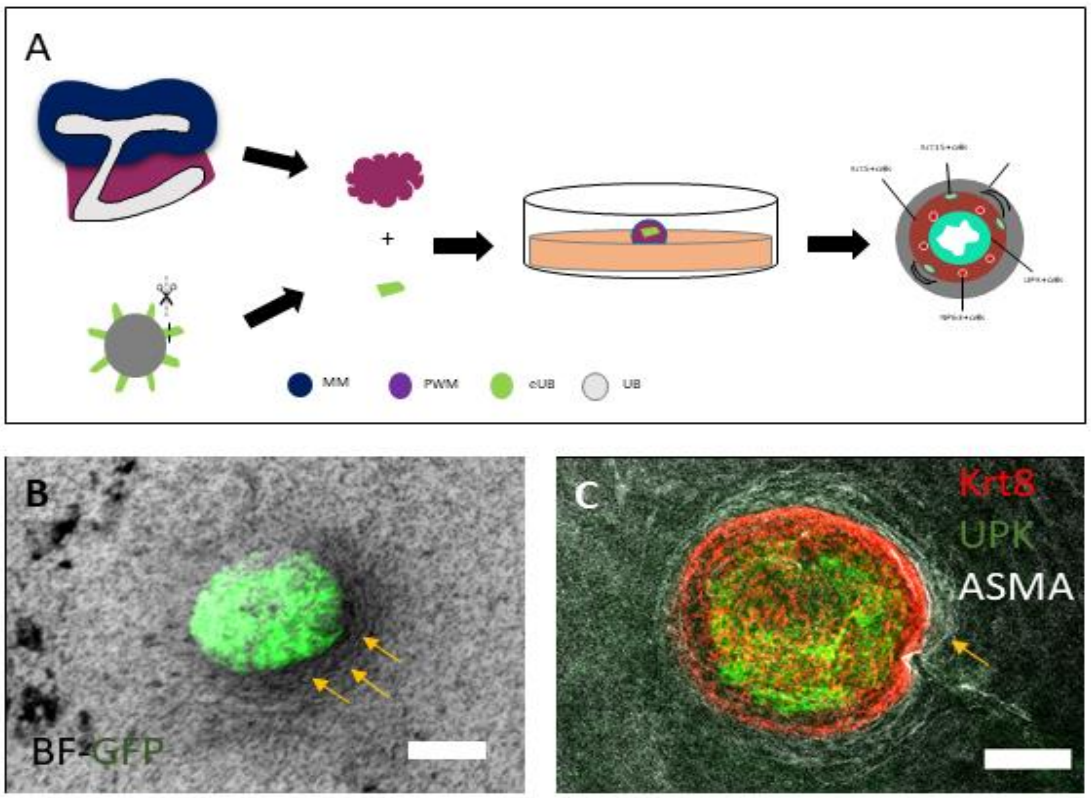

Figure 4.7 Urothelial differentiation of eUBs when combined with isolated PWM. (A) Illustration shows the steps of the combination of eUBs and PWM cells (B) Bright-field image with GFP channel showing a combined tissue of GFP-eUB with isolated PWM (arrows). (C) Immunofluorescence image of the combination tissue showing UPK expression in the luminal side and expression of KRT8 in the whole epithelium and surrounded by a layer expressing smooth- muscle actin (ASMA). Scale bar=100µm.

Urothelium consists of three distinct cell types; superficial, intermediate, and basal cells, each with its own specific markers (Wu et al., 2009). Basal layer cells express Krt5+ and NP63+, intermediate cells express weak UPK+ and NP63+ but they do not express KRT5, while the superficial apical cells express only UPK (Shin et al., 2011). To investigate the similarities between the tissue produced by combination of the eUBs with the PWM and the natural ureter, detection of different urothelial cell markers was performed using immunofluorescence analysis.

Histological sections of the eUB-derived ureter-like structures showed an organization similar to that of the of the natural ureter, with an inner layer of uroplakin III+ cells, a marker specific to superficial cells. A strong expression of the basal (B) cell marker Krt5 (Mysorekar et al., 2002; Wu et al., 1999; Bohnenpoll et al., 2013) could be detected in the cells that lie between the basement membrane and the superficial cell layer as shown in Fig. 4.8A, (3/3 examples examined; 100%, CI95% ± 17%).

A lumen could be detected in some samples which sometimes appeared collapsed and sometimes inflated (Fig. 4.8A, B). Occasional cells within the B cells' zone showed KRT15 expression, this could be seen in 5/5 examples tested (100%, CI95% ± 10%; Fig. 4.8B), as in natural ureter (Tai et al., 2013). Cells expressing very weak UPK and KRT5- could be detected in some parts in the zone dominated by the basal cells (Fig. 4.8A). A strong expression of NP63 could be detected in them (4/4 samples were tested 100%, CI95% ± 12.5%; Fig. 4.8C), a pattern characteristic of intermediate ('I') cells (Mysorekar et al., 2002; Wu et al., 1999). Co-expression of Np63 and the basal cell marker Krt15 is detected in some cells in the urothelium of wild-type mice (Tai et al., 2013). Fig. 4.8D shows similar co-expression in the ES-cell derived ureter-like structures (3/3 samples tested, 100%, CI95% ± 17%).

Collectively, these experiments indicate that the combination of the eUB and PWM cells show characteristic similarity to the natural fetal ureter, including expressing markers of different urothelial cells and the ability to organize the mesenchyme to differentiate into smooth muscle cells with contractile activity.

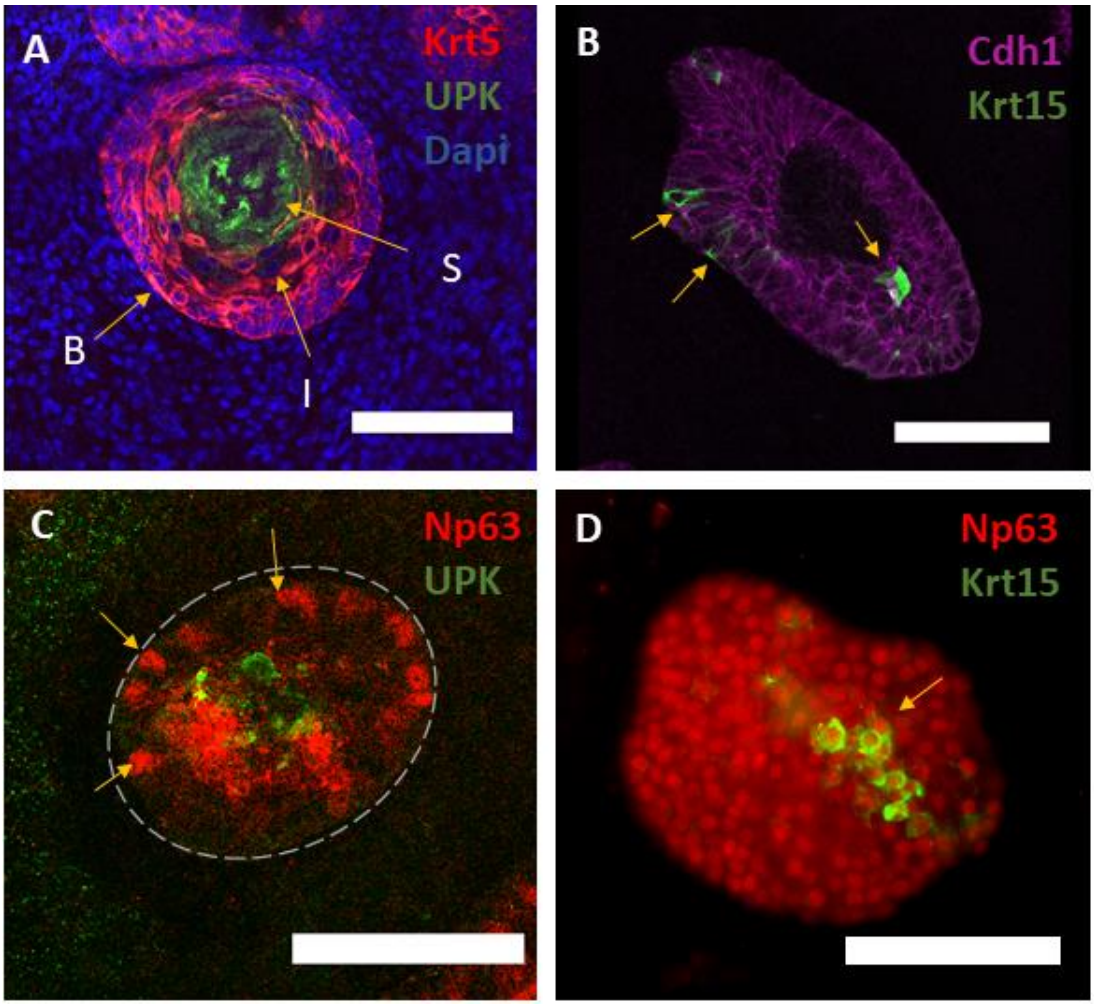

Figure 4.8 eUBs combined with PWM express various urothelial cell markers. (A) Shows a section of a combined eUB with PWM expressing krt5 in basal cells ('B'), UPKIII in superficial ('S') cells, and krt5- intermediate ('I') cells in between the two. (B) Krt15 expression detected in some cells in the B cell layer; the rest express the epithelial marker (Cdh1) (C) Showing the expression of NP63, intermediate cell marker, and other cells expressing UPK. (D) Shows cells co-express the basal marker krt15 and NP63 (arrow). Scale bar 100=µm.

4.2.6 Ureter-like tissues, derived from the combined eUBs and peri-Wolffian mesenchyme, display spontaneous contractions

As described previously, the eUBs grafted in the PWM differentiate into ureter-like compound 'tissues' containing UPK^+ urothelium and smooth muscle which started to show rhythmic contractions after 7 days in culture. These movements were strongly reminiscent of natural ureteric peristalsis. The asynchronous contraction of the host ureter and the graft indicates that the smooth muscle that developed around the graft contracts autonomously and independently of the adjacent host ureter.

To confirm this, a combination of the eUB and isolated peri-Wolffian mesenchyme without host kidney were filmed using time lapse. These independent ureter-like structures have also showed spontaneous rhythmic contractions (video 4.3), of period 11s (SEM 0.8s) in one recoded movie and 20s (SEM 0.7s) in another video as analysed by Prof. Jamie Davies and depicted in Fig. 4.9A, B. This indicates the functionality of the smooth muscles that developed around the graft as well as the presence of a pace-maker activity. These pace-maker cells most probably are the atypical smooth muscle cells which are normally present in the pelvis of the kidney and the proximal ureter (Lang and Hashitani, 2019).

Thorough analysis of the recorded videos showed that there were very small contractions that can be detected in between the large ones which together produced a constant sequence, with periods 6.4s (SEM 0.4s) and 7.5s (SEM 0.5s). Using electrical measurements, previous studies have shown that the electrical pace-maker activity of the ureteric smooth muscle cells operates at frequency 2-4x of gross peristaltic contraction- this is because of the refractory period that occurs in the smooth muscle contractions (Lang et al., 2010; Burdyga & Wray, 2005); the small contractions that could be detected between the large ones may reflect this underlying clock. Noticeably, there were no small contractions detected in the eUBs grafted in the PWM of a host kidney, probably because the tightly packed mesenchyme in these prevented the

visibility of the small contractions.

The behaviour of PWM around a grafted eUB, enveloping it and producing a smooth muscle layer, provides strong evidence of reciprocal inductive signalling, from epithelium to mesenchyme, to form the ureter. The identity of these signals remains unknown, although there is evidence for involvement of Shh as a urothelium-secreted, muscle-promoting factor (Weiss et al., 2013). The mechanisms that order the smooth muscle in a way that promotes relatively organized peristaltic actions are also not fully understood.

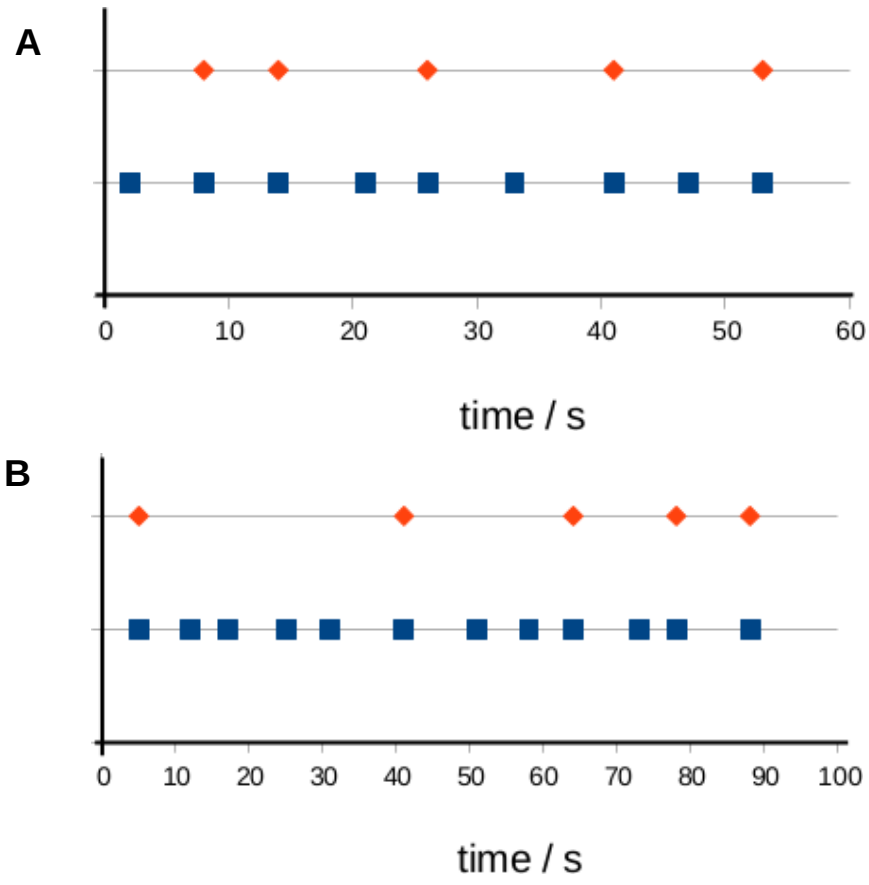

Figure 4.9 Contractions in eUBs combined with peri-Wolffian mesenchyme. (A) and (B) show the timing of the small contractions, and of large contractions (red, these large contractions being comparable to those in Fig. 4.6), in two examples. In (A) contractions timings were 2, 8, 14, 21, 26, 33, 41, 47 and 52s and in (B) they were 5, 12, 17, 25, 31, 41, 51, 58, 64, 73, 78, 88s (blue shows small and large, red shows only large contractions. ***(Analysis performed by Prof. Jamie Davies for a jointly authored paper).***

4.2.7 eUB can differentiate into CDs and ureter at the same time using grafting

Based on the above results, eUBs can differentiate into collecting ducts and/or ureters when transplanted into the MM and PWM, respectively. This suggests that there is a possibility of getting both CDs and a ureter from the same eUB, similar to the natural UB.

While working on grafting, I have noticed that in one of the cultures, the eUB was accidentally placed in the middle zone between the MM and the PWM. The proximal part of the graft adjacent to the MM showed branching and apparently formed nephrons, while the distal part which was close to the PWM become slightly elongated and did not show branching (vid 4.4).To explore that, I set some grafting cultures where the eUBs were intentionally placed in the region between the MM and the PWM (in which, at the level of the renal pelvis), and the same result was obtained (3/3 samples tested, 100%, CI95% ± 17%; Fig. 4.10 A,C). The part set in the PWM showed positive UPK expression and induced the differentiation of smooth muscle around it, which could be detected using anti body against SMA (Fig. 4.10 B). The other end, set in the MM showed branching, induced nephrons to form and to express the nephron marker PODXL and connected to them.

Using the immunofluorescence stain for the apical marker PKC, the lumen appeared continuous between the graft and the surrounding nephrons which confirms their connection (Fig. 4.10 D, E). After 7 days in culture, the non-branching end started to show rhythmic contractions while the branched end did not (3/3 samples tested and recorded using Nikon microscope; 100%, CI95% ± 17%; vid 4.5). This suggests that engineering kidney organoids with ureters attached is possible but requires both types of mesenchyme to be organized around the eUB in a fashion similar to the natural ureteric mesenchyme.

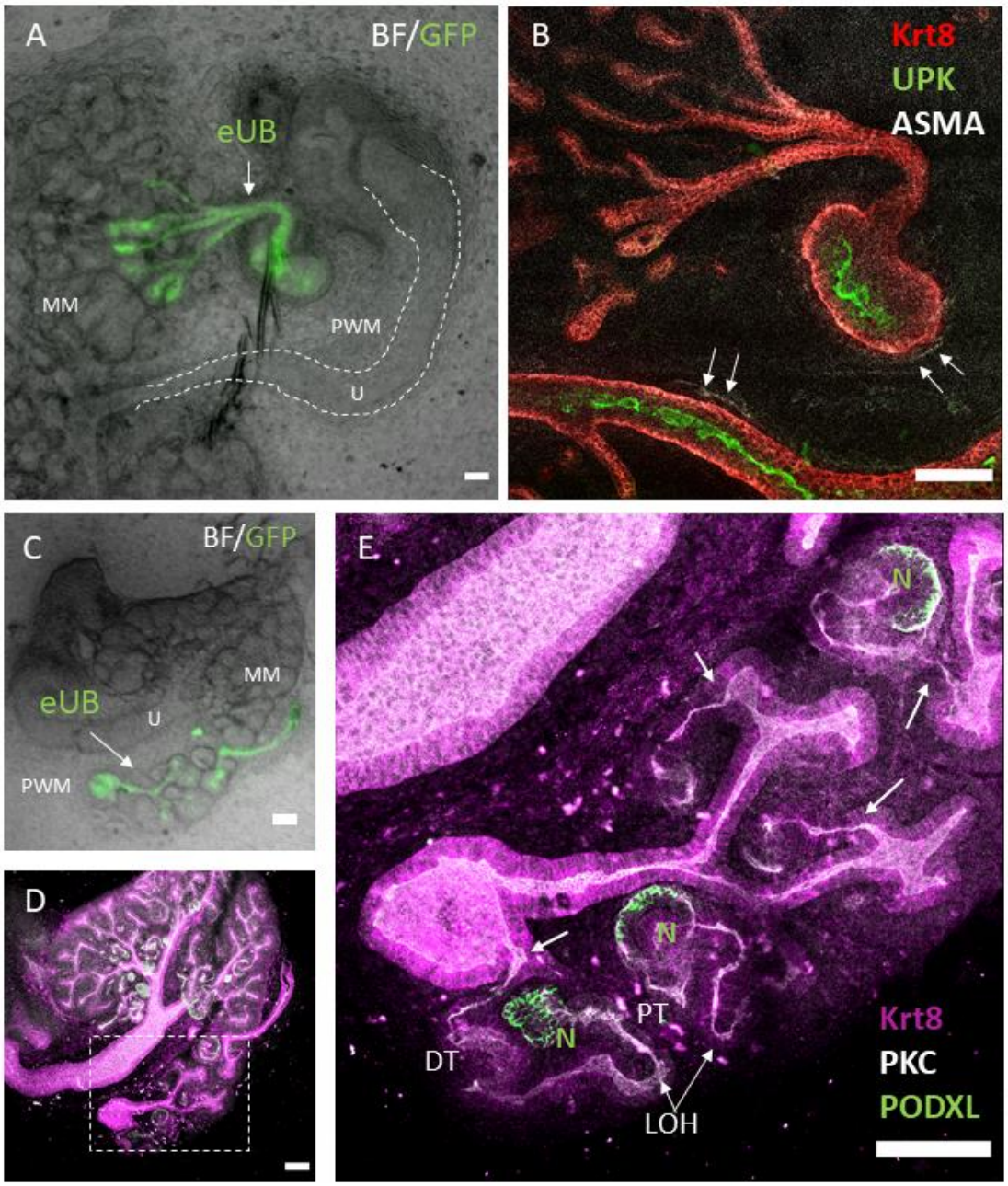

Figure 4.10 eUBs differentiate into both CDs and a ureter when grafted between the MM and the PWM. (A) Bright field image with GFP channel showing the GFP-eUB grafted between the MM and PWM showing branching from one side. (B) Immunofluorescence stain of A, showing UPK expression in the unbranched side of the grafted eUB and the host ureter, and cells expressing SMA around the graft and the ureter (arrows). (C) Bright field image with GFP channel showing another GFP-eUB grafted between the MM and PWM, showing branching from one side. (D) Immunofluorescence stain of C showing PODXL expressing nephrons connected to the krt8 positive eUB branches from one side, as the natural collecting ducts nearby. (E) Magnification of the boxed area in D shows connection of the graft to nephrons

(arrows). N; nephrons, DS; distal tubule, PT; proximal tubule, LOH; loop of Henle. Scale bar=100μm.

4.3 Discussion

This chapter describes an advance in techniques for generating tissues of the excretory system, specifically ureter, from embryonic stem cells. The general aim of producing renal and related tissues from stem cells is important for several reasons. The production of simple kidney models (‘organoids’) has already provided new insights into organ development, offered human-based systems for the study of pathophysiology, and shown promise as a means of screening potential drugs for efficacy and toxicity (Morizane et al., 2017). Several research groups in the field are working toward the long-term aim of engineering complete functional kidneys for transplant purposes (Morizane & Bonventre, 2017; Taguchi & Nishinakamura, 2017). This might be a new strategy to treat patients with chronic kidney disease (CKD), however these techniques need to be transferred from mouse to human in order to be clinically useful.

In this chapter, I have showed that mESC-derived eUBs are capable of differentiating into either collecting ducts or ureter, the choice being governed by surrounding mesenchyme. Moreover, I was able to generate ureter-like structures in vitro from eUBs, by combining them with mouse fetus-derived PWM cells. These tissues had similar epithelial characteristics to the fetal ureter and included smooth muscle layers that showed spontaneous peristaltic contractions which were a little slower than the natural ureter.

Studies using human cells have reported methods to induce human ES and iPS cells to differentiate into urothelial cells (Osborn et al., 2014). However, the structures produced lacked the three-dimensional shape and the smooth muscle cell lining of ureters. Recently, Mullenders et al., published a paper describing the generation of ureteric organoids derived from adult human tissue and from bladder carcinoma (Mullenders et al., 2017). Their organoids

formed cyst-like spheroids with a lumen but did not show mesenchymal organization or smooth muscle formation and there was no evidence of peristaltic contractions. The method I described here is distinctive in combining the engineered UBs with fetal peri-Wolffian mesenchymal cells to produce ureter-like structures with multilayer epithelium and a smooth muscle coat that can show spontaneous contractions.

Using transplantation studies, Bohnenpoll and colleagues in 2013 showed that the ureteric stalk (the epithelial part forms the presumptive ureter) when transplanted into the MM, gives rise to a collecting duct like branching epithelium. In 2017, Mills et al. performed the reverse experiment by transplanting the ureteric bud tips (future collecting ducts) into the peri-ureteric mesenchyme. The UB epithelium did not branch and expressed UPK which is a unique urothelial marker. This indicates the plasticity of the UB epithelium to take different fates in response to different types of mesenchymal signals. This has not been tested before in the ES cell-derived eUBs and the grafting experiments in this chapter confirm that eUBs have a plastic nature at least in their early stages.

The plasticity of the engineered ureteric bud (eUB) structures to form either collecting duct or ureter does provide some evidence that eUBs are realistic analogues of natural UBs. Natural UBs have the same plasticity, differentiating into collecting duct when grafted into metanephric mesenchyme (MM) and into urothelium when grafted into PWM (Sweeney et al.,2007; Bohnenpoll et al.,2013; Mills et al 2017). This plasticity also exists when the eUBs are combined with a pure mesenchyme in absence of a host kidney which suggests that the interaction is confined between the epithelium and the mesenchyme.

The method of recombination of eUB epithelium with either MM or the PWM that has been used in this chapter is similar to what has been described by Taguchi and Nishinakamura, 2017 and described earlier by Grobstein, 1953. Another model for exploring renal self-organization in culture was described elsewhere (Unbekandt et al., 2010; Ganeva et al., 2011). The Ganeva

organoids were similar to those of Grobstein with one exception; the UB cells were enzymatically dissociated and cultured before the recombination, which represents a suitable model for studying the formation of renal organoids from single cell suspension. In this chapter, I have used the Grobstein system, as the ES-cell derived eUBs are structurally comparable to the intact natural UB at its early stages yet these eUBs were formed from stem cell suspensions in the first place.

The eUBs in MM form branching trees connected to nephrons in a fashion similar to the natural collecting ducts, while in PWM the eUBs form ureter-like structures surrounded by a smooth muscle layer. Grafting the eUBs in between the two mesenchymes formed mini kidney-like structures, with branching collecting duct from one side and a single ureter-like from the other side, which suggests the possibility of producing a whole kidney organoid with a ureter if the anatomical arrangement of both MM and PWM was achieved.

Previous studies have shown that the ureteric epithelium expresses Shh, which induces mesenchymal cell proliferation and expression of BMP4 (Yu et al., 2002). BMP4 induces the mesenchyme itself to differentiate into smooth muscle and promotes the urothelial development (Miyazaki et al., 2003). Inhibition of Shh causes defective smooth muscle maturation and failure of the stromal cell layer to develop (Yu et al., 2002). Moreover, BMP4 induces the differentiation of the UB stalk into urothelium by inducing UPK expression at the apical layer which plays a role in the urothelial water sealing mechanism (Jenkins and Woolf, 2007). Additionally, Tshz-3 is known to be an essential factor in ureteric smooth muscle development (Caubit et al., 2008). A defect in Tshz-3 expression causes functional hydronephrosis without anatomical obstruction due to absence of the contractile smooth muscle markers at the renal pelvis. Tshz-3 defect causes a defect in the expression of the key smooth muscle regulator MYCOD, while the expression of SHH and BMP4 were not affected (Wang and Olson, 2004).

Ureter contractions are controlled by the action of the pacemaker cells which lie mainly in the pelvi-ureteric junction PUJ (Gosling, 1970). In vitro-isolated

ureters that were separated from their kidneys have the ability to generate proximal to distal peristaltic waves independently (Caubit et al., 2008) suggesting the presence of more than one pacemaker cell population. The eUB grafted in PWM alone or in the presence of a host kidney also show spontaneous contractions, which indicates that they develop pacemaker cells.

The eUBs combined with PWM in presence of a host kidney or in absence develop contractions comparable to the natural ureter but a little slower, probably because the non-tubular shape of these grafts might have affected the efficiency of their contraction.

It should be noted that, while the urothelial components of the engineered ureters were differentiated from mES cells, all the mesenchymal and smooth muscle components arose from ex-fetu PWM cells. Production of all-ES-derived ureters awaits the development of methods to differentiate ES cells into PWM cells, to combine with the eUBs and induce the combined tissue to elongate into a ureteric tube.

Chapter 5. Connection of the ES cell-derived eUBs to the host kidney CDs or ureter

Work in this chapter has been accepted for publication in ***Organogenesis Journal, March 2021.***

5.1 Introduction

Currently, kidney organoids provide excellent models for studying organ development, disease pathogenesis, and for drug screening and, if they are transplanted in vivo, these organoids acquire vasculature (Van de berg et al., 2018; Xinaris et al., 2012). However, many challenges need to be overcome for these organoids to be of any clinical use, including organoid size and maturation, which cannot be improved by current culture techniques (Koning et al.,2020).

Alternative methods are needed to accelerate the utilization of organoids, and one of these might be using multiple organoids to replace parts of a damaged kidney. This will depend on their ability to connect and integrate into the host kidney tubular system and to drain the urine produced by them.

In this chapter, I demonstrate a modified grafting method that can provoke the ES cell-derived eUBs to connect to the CD system and the ureter of a host kidney. This was based on an observation during the optimisation of the grafting technique described in the previous chapter, where some contact was noticed between graft and host in rare samples.

Investigation of this revealed that introducing an incision in the host CD or ureter at the site of grafting promotes connection between graft and host, and it still differentiates according to the tissue surrounding it (the mesenchyme). Immunofluorescence analysis of the connection site revealed that both the eUB and the host share a continuous open lumen, which would be essential for graft drainage. Furthermore, when connection was made to a ureter, the graft showed synchronous contractions with host ureter. This was done using immature host tissues as well as older kidneys in culture. These results might

be a foundation for developing new methods that allow the use of ES cell-derived organoids for kidney regeneration.

5.2 Results

5.2.1 Connection of ES cell-derived eUBs to host collecting ducts

When eUBs were grafted into ex-fetu nephrogenic areas, as described before, they generally remained independent of host UB-derived epithelium. When developing the grafting technique, however, I noticed that this independence seemed to be lost in occasional damaged samples, and that the graft sometimes appeared to attach to a host ureteric bud-derived epithelium. Therefore, I hypothesised that nicking of the host kidney epithelium might be used to induce connection between graft and host.

To test this, I set some grafting cultures in which a deliberate cut was made in the host epithelium with a sharp needle, just before the eUB was grafted nearby. First, as described in the previous chapters, I used Hoxb7-GFP mESCs to make the eUBs using the Taguchi protocol. GFP fluorescence of the eUBs was essential to recognize graft from host.

At day 10 of the differentiation protocol, eUBs were manually dissected from the main spheroids and grafted into the metanephric mesenchyme area of an E11.5 kidney and cultured on Transwell inserts for 5 days (see chapter 2 for details). With no injury performed, the graft remained separate from host collecting ducts and showed branching and nephron formation as natural CDs (Fig. 5.1). No connection was detected between eUB grafts and host (0/6 samples examined, 0%, $CI^{95\%} \pm 8.3\%$).

Interestingly, when no cut was made, the host collecting ducts seemed to avoid contact with the graft either by ceasing their expansion (Fig. 5.1A-C) or tilting their branches away from the graft forming odd-shaped trees (Fig. 5.1D, E). This behaviour is in fact similar to what had been described in Davies et al.,

2014 between two adjacent kidneys in culture. When two kidneys were cultured close to each other, their branches appeared to avoid contact with one another forming distorted trees. It is reported that molecular signals including Bmp7 are responsible for this behaviour (Davies et al., 2014).

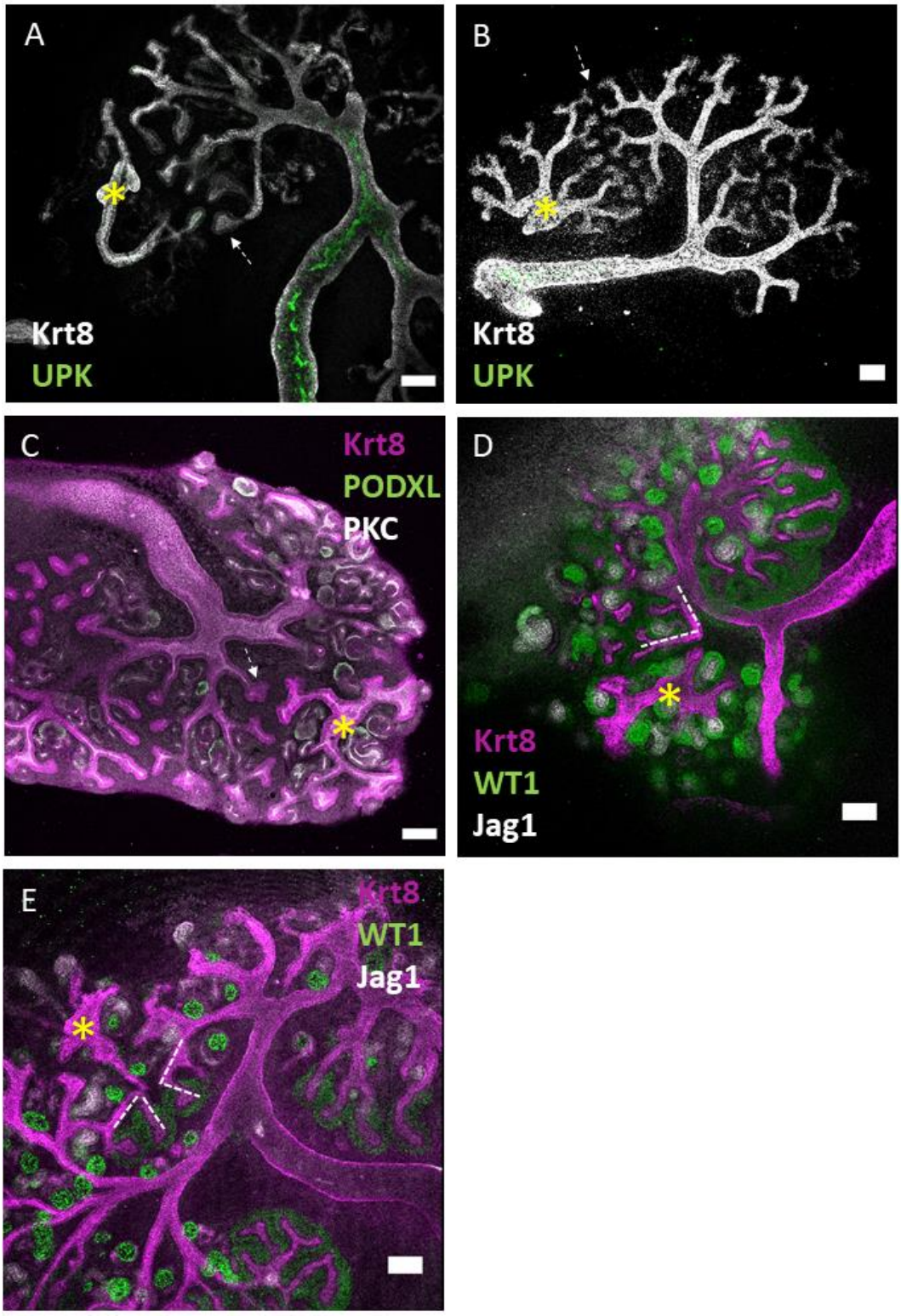

Figure 5.1 Avoidance of contact between eUB grafts and CD branches of host kidneys. (A-E) Show eUB grafts in the MM of host kidneys marked by yellow asterisk* and the CDs of the host that face the grafts, avoiding contact by stopping their expansion (arrow), or changing their branching direction (dotted lines). Scale bar=100µm.

When a cut was made in the host collecting duct system using a sharp needle (as shown in Fig. 5.2A), and the eUB was grafted as close as possible to it, contact being the intention, the grafted Hoxb7-GFP eUB made its own tree-like duct system and, in approximately 50% of the experiments, this connected with the host collecting duct tree (Fig. 5.2B, D). Connection was seen in 10/20 samples examined (50%; 95%CI ±24%, the rest did not connect anywhere).

The eUBs connecting to host collecting ducts formed structures that showed characteristics of CDs, including branching and nephron induction (Fig. 5.2B, D), and as would be anticipated of collecting ducts, there was no expression of the urothelial marker UPK (Fig. 5.2C). The eUB graft was capable of inducing formation of nephrons that expressed the early nephron markers WT1, and Jag1 (Fig. 5.2E) that connected to it.

For further analysis of the connection between eUB and host UB-derived tubules, time lapse video recordings were made using a confocal microscope. Samples were filmed directly after grafting and recorded for 3 days (Video 5.1, 5.2). In these videos, the GFP-eUBs appeared to be interacting with the surrounding metanephric mesenchyme, showed branching and apparently induced a nephrogenic response. The part close to the host collecting duct seemed to blend into the main CD tree and appeared as just another branch. Some GFP cells seemed to extend into the natural host tubes, which suggests integration of the graft into the kidney tubular system and some cell mobility (Video 5.1, 5.2).

Compared with the repulsive behaviour that occurred between the graft and the intact epithelial host tubules, the intentional incision made in the wall of the host tubules appeared to have encouraged the connection.

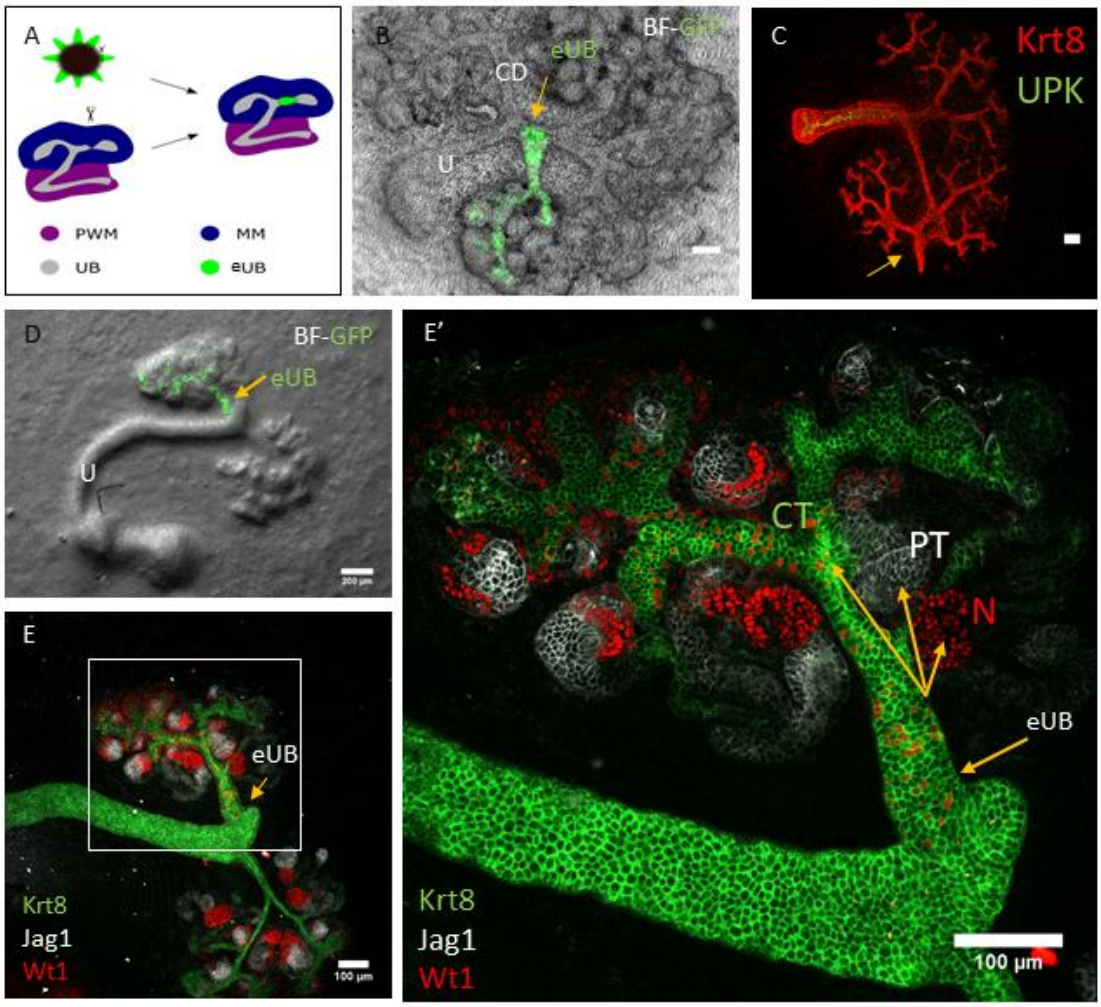

Figure 5.2 eUBs can connect to the CDs of host kidneys in culture. (A) Steps of induction of eUB connection to mouse kidney CD. (B) Bright-field image with GFP channel showing the GFP-eUB graft branched and connected to the CD system of the host kidney. (C) Immunofluorescence image of the eUB (arrowed), connected to the collecting duct tree and does not express UPK. (D) Combined BF and GFP image showing GFP-eUB showing branching and connect to the CD system of a host kidney. (E) Immunofluorescence stain of D, showing eUB branching and associated nephron formation. (E') Higher magnification image of E showing WT1+, Jag1+ nephrons connect to the eUB-derived collecting duct subsystem. N; Nephron, CD; collecting duct, PT; proximal tubule. Scale bar=100 µm.

5.2.2 Connection of the eUBs to the host kidney ureter in culture

In the previous chapter, I showed that ureteric buds engineered from ES cells are capable of differentiating into ureter-like structures, when combined with cells of the PWM, with or without host kidney. These structures expressed markers characteristic of fetal urothelium and induced the differentiation of smooth muscle cells around them. In most cases, the eUB remained separate from host ureter and showed simultaneous contractions after 7 days in culture.

Having shown that the intentional damage of collecting duct epithelium can induce the connection between the eUB graft and the host kidney, and this subsequently will differentiate into a collecting duct-like branch, I asked whether the same can happen when grafting is performed near to a ureter instead. To test this, I set some grafting cultures in which the cut was made into a host ureter before eUBs were grafted nearby (Fig. 5.3A).

Data from the previous chapter showed that the Hoxb7-GFP eUBs maintained GFP expression throughout the culture either in MM or in PWM. This had helped the connection to be clearly detectable between eUBs and ureter after a few days in culture. Fig. 5.3B, D shows GFP-eUBs connect to the ureter (13/20 samples showed connection to the host ureter; 65%, 95%CI± 22.5; while the others did not connect anywhere).

Immunofluorescence analysis showed strong UPK expression in the graft site as well as in the host ureter (Fig. 5.3C, E, E''). These eUBs acquired a coat of smooth muscle cells, expressing smooth muscle actin (ASMA) as showed in (Fig. 5.3E, E')**.**

In control samples, with no damage performed, no connections were seen (0/6 samples examined, 0%, $CI^{95\%} \pm 8.3\%$) suggesting that the intentional damage to the wall of the ureter encouraged its connection with the eUB graft.

To investigate the connection further, I carried out time-lapse recording of the connection process between eUB graft and host ureter (videos 5.1). This was

done by placing the samples in a special chamber (37°C and 5%CO_2) of the Nikon microscope, directly after grafting, and events were recorded for 3 days (as described before).

In the recordings, eUB grafts seem to interact with the surrounding mesenchyme and as would be expected of a ureter, these grafts show slight elongation with no branching. In addition, some GFP cells can be seen extending into the main trunk of the host ureter, which suggests integration of the graft into the ureteric tissue and cell mobility.

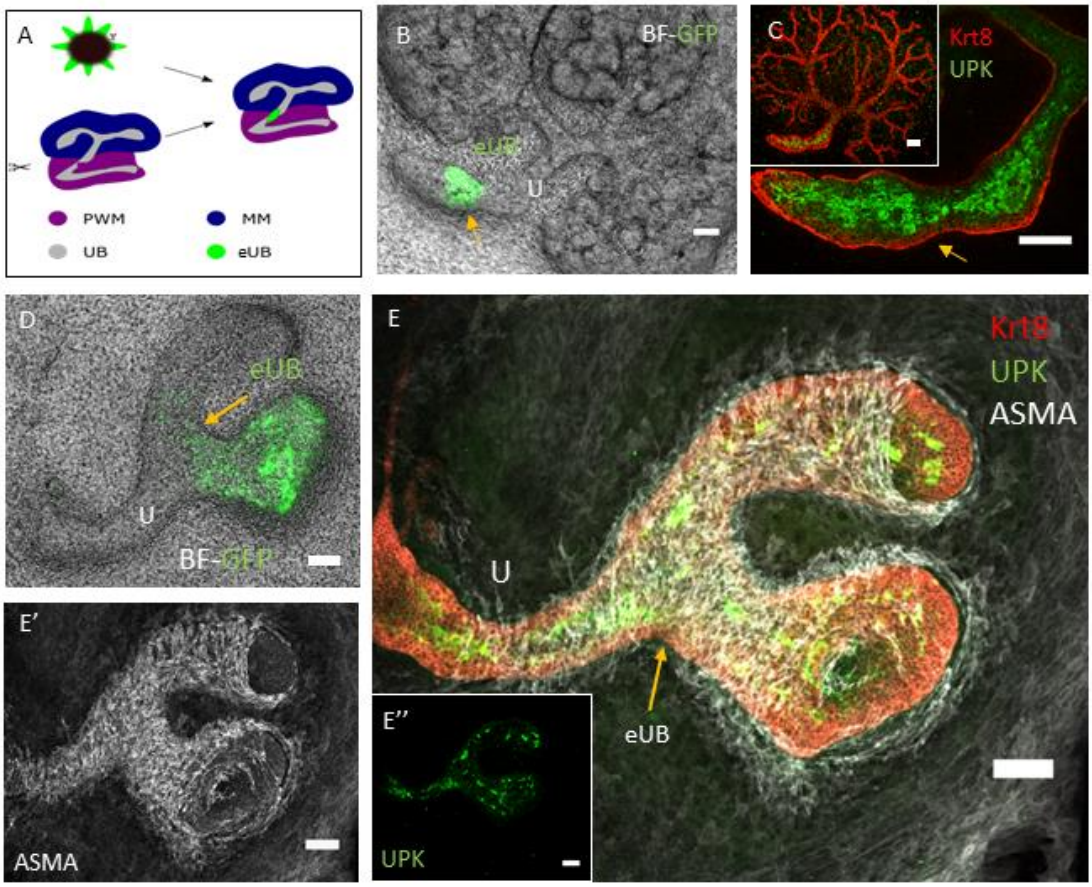

Figure 5.3 eUBs connect to ureters of host kidneys in culture. (A) Steps of eUB connection to mouse kidney ureter. (B) Bright field image with GFP channel showing the GFP-eUB grafted and connected to the ureter (arrow) of a host kidney in culture. (C) Magnified immunofluorescence image, showing the eUB connected to the host ureter, and expressing UPK, (the graft is marked with an arrow, as in B). (D) Shows another eUB graft connects to a host ureter (arrow). (E) Immunofluorescence image of (D) shows the expression of Krt8, UPK and ASMA in both the graft and the host. (E') Individual ASMA channel of E, showing a smooth muscle layer surrounded the host ureter and the connected graft (E'') Isolated UPK channel shows the expression of UPK in both the connected graft and the ureter. Scale bar =100μm.

5.2.3 eUBs share an open lumen with host CDs and ureteric stalk

The kidney receives around 20% of the cardiac output and nephrons are kidneys' functional unit (Saxén and Sariola, 1987). The main function of the nephron is to filter the plasma and excrete waste while recovering useful substances such as glucose and amino acids (Stott et al., 1983; Wang et al., 1993). Distal tubules, the final segment of nephrons, drain into collecting ducts which converge to renal papillae that drain into the pelvis of the kidney and the ureter (Sarin et al., 1990). For incorporated eUBs to function, they need to share a continuous open lumen with the nearby host kidney.

For that, I needed to examine the site of connection between eUB grafts and host epithelium, and whether they were connected to the host collecting duct and / or the ureter or just attached with no common lumen.

To test that, I first tried to detect the lumen using ink injection in the kidney tubules and see if the ink would flow through the whole CD system including the connected graft. Initially, I started with normal cultured kidneys and used micro-injection needles to introduce ink into the kidney tubular system. After several attempts, this technique was found to be impractical, as conventional culture allow kidneys to flatten out which apparently precludes fluid flow in its tubules.

Alternatively, I decided to use immunofluorescence analysis to visualize the boundaries of the lumen by staining for the apical marker of the epithelia using antibody to the apical protein, anti-protein kinase C zeta (PKC-zeta). This PKC-zeta is one of the PKC family that play a role in a range of cell functions including cell growth and differentiation as well as membrane function (Sacktor et al.,1993).

Confocal images showed that the luminal apical surface of cells form sheets that ran along, not across, the tubules at the junction, meaning that the lumen was continuous across the boundary between the eUB graft and host collecting duct making a contiguous luminal space (Fig. 5.4 B, C). This was

clear in 6/6 examples examined of eUBs connected to the host collecting duct (100%, CI95% ± 8.33%).

The same method was used to detect the lumen in grafts connected to ureters of host kidneys. In these samples, staining for the apical marker PKC showed that the lumen was continuous along the boundary between the eUB graft and host ureter in 5/5 examples examined (100%, CI95% ± 10%; Fig. 5.4 E, F**)**. This suggests that these eUB grafts can make incision-induced connections with host CDs and ureter that shows a clear patent lumen, which is vital for the graft function.

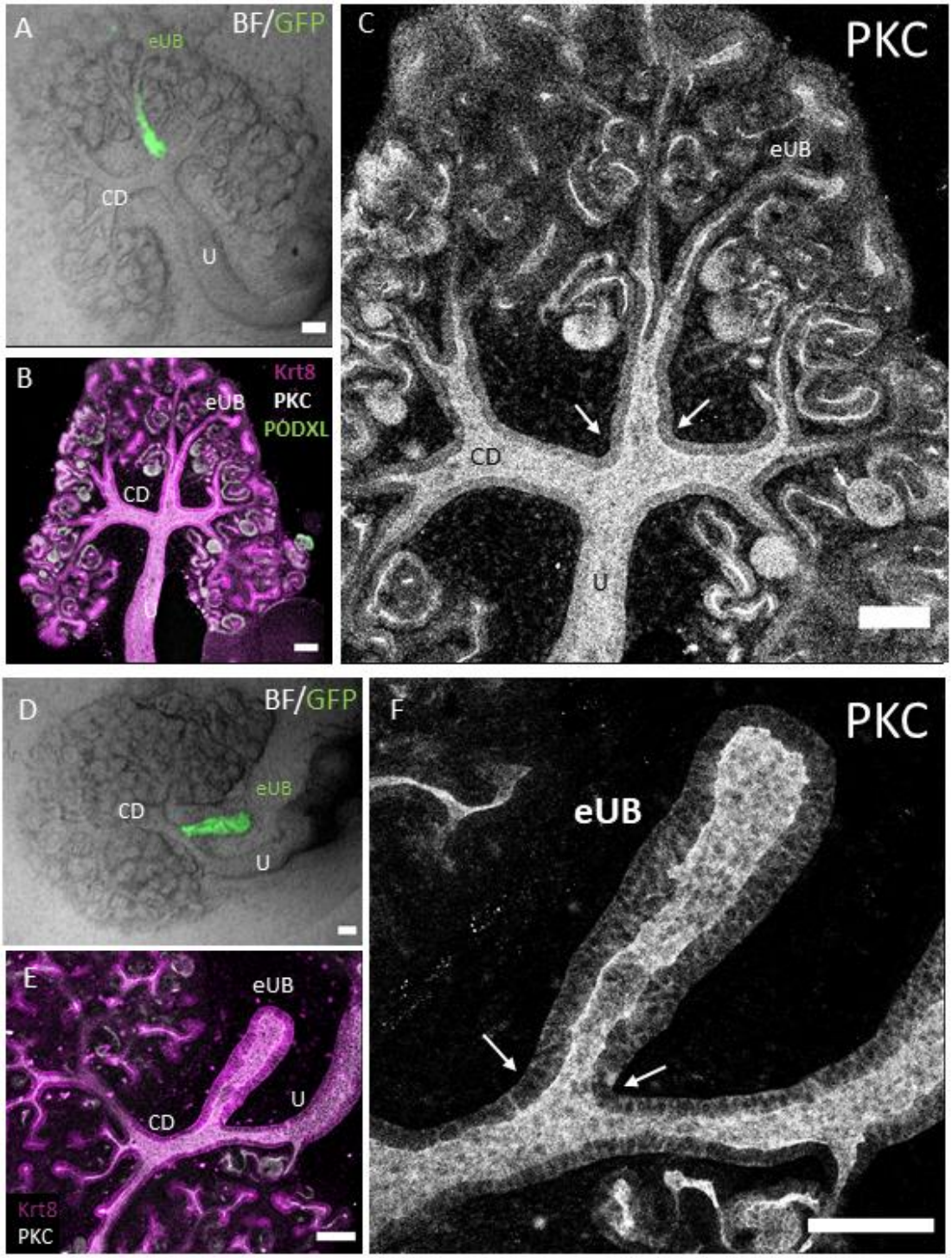

Figure 5.4 eUBs share open lumen with the CDs/or ureter connected to it. (A) Bright field image with GFP channel showing eUB graft connected to the collecting duct system of a cultured kidney and showed branching. (B) Immunofluorescence stain of A showing continuous open lumen between the graft and the host collecting ducts, can be detected by the apical domain protein kinase C (PKC), and the epithelial marker Krt8. (C). Individual PKC channel, for clarity, arrows point to the connection site. (D) Combined BF& GFP image of a GFP-eUB connected to the ureter of a cultured

kidney, to reveal the graft position (E) Immunofluorescence stain of the apical marker PKC and the Krt8 (epithelial marker) showing continuous open lumen between the host ureter and the graft (arrows). (F) Magnified individual channel of PKC, for clarity, arrows point to the connection site. Scale bar=100µm.

5.2.4 eUBs connected to a host kidney ureter show synchronous contractions

The function of the smooth muscle of the ureter is to push urine down to the bladder (Kiviat et al.,1973). These contractions occur in the form of waves that propagate from proximal to distal. Failure in this process causes functional obstruction and subsequent back pressure-induced kidney injury (Mendelsohn 2004). Ureteric contractions are believed to be myogenic in origin and initiated by a group of pace-maker cells that are similar to the pacemaker cells of the gut and can be identified by c-kit expression (Santicioli and Maggi, 1998; David et al., 2005).

Data from the previous chapter revealed that eUBs grafted in a host kidney PWM showed spontaneous contractions. These contractions resembled the contractions of the host ureter in terms of periodicity but were independent in terms of phase and frequency. This suggests the presence of autonomous pace-maker activity in the graft tissue.

This raised the question about the capability of the connected grafts to show contractions and whether these contractions, if present, would operate synchronously with the movements of the connected ureters.

To investigate this, I set up connection cultures where eUBs were induced to connect to host ureter and time lapse video recordings were carried out after 7 days in culture using a confocal microscope (video 5.4).

When the eUBs were induced to connect to host kidney ureter, they showed synchronous contractions (video 5.4). Thorough analysis of the recorded videos showed that the GFP-graft contractions coincided with those in the part

of the UB to which it had linked (Fig. 5.5). This behaviour was observed in 3/3 samples tested and filmed using time-lapse (100%, CI95% ± 17%).

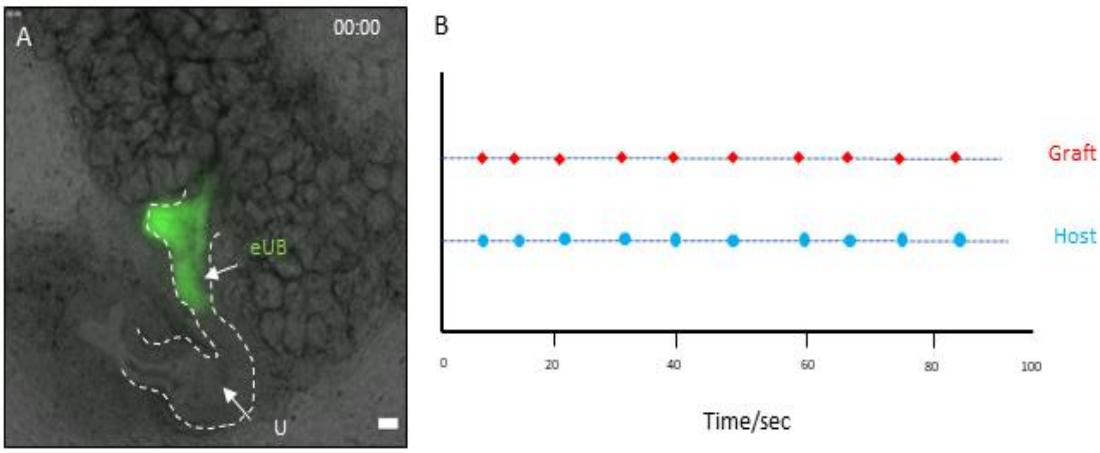

Figure 5.5 Contractions of eUB graft and connected host ureter. (A) shows the first frame of the recorded video (video 3S); the connected graft can be distinguished by the GFP fluorescence, and the arrows point to places at which contractions in the GFP-graft and the adjacent ureter were timed. (B) Shows a graph that illustrates the timings at which the contractions were observed, shown as red and blue dots on the time scale. Synchronous contraction between the graft and the host could be detected, and timings of the contractions was seen at 9.0, 14.0, 22.0, 32.0, 40.0, 49.0, 60.0, 67.0, 75, 84.0 S.

5.2.5 eUBs can connect to older kidneys in culture, and those connected to the ureter show contractions

The data from the previous section (5.2.2) showed that eUBs can be induced to connect to CDs or ureters of host kidneys in culture by inflicting a small incision in the adjacent host epithelium. However, these kidneys were immature fetal kidneys at developmental age E11.5.

In this section I aimed to investigate if the eUBs can be encouraged to connect to older kidneys in culture, or is this just an advantage of immature tissues. This is essential for the possible future applications of using these grafts in kidney regeneration.

To test this, I set some connection experiments using older kidneys and started with E11.5 kidneys cultured for 9 days, then grafting was performed in both MM and PWM. The grafted eUBs showed connection to the CDs and the ureter as showed in Fig. 5.6, (3/3 samples tested, 100%, CI95% ± 17%). The connection succeeded but, due to the prolonged time in culture, the condition of the host kidneys made the interpretation of the eUB graft differentiation difficult. Nevertheless, UPK expression could be detected in grafts connected to the ureter (Fig. 5.6B, D). To overcome the problem of long culture times, grafting was repeated using relatively older kidneys, E13.5 which were cultured for an additional 4 days before grafting was attempted.

The eUBs grafted in the PWM showed connection, which was seen in 10/10 samples tested (100%, CI95% ± 5%, Fig. 5.7A-C). The connected grafts expressed UPK and acquired a layer of SMA expressing cells (Fig. 5.7A'-C').

For more analysis of the connection, time lapse video recordings were performed, and events were recorded for 3 days after grafting (video 5.5). GFP grafts were placed in close contact with the site of the cut, and recordings show that the tiny space between the graft and the ureter was being filled and cells from the surrounding mesenchyme appeared to cover the graft from outside. Later, the GFP-eUB grafts connected to host ureter and some GFP cells could be observed incorporated into the ureteric tissue indicating cell mobility.

To investigate if these connected grafts could develop contractions, another time lapse recording was performed after 7 days in culture (video 5.6). The recordings revealed that the connected grafts showed rhythmic contractions (10/10 samples tested and recorded using confocal microscope,100%, CI95% ± 5%, video 5.6).

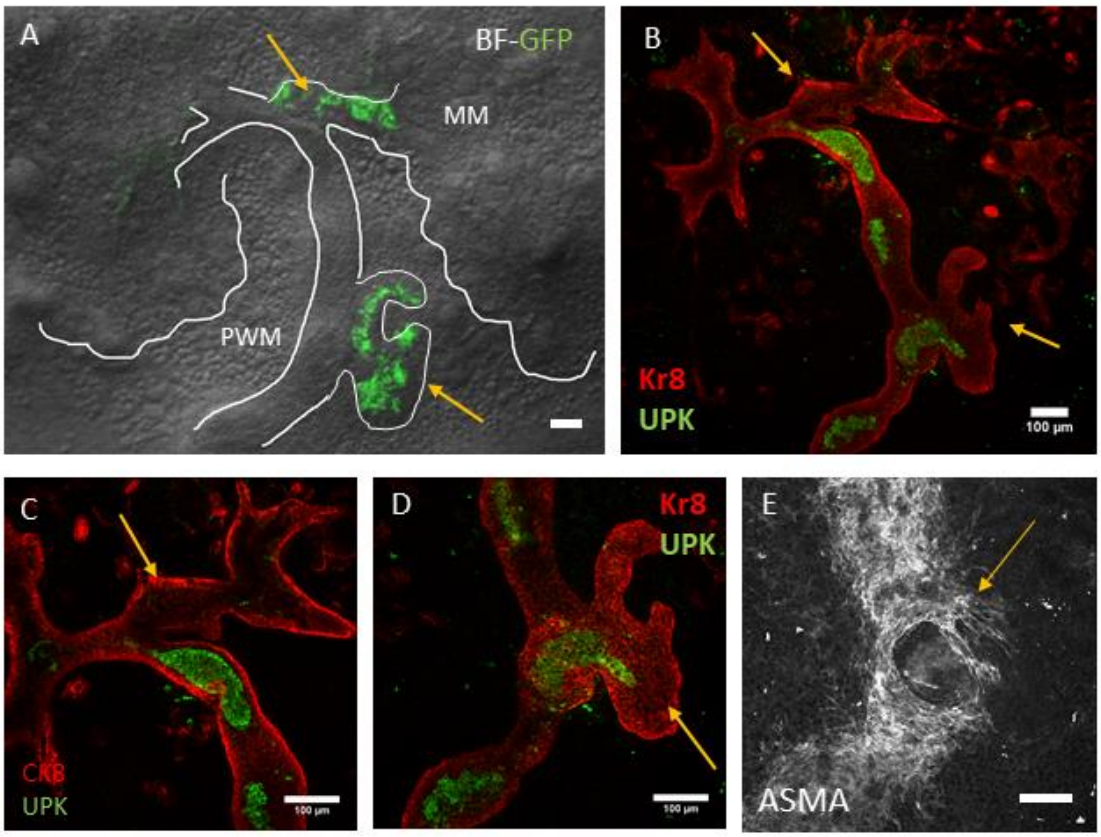

Figure 5.6 eUBs connect to CDs and ureter of older kidneys in culture. (A) Bright field image with GFP channel showing the position of the grafted GFP eUBS (yellow arrows) one in the MM and another one in the PWM. (B) Immunofluorescence satin of A shows connection of the eUB to the CDs (marked with the higher arrow) and another one connected to the ureter (marked with the lower arrow). (C) Shows the eUB graft connected to the CDs (arrow points to the graft). (D) Shows the eUB graft connected to the ureter and shows UPK. (E) A separate SMA channel of D shows the expression in both graft and host, some SM cells are seen around the graft (arrow).

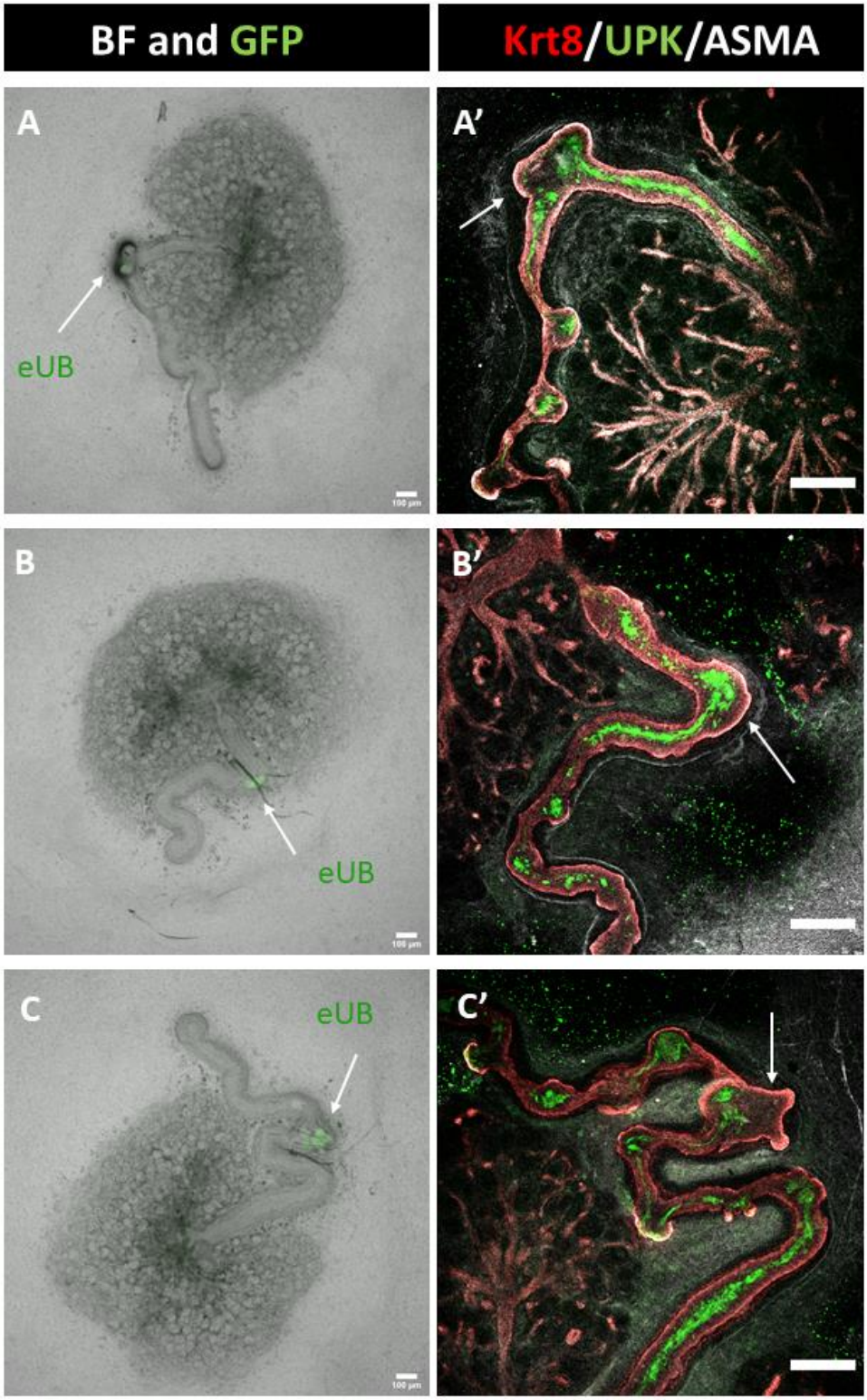

Figure 5.7 eUBs connect to ureters of older kidneys and show ureter characteristics. A, B, C. Are bright field images with GFP channel showing GFP-eUB (white arrows) connected to the ureter of older kidneys in culture. A', B', C'. Immunofluorescence stain of A, B, C showing the connected grafts (arrows) expressing urothelial marker UPK and epithelial marker krt8.

To investigate the eUBs connection to the CDs of older kidneys, I set some connection cultures where the eUBs were grafted in the MM after making a cut in the host collecting duct nearby (E13.5 cultured for 4 days). Time lapse video recordings were performed directly after grafting and lasted for three days (video 5.7).

Early after grafting, it was possible to observe the GFP-eUBs and the videos showed an apparent interaction between graft and host (10 samples were tested and recorded using time lapse). After 5 days in culture, the eUB grafts could not be detected and the MM appeared darker and possibly degenerating. Fixing and staining those samples showed degeneration in the collecting ducts probably because of the longer culture time. In vivo implantation might be a good alternative because of the advantage of a blood supply.

5.3 Discussion

In the previous chapter, I showed that the mESCs-derived eUBs were capable of differentiating into collecting ducts and/or ureters, according to the surrounding mesenchyme.

A very interesting finding of these experiments was that the eUBs had made connections to the epithelial tubules in some damaged samples. Further testing revealed that deliberate injury to the host kidney could induce connections to the graft. The graft differentiated according to the engraftment site and these connections exhibited a continuous lumen between the graft and the host.

The ability of eUBs to connect to existing epithelia of a kidney (collecting ducts, pelvis or ureter depending on graft location) was an unexpected feature, because this is not a feature of natural ureteric/ CD development. In fact, studies have reported mutual repulsion between the adjacent branches of collecting duct trees (Davies et al., 2014). In kidney development, the ureter and collecting ducts develop by branching morphogenesis from the UB, with

no need for any connection to be made. However, within the kidney, it is necessary for the nephrons to make a connection between their distal pole and the CD branch that provoked their development in the first place (Saxen, 1987). This indicates that ureteric epithelia may retain an inherent capacity to make connections that produce open-lumen communications among the tubules involved. However, the mechanisms of this are still not fully understood.

I founded that damage (nicking) to the host collecting duct or ureter is essential for connections to occur. It is worth noting that one end of the isolated eUB had been cut as an unavoidable step in its isolation from its parent spheroid. During grafting, there was no way to track which graft end is the one opposed to the host cut, either the cut or the intact end, so it was random. The nearly 50% success rate of the connection is consistent with the idea that the connection demands both apposed ends to be cut, though the data do not prove this.

Regeneration of epithelial wounds occurs by two methods, either proliferation of the undamaged cells or deposition of connective tissue and scar formation. Regeneration is the process of complete restoration of damaged tissue, and this depends on the type of tissue injured and the extent of damage; small clean epithelial cuts tend to regenerate completely. If the injury is extensive or for some reason the cells cannot proliferate effectively, the injured tissue tends to close the gap by deposition of fibrous material which later results in scar formation. Cell proliferation occurring in the process of tissue repair is controlled by growth factors and signalling molecules secreted as a response to tissue injury and lead to proliferation of cells of the injured tissue, vascular endothelial cells and fibroblasts (Kumar et al., 2014).

There are various possible explanations why damage is required for the connection to happen. A simple mechanical reason is that, if two intact tubes met, they would do so basal surface-to-basal surface, and there would be no apparent reason for their cells to exchange current neighbour relationships for new neighbour relationships with cells of the other epithelium. Once there is a

gap in one side of the host epithelium, cells at the edges of the gap will proliferate to close that gap and make adhesions either with cells of the graft or with the cells of their own kind across the gap, and this might raise the chances of the connection between graft and host to occur, instead of host-host healing.

There may be other reasons related to the production of signalling molecules. It is known that contact between the UB-derived epithelium is prohibited by their secreting and avoiding BMP7 (Davies et al., 2014). For example, if two kidneys were cultured adjacent to each other, their growing collecting ducts tend to avoid contact by tilting their branches away creating odd-shaped trees. This was also noticeable in the samples where eUBs were grafted in the metanephric mesenchyme without nicking the host CDs (Fig. 5.1).

In general, injuring the epithelium changes the production of signals (Maddaluno et al., 2017). Altering the signalling environment might result in increasing the probability of the connection to happen either by reduction in the repulsive signals or through production of attractive signals; the exact mechanism is unknown. Another possibility is that wound-derived signals might have induced some sort of epithelium-to-mesenchymal transition, or at least weakening of the remaining cell-cell adhesions in adjacent regions of the graft. Whatever the mechanism of connection of the eUB graft and host epithelium, the fact that a simple mechanical intervention can induce it to happen raises an exciting new possibility for renal regeneration.

In general, researchers discuss three strategies for kidney regeneration; one includes the induction of the endogenous repair through recruitment of natural kidney stem cells (Hopkins et al., 2009). Another requires the integration of exogenous cells, such as stem cells, into the damaged kidney tissue to repair it (Sagrinati et al., 2008), and third one focuses on creating a whole new kidney from stem cells for the purpose of transplantation (Naganuma & Nishinakamura, 2019).

The observation that ES cell-derived eUBs can connect and integrate into host epithelia raises the interesting possibility of creating new tissues to replace parts of damaged kidneys and grafting them in to connect to the CDs/ ureter of the host organ. This requires the connections to be possible even in older mature host kidneys. Data presented in this chapter demonstrated that the connection is possible in older kidneys in culture at least at the time points described. The next step would be to test the connection to adult kidneys, perhaps through culturing adult kidney tissue slices.

The connection was successful in all samples in which eUBs were induced to connect to older ureters, and all showed contractions after 7 days in culture. In MM, connection could be detected in some samples, however the condition of the MM interfered with the proper analysis of the connection. As known from previous studies, maturation and function of renal tissue rely on their vascularization and this is limited in static culture (Munro et al., 2017). It might be worth performing further analysis for the connection using adult kidneys in vivo.

Collectively, eUB grafts can connect to younger as well as older kidneys in culture, at least at the time points examined. This may open a new avenue in kidney regeneration, by allowing replacement of parts of a damaged kidney rather than replacement of the whole. This is not limited to kidney regeneration but may also extend to other parts of the lower urinary system such as the bladder and urethra, according to a recent study published by Joseph et al., 2018 which describes an unexpected role of Wolffian duct progenitors in bladder regeneration after injury.

Chapter 6. DISCUSSION

This chapter is dedicated to discussing the current approaches in the field of ureter engineering and potential applications of the work described in this thesis on the future of urinary tissue engineering and regeneration.

6.1 Summary

This project aimed to improve the existing kidney organoid model that lacked a single urinary exit, by adding a ureter. This is important, not only to improve the anatomical realism of these organoids, but also to provide transplanted organoids with a drainage pathway once they have been vascularized (Naguama and Nishinakamura, 2019).

The kidney tubular system, including CDs and ureters, derives from single epithelial outgrowth, the ureteric bud (reviewed by Saxen, 1987). Previous studies reported that the fate of the natural ureteric bud is governed by signals from the surrounding mesenchyme (Sweeney et la., 2008; Bohnenpoll et al., 2013). The MM mesenchymal signals include GDNF as a key signalling molecule that induces UB branching, while the peri-Wolffian mesenchyme expresses BMP4, which is the main factor in the process of urothelial differentiation (Michos et al., 2007; Costantini &Shakya, 2006). Using engineered UBs derived from mESCs and mouse fetal mesenchymal cells, I verified that eUBs possess the same plasticity as the natural UB.

The effect of the peri-Wolffian mesenchyme in urothelial development can be mimicked by the addition of BMP4 (Miyazaki et al., 2000; Mills et al., 2017). Based on that, I first tried to use the BMP4 bead strategy previously adopted by Mills et al., 2017 to induce urothelium in renogenic cell-derived organoids, in order to develop a ureter in Taguchi organoids. This method turned out to be impractical in these organoids, as they grow in an extracellular matrix-like gel which impedes the application of the beads.

The Mills method induced urothelial differentiation in renal cell-derived organoids, but these urothelial structures apparently did not develop smooth muscles or show peristaltic contractions (Mills et al., 2017).

It is believed that ureter mesenchyme is needed for smooth muscle development (Bohnenpoll et al., 2013). I therefore recruited host kidney mesenchymal cells either metanephric mesenchyme, or peri-Wolffian mesenchyme to differentiate the ES cell-derived eUBs toward a ureteric fate or CD fate, using grafting. I took two approaches to connect these eUB-derived CD/ureter-like tissues to host kidneys.

The first approach was to apply a micro-incision in the host tubular system at the site of engraftment to enhance connection between graft and host. The second approach was to build both CDs and ureter using the same eUB, by grafting into a mid-point between the two kidney mesenchymes. The latter was based on the results of grafting independent eUBs into MM or PWM.

Both methods produced ureter-like structures that showed spontaneous contractions. While the incision-based strategy produced only ureteric tissue that connected to the host ureter, it showed the possibility to work in older kidneys. The second method produced both a collecting duct tree and a contractile ureter-like structure in a realistic anatomical organization yet was only possible when using fetal tissues. This might have been because the signalling environment is thought to be different in older kidneys (Sweeney et al., 2008). Nevertheless, this could be an effective strategy to generate kidney organoids with a single urinary exit, first by developing protocols to differentiate the ES cells into PWM, and then finding ways to arrange the two renal mesenchymes in the correct developmental frame.

6.2 Clinical context of the work

The ureter is not a complicated structure like the kidney, yet it is by no means simple. In addition to its multilayer urothelium, the ureteric wall consists of an

active contractile smooth muscle layer arranged in two directions, lined by mucosa from the inside and adventitia from the outside (Bohnenpoll et al.,2013).

There are several disorders where the ureter, bladder and urethra can be damaged locally, for example in tumours, mechanical injury during gynaecological and pelvic surgeries, infections, and congenital anomalies (Tyritzis & Wiklund, 2015). These conditions need to be treated effectively to prevent extensive damage of the affected organ and the negative effect on the kidneys and other body organs.

Currently, physicians use reconstructive surgery to repair the damage and restore the lost function using 'autologous' tissue, most commonly an intestinal lobe (Gild et al., 2018). This is unsurprisingly associated with many complications such as metabolic disturbances, urolithiasis, and malignancy, particularly because these tissues are not prepared structurally to carry out the urinary excretion function. Despite the complications, this remains the gold standard method in treating urinary tract defects since no better option is available. Using an original urological tissue is preferable to tissue substitution, but the amount of redundant autologous urological tissue is very limited (Zamani et al., 2018).

Another proposed strategy to treat urinary tract defects is the use of scaffolds, which can be a natural decellularized tissue (Osman et al., 2004) or synthetic (Kloskowski et al., 2014). This approach appeared promising in terms of the size and the tubular shape of the tissue produced, but several post-operative complications are frequently reported including tissue fibrosis and stricture, obstruction, poor cellularization and renal hydronephrosis (Zamani., 2018). Pre-seeded scaffolds offered better outcomes in terms of cellular functions but similar complications such as obstruction, graft contracture, and hydronephrosis have been reported (Xue et al., 2016; El-Hakim et al., 2005). Engineering ureteric tissues, from patients own cells, and use it to replace the damaged parts might be a better solution.

6.3 Advantages and challenges

The distinctive microanatomical similarity and the functional contractility of the engineered ureteric tissue produced in this project, as well as their ability to connect and integrate into tissues of older kidneys, are favourable features compared with previous trials in ureteric engineering that lacked the original tissue resemblances and failed to show smooth muscle contractions (Xie et al., 2000; Kloskowski et al., 2014; de Jonge P. et al., 2018). Nevertheless, the fetal size and shape of these engineered tissues are still problematic.

Developing ways to increase the size of engineered tissues as well as their elongation into a tube is required for the proper use of these structures for repairing adult urinary tract defects. This could be either by transplanting them in vivo for some time to allow them to grow and mature, or by finding ways to grow them in vitro.

The connection and integration ability of the engineered tissue to older kidneys yield the potential for other tissue engineering and tissue regeneration applications not only for kidney and ureter but also for other urinary tissues such as the bladder and urethra. This was based on a recent study published by Joseph et al., 2018, which states that WD epithelial cells can support bladder regeneration. This could be used to repair a damaged part directly by implantation or indirectly as cellular component for a scaffold.

This method, however, was less successful in the metanephric mesenchymal region in older kidney, because the prolonged time of culture in vitro is likely to have affected the survival of both collecting ducts and eUB grafts. In vivo implantation might be a better approach as the presence of blood supply may be an advantage that could improve the survival and maturation of these grafts (Homan et al., 2019). Once this has been achieved, these tissues made from patient’s own iPS cells, could be used to replace parts of failed or resected kidneys instead of replacing the whole organ.

6.4 From mouse to human

Most of the current knowledge about kidney development and disease pathophysiology was obtained from animal studies, however these models have limitations. Although a lot of similarities to human tissue exist, there are significant differences between the mouse, the most studied animal model, and human genome (Pope et al., 2014; Yue et al., 2014).

Translating these techniques from mouse to human tissue is challenging because of the practical and ethical reasons that precludes the use human fetal material in such studies. Using human iPS cells to generate kidney organoids is a good alternative but the human models have been less successful than the mouse models (Little, 2019). This might be due to a lack of the proper knowledge of the accurate human developmental cues, nonetheless certain animal models may be quite informative (Taguchi and Nishinakamura, 2017).

An old study about cell association performed by Moscana, 1956 proposed that tissue specificity is stronger than the species differences. In other words, he found that tissues of the same histological type tend to integrate with each other when mixed, even if they are derived from different species, while mixing cells from two different tissue types, they tend to sort out despite being from the same animal. This had also been discussed by Steinberg in 1963 with his differential adhesion theory, however the exact mechanism is still not fully understood. Taking together the results of eUBs characterization, branching abilities as well as their integration with host epithelia, there is a solid evidence that the engineered eUBs derived from ES cells are the same tissue type as the natural UB.

An interesting approach that might help to improve our understanding of the human molecular signals and assess the differentiation status of human stem cell-derived kidney organoids despite the absence of comparative human tissue would be the formation of hybrid models. This could include testing the integration between iPSc derived UBs and natural fetal mouse UB using

reaggregation technique and explore the possibility of interaction between human cell derived UBs and mouse fetal mesenchymal cells using grafting technique.

6.5 Vascularization

The blood supply of kidneys and ureters arises from branches of the renal arteries, common iliac and gonadal arteries (Hallgrímsson et al., 2003). One disadvantage of the current organoids is their altered micro-physiological environment due to the lack of blood supply which might change some cellular characteristics (Homan et al., 2019).

Vascularization is essential not only for organoid survival in vivo, but also for organoid tissue maturation and function (Homan et al., 2019). Previous studies indicated that kidney organoids organized host-derived vascularization when transplanted into adult rodents. This has been shown using renogenic cell-derived organoids (Xinaris et al.,2012) and stem cell-derived organoids (van de Berg et al., 2018). Vascularization results of organoid in vivo implantation experiments are promising, yet more work is needed to incorporate vasculature into these organoids which is necessary for their cellular maturation and functional abilities.

The effect of vascularization on ES cell-derived kidney organoids with ureter or on engineered ureters alone has not yet been explored. This could be done by engrafting these organoids into the chorioallantoic membrane of developing chicks, or by in vivo transplantation into an adult rodent.

6.6 Final remarks

Formation of kidney organoids that connect to a contractile ureter as a single exit was the main aim of this thesis. I managed to generate ureter-like structures using ES cell-derived eUBs and mouse fetal PWM cells. These

eUBs could be induced to connect to host kidney in culture or form mini kidney -like organoids with ureter, using different grafting techniques. However, this could only be achieved using mouse fetal mesenchymal cells.

The next step would be to find ways to generate stem cell-derived peri-Wolffian mesenchyme (iPWM) and arrange them anatomically along with induced metanephric mesenchyme (iMM) around an engineered UB to attain an entirely induced organoids (stem cell-derived), with a single urinary exit. Additionally, testing the connection property using adult murine kidneys either in vivo or in vitro Once this has been achieved, introducing vascularization would be the next sensible step.

Finally, for this to be clinically valuable, more work is needed in order to tackle the challenges stated above and to transfer these methods from mouse to human. An additional experimental step using large animals is usually required before going to human trials, particularly for new and high-risk techniques.

7. References

Agarwal, S., & John, P. A. (1988). Studies on the development of the kidney of the guppy, Lebistes reticulatus, part 1. The development of the pronephros. *J Anim Morphol Physiol*, *35*, 17-24.

Airik, R., & Kispert, A. (2007). Down the tube of obstructive nephropathies: the importance of tissue interactions during ureter development. *Kidney international*, *72*(12), 1459-1467.

Airik, R., Bussen, M., Singh, M.K., Petry, M. and Kispert, A. (2006) Tbx18 regulates the development of the ureteral mesenchyme. J. Clin. Invest., 116, 663–674.

Airik, R., Trowe, M. O., Foik, A., Farin, H. F., Petry, M., Schuster-Gossler, K., ... & Kispert, A. (2010). Hydroureternephrosis due to loss of Sox9-regulated smooth muscle cell differentiation of the ureteric mesenchyme. *Human molecular genetics*, *19*(24), 4918-4929.

Alcorn, D., Maric, C., Mc Causland, J., 1999. Development of the renal interstitium. Pediatr.Nephrol.13,347–354.

Barbuti, A., & DiFrancesco, D. (2008). Control of cardiac rate by "funny" channels in health and disease. *Annals of the New York Academy of Sciences*, *1123*(1), 213-223.

Basson, M. A., Akbulut, S., Watson-Johnson, J., Simon, R., Carroll, T. J., Shakya, R., ... & Wilson, P. D. (2005). Sprouty1 is a critical regulator of GDNF/RET-mediated kidney induction. *Developmental cell*, *8*(2), 229-239.

Batourina, E., Choi, C., Paragas, N., Bello, N., Hensle, T., Costantini, F. D., ... & Mendelsohn, C. L. (2002). Distal ureter morphogenesis depends on epithelial cell remodeling mediated by vitamin A and Ret. *Nature genetics*, *32*(1), 109-115.

Batourina, E., Gim, S., Bello, N., Shy, M., Clagett-Dame, M., Srinivas, S., ... & Mendelsohn, C. (2001). Vitamin A controls epithelial/mesenchymal interactions through Ret expression. *Nature genetics*, *27*(1), 74-78.

Becker, A., & Baum, M. (2006). Obstructive uropathy. Early human development, 82(1), 15-22.

Bellairs, R. (1986). The primitive streak. Anatomy and embryology, 174(1), 1-14.

Bertram, J. F. (2001). Counting in the kidney. Kidney international, 59(2), 792-796.

Biel, M., Wahl-Schott, C., Michalakis, S., & Zong, X. (2009). Hyperpolarization-activated cation channels: from genes to function. Physiological reviews, 89(3), 847-885.

Bohnenpoll T, Wittern AB, Mamo TM, Weiss AC, Rudat C, Kleppa MJ, Schuster-Gossler K, Wojahn I, Lüdtke TH, Trowe MO, Kispert A. (2017) A SHH-FOXF1-BMP4 signaling axis regulating growth and differentiation of epithelial and mesenchymal tissues in ureter development. PLoS Genet. 2017 Aug 10;13(8):e1006951.

Bohnenpoll, T., & Kispert, A. (2014, December). Ureter growth and differentiation. In Seminars in cell & developmental biology (Vol. 36, pp. 21-30). Academic Press.

Bohnenpoll, T., Bettenhausen, E., Weiss, A. C., Foik, A. B., Trowe, M. O., Blank, P., ... & Kispert, A. (2013). Tbx18 expression demarcates multipotent precursor populations in the developing urogenital system but is exclusively required within the ureteric mesenchymal lineage to suppress a renal stromal fate. Developmental biology, 380(1), 25-36.

Bouchard, M., Pfeffer, P., & Busslinger, M. (2000). Functional equivalence of the transcription factors Pax2 and Pax5 in mouse development. Development, 127(17), 3703-3713.

Bouchard, M., Souabni, A., Mandler, M., Neubuser, A. & Busslinger, M. Nephric lineage specification by PAX2 and PAX8. Genes Dev. 16, 2958-2970 (2002).

Bremer M, Doerge RW: Statistics at the Bench, NY, Cold Spring Harbor Laboratory Press, 2010

Brenner-Anantharam, A., Cebrian, C., Guillaume, R., Hurtado, R., Sun, T. T., & Herzlinger, D. (2007). Tailbud-derived mesenchyme promotes urinary tract segmentation via BMP4 signaling. Development, 134(10), 1967-1975.

Brophy, P. D., Ostrom, L., Lang, K. M., & Dressler, G. R. (2001). Regulation of ureteric bud outgrowth by Pax2-dependent activation of the glial derived neurotrophic factor gene. Development, 128(23), 4747-4756.

Brunskill, E. W., Aronow, B. J., Georgas, K., Rumballe, B., Valerius, M. T., Aronow, J., ... & Potter, S. S. (2008). Atlas of gene expression in the developing kidney at microanatomic resolution. *Developmental cell*, *15*(5), 781-791.

Burdyga, T., & Wray, S. (2005). Action potential refractory period in ureter smooth muscle is set by Ca sparks and BK channels. Nature, 436(7050), 559-562.

Bussen, M, et al. The T-box transcription factor Tbx18 maintains the separation of anterior and posterior somite compartments. Genes Dev. 2004. **18**:1209-1221.

Cain, J. E., Islam, E., Haxho, F., Blake, J., & Rosenblum, N. D. (2011). GLI3 repressor controls functional development of the mouse ureter. The Journal of clinical investigation, 121(3), 1199-1206.

Carroll, T. J., Park, J. S., Hayashi, S., Majumdar, A. and McMahon, A. P. (2005). Wnt9b plays a central role in the regulation of mesenchymal to epithelial transitions underlying organogenesis of the mammalian urogenital system. Dev. Cell 9, 283-292.

Caubit, X., Lye, C. M., Martin, E., Coré, N., Long, D. A., Vola, C., … & Fasano, L. (2008). Teashirt 3 is necessary for ureteral smooth muscle differentiation downstream of SHH and BMP4. Development, 135(19), 3301-3310.

Cebrian, C., Borodo, K., Charles, N. and Herzlinger, D. A. (2004). Morphometric index of the developing murine kidney. Dev. Dyn. 231, 601-608.

Chevalier, R. L., & Peters, C. A. (2003). Congenital urinary tract obstruction: proceedings of the state-of-the-art strategic planning workshop—National Institutes of Health, Bethesda, Maryland, USA, 11–12 March 2002. Pediatric Nephrology, 18(6), 576-606.

Chishti, A. S., Alam, S., & Kiessling, S. G. (Eds.). (2014). Kidney and Urinary Tract Diseases in the Newborn. New York: Springer.

Constantinou, C. E. (1978). Contractility of the pyeloureteral pacemaker system. Urologia internationalis, 33(6), 399-416.

Costantini, F. & Shakya, R. GDNF/RET signaling and the development of the kidney. Bioessays 28, 117-127 (2006).

Costantini, F., & Kopan, R. (2010). Patterning a complex organ: branching morphogenesis and nephron segmentation in kidney development. Developmental cell, 18(5), 698-712.

Costantini, F., and Shakya, R. (2006). GDNF/Ret signaling and the development of the kidney. Bioessays 28, 117–127.

Crelin, E. S. (1978). Normal and abnormal development of ureter. Urology, 12(1), 2-7.

Cullen-McEwen, L. A., Caruana, G., & Bertram, J. F. (2005). The where, what and why of the developing renal stroma. Nephron Experimental Nephrology, 99(1), e1-e8.

Das, A., Tanigawa, S., Karner, C. M., Xin, M., Lum, L., Chen, C., ... & Carroll, T. J. (2013). Stromal–epithelial crosstalk regulates kidney progenitor cell differentiation. Nature cell biology, 15(9), 1035-1044.

David, S. G., Cebrian, C., Vaughan, E. D., & Herzlinger, D. (2005). C-kit and ureteral peristalsis. The Journal of urology, 173(1), 292-295.

Davies JA, Chang C-H, Lawrence ML, Mills CG, Mullins JJ (2014) Engineered kidneys: principles, progress and prospects. Adv. Regen Biol. 1: 24990
Davies, J. A., & Chang, C. H. (2014). Engineering kidneys from simple cell suspensions: an exercise in self-organization. Pediatric Nephrology, 29(4), 519-524.

Davies, J. A., Hohenstein, P., Chang, C. H., & Berry, R. (2014). A self-avoidance mechanism in patterning of the urinary collecting duct tree. BMC Dev Biol, 14:35. doi: 10.1186/s12861-014-0035-8.

de Jonge, P., Simaioforidis, V., Geutjes, P., Oosterwijk, E., and Feitz, W. (2018). Ureteral reconstruction with reinforced collagen scaffolds in a porcine model. J. Tissue Eng. Regener. Med. 12, 80–88. doi: 10.1002/term.2366

Dressler, G. R. (1999). Kidney development branches out. Developmental genetics, 24(3-4), 189-193.

Dressler, G. R., Deutsch, U. R. B. A. N., Chowdhury, K. A. M. A. L., Nornes, H. O., & Gruss, P. E. T. E. R. (1990). Pax2, a new murine paired-box-containing gene and its expression in the developing excretory system. Development, 109(4), 787-795.

Dudley, A. T., Godin, R. E., & Robertson, E. J. (1999). Interaction between FGF and BMP signaling pathways regulates development of metanephric mesenchyme. Genes & development, 13(12), 1601-1613.

Duester, G. (2001). Genetic dissection of retinoid dehydrogenases. Chemico-biological interactions, 130, 469-480.

Dunn N. R., Winnier G. E., Hargett L. K., Schrick J. J., Fogo A. B., Hogan B. L. (1997). Haploinsufficient phenotypes in Bmp4 heterozygous null mice and modification by mutations in Gli3 and Alx4. Dev. Biol. **188**, 235–247

Enomoto, H., Crawford, P. A., Gorodinsky, A., Heuckeroth, R. O., Johnson, E. M., & Milbrandt, J. (2001). RET signaling is essential for migration, axonal growth and axon guidance of developing sympathetic neurons. Development, 128(20), 3963-3974.

Eswarakumar, V. P., Lax, I., & Schlessinger, J. (2005). Cellular signaling by fibroblast growth factor receptors. Cytokine & growth factor reviews, 16(2), 139-149.

Evans, M. J., & Kaufman, M. H. (1981). Establishment in culture of pluripotential cells from mouse embryos. nature, 292(5819), 154-156.

Fatehullah, A., Tan, S. H., & Barker, N. (2016). Organoids as an in vitro model of human development and disease. Nature cell biology, 18(3), 246-254.

Figueira EC, Di Girolamo N, Coroneo MT, Wakefield D (2007) The phenotype of limbal epithelial stem cells. Invest Ophthalmol Vis Sci 48: 144-156. doi:10.1167/iovs.06-0346.

Fourman, J., & Moffat, D. B. (1971). The blood vessels of the kidney. Wiley-Blackwell.

Freedman BS, Brooks CR, Lam AQ, Fu H, Morizane R, Agrawal V, Saad AF, Li MK, Hughes MR, Werff RV, Peters DT, Lu J, Bac-cei A, Siedlecki AM, Valerius MT,

Musunuru K, McNagny KM, Steinman TI, Zhou J, Lerou PH, Bonventre JV (2015) Modelling kidney disease with CRISPR-mutant kidney organoids derived from human pluripotent epiblast spheroids. Nat Commun 6:8715

Frimann-Dahl, J. (1961). Normal variations of the left kidney: an anatomical and radiologic study. Acta radiologica, (3), 207-216.

Gandhi, D., Molotkov, A., Batourina, E., Schneider, K., Dan, H., Reiley, M.,Laufer, E., Metzger, D., Liang, F., Liao, Y. et al. (2013). Retinoid signaling in progenitors controls specification and regeneration of the urothelium. Dev. Cell **26**, 469-482. doi:10.1016/j.devcel.2013.07.017

Ganeva, V., Unbekandt, M., & Davies, J. A. (2011). An improved kidney dissociation and reaggregation culture system results in nephrons arranged organotypically around a single collecting duct system. Organogenesis, 7(2), 83-87.

Garza LA, Yang CC, Zhao T, Blatt HB, Lee M et al. (2011) Bald scalp in men with androgenetic alopecia retains hair follicle stem cells but lacks CD200-rich and CD34-positive hair follicle progenitor cells. J Clin Invest 121: 613-622. doi: 10.1172/JCI44478. PubMed: 21206086.

Georgas, K., Rumballe, B., Valerius, M. T., Chiu, H. S., Thiagarajan, R. D., Lesieur, E., ... & Little, M. H. (2009). Analysis of early nephron patterning reveals a role for distal RV proliferation in fusion to the ureteric tip via a cap mesenchyme-derived connecting segment. Developmental biology, 332(2), 273-286.

Gild, P., Kluth, L. A., Vetterlein, M. W., Engel, O., Chun, F. K., and Fisch, M. (2018). Adult iatrogenic ureteral injury and stricture–incidence and treatment strategies. Asian J. Urol. 5, 101–106. doi: 10.1016/j.ajur.2018.02.003

Golenhofen, K., & Hannappel, J. (1973). Normal spontaneous activity of the pyeloureteral system in the guinea-pig. Pflügers Archiv, 341(3), 257-270.

Gosling, J. A., & Dixon, J. S. (1970). Further observations on upper urinary tract smooth muscle. Zeitschrift für Zellforschung und Mikroskopische Anatomie, 108(1), 127-134.

Gosling, J. A., & Dixon, J. S. (1971). Morphologic evidence that the renal calyx and pelvis control ureteric activity in the rabbit. American Journal of Anatomy, 130(4), 393-407.

Grieshammer, U. et al . SLIT2-mediated ROBO2 signaling restricts kidney induction to a single site. Dev. Cell 6, 709-717 (2004).

Grobstein, C. (1953). Inductive epithelio-mesenchymal interaction in cultured organ rudiments of the mouse. Science, 118(3054), 52-55.

Grobstein, C. (1953). Morphogenetic interaction between embryonic mouse tissues separated by a membrane filter. Nature, 172(4384), 869-871.

Grote, D., Boualia, S. K., Souabni, A., Merkel, C., Chi, X., Costantini, F., ... & Bouchard, M. (2008). Gata3 acts downstream of β-catenin signaling to prevent ectopic metanephric kidney induction. PLoS Genet, 4(12), e1000316.

Grote, D., Souabni, A., Busslinger, M., & Bouchard, M. (2006). Pax2/8-regulated Gata3 expression is necessary for morphogenesis and guidance of the nephric duct in the developing kidney. Development, 133(1), 53-61.

Hale, E. H. (1952). The Kidney: Structure and Function in Health and Disease. Journal of the National Medical Association, 44(3), 239.

Hallgrímsson, B., Benediktsson, H., & Vize, P. D. (2003). Anatomy and histology of the human urinary system. In The Kidney (pp. 149-164). Academic Press.

Hatini, V., Huh, S.O., Herzlinger, D., Soares,V.C., Lai,E., 1996. Essential role of stromal mesenchyme in kidney morphogenesis revealed by targeted disruption of Winged Helix transcription factor BF-2. Genes Dev.10,1467–1478.

Hellmich, H. L., Kos, L., Cho, E. S., Mahon, K. A., & Zimmer, A. (1996). Embryonic expression of glial cell-line derived neurotrophic factor (GDNF) suggests multiple developmental roles in neural differentiation and epithelial-mesenchymal interactions. Mechanisms of development, 54(1), 95-105.

Hicks, R. M. (1965). The fine structure of the transitional epithelium of rat ureter. The Journal of cell biology, 26(1), 25-48.

Hinchliffe, S. A., Sargent, P. H., Howard, C. V., Chan, Y. F., & Van Velzen, D. (1991). Human intrauterine renal growth expressed in absolute number of glomeruli assessed by the disector method and Cavalieri principle. Laboratory investigation; a journal of technical methods and pathology, 64(6), 777.

Homan, K. A., Gupta, N., Kroll, K. T., Kolesky, D. B., Skylar-Scott, M., Miyoshi, T., ... & Lewis, J. A. (2019). Flow-enhanced vascularization and maturation of kidney organoids in vitro. Nature methods, 16(3), 255-262.

Hopkins, C., Li, J., Rae, F., & Little, M. H. (2009). Stem cell options for kidney disease. The Journal of Pathology: A Journal of the Pathological Society of Great Britain and Ireland, 217(2), 265-281.

Humphreys, B. D., Valerius, M. T., Kobayashi, A., Mugford, J. W., Soeung, S., Duffield, J. S., ... & Bonventre, J. V. (2008). Intrinsic epithelial cells repair the kidney after injury. Cell stem cell, 2(3), 284-291.

Hurtado, R., Bub, G., & Herzlinger, D. (2010). The pelvis–kidney junction contains HCN3, a hyperpolarization-activated cation channel that triggers ureter peristalsis. Kidney international, 77(6), 500-508.

Imberty A, Casset F, Gegg CV, Etzler ME, Perez S (1994) Molecular modelling of the Dolichos biflorus seed lectin and its specific interactions with carbohydrates: alpha-D-N-acetylgalactosamine, Forssman disaccharide and blood group A trisaccharide. Glycoconj J 11, 400–413

James, R. G., & Schultheiss, T. M. (2005). Bmp signaling promotes intermediate mesoderm gene expression in a dose-dependent, cell-autonomous and translation-dependent manner. Developmental biology, 288(1), 113-125.

Jenkins, D., & Woolf, A. S. (2007). Uroplakins: new molecular players in the biology of urinary tract malformations. Kidney international, 71(3), 195-200.

Joseph, D. B., Chandrashekar, A. S., Abler, L. L., Chu, L. F., Thomson, J. A., Mendelsohn, C., & Vezina, C. M. (2018). In vivo replacement of damaged bladder urothelium by Wolffian duct epithelial cells. Proceedings of the National Academy of Sciences, 115(33), 8394-8399.

Kent, J., Wheatley, S. C., Andrews, J. E., Sinclair, A. H. and Koopman, P. (1996). A male-specific role for SOX9 in vertebrate sex determination. Development 122, 2813-2822.

Kim D, Dressler GR. (2005) Nephrogenic factors promote differentiation of mouse embryonic stem cells into renal epithelia. J Am Soc Nephrol. 16(12):3527-34

Kispert, A. (2013). Tbx18 expression demarcates multipotent precursor populations in the developing urogenital system but is exclusively required within the ureteric mesenchymal lineage to suppress a renal stromal fate. Developmental biology, 380(1), 25-36.

Kispert, A., Vainio, S., Shen, L., Rowitch, D. H. and McMahon, A. P. (1996). Proteoglycans are required for maintenance of Wnt-11 expression in the ureter tips. Development 122, 3627-3637.

Kiviat, M. D., Ross, R., & Ansell, J. S. (1973). Smooth muscle regeneration in the ureter: electron microscopic and autoradiographic observations. The American journal of pathology, 72(3), 403.

Kloskowski, T., Jundziłł, A., Kowalczyk, T., Nowacki, M., Bodnar, M., Marszałek, A., et al. (2014). Ureter regeneration–the proper scaffold has to be defined. PLoS One 9:e106023. doi: 10.1371/journal.pone.0106023

Kloth, S., Aigner, J., Schmidbauer, A., & Minuth, W. W. (1994). Interrelationship of renal vascular development and nephrogenesis. Cell and tissue research, 277(2), 247-257.

Kobayashi, A., Mugford, J. W., Krautzberger, A. M., Naiman, N., Liao, J., & McMahon, A. P. (2014). Identification of a multipotent self-renewing stromal progenitor population during mammalian kidney organogenesis. Stem cell reports, 3(4), 650-662.

Koning, M., van den Berg, C. W., & Rabelink, T. J. (2020). Stem cell-derived kidney organoids: engineering the vasculature. Cellular and Molecular Life Sciences, 77(12), 2257-2273.

Köster, M., Plessow, S., Clement, J. H., Lorenz, A., Tiedemann, H., & Knöchel, W. (1991). Bone morphogenetic protein 4 (BMP-4), a member of the TGF-β family, in early embryos of Xenopus laevis: analysis of mesoderm inducing activity. Mechanisms of development, 33(3), 191-199.

Kreidberg, J. A. (1996). Gene targeting in kidney development. Medical and Pediatric Oncology: The Official Journal of SIOP—International Society of Pediatric Oncology (Societé Internationale d'Oncologie Pédiatrique, 27(5), 445-452.

Kriz, W., & Kaissling, B. (1992). Structural organization of the mammalian kidney. The kidney: physiology and pathophysiology, 3, 587-654.

Kriz, W., & Koepsell, H. (1974). The structural organization of the mouse kidney. Zeitschrift für Anatomie und Entwicklungsgeschichte, 144(2), 137-163.

Kumar, S., Bogle, R., & Banerjee, D. (2014). Why do young people with chronic kidney disease die early?. World journal of nephrology, 3(4), 143.

Kume, T., Deng, K. & Hogan, B. L. Murine forkhead/winged helix genes Foxc1 (Mf1) and Foxc2 (Mfh1) are required for the early organogenesis of the kidney and urinary tract. Development 127, 1387-1395 (2000).

Lam, A. Q., Freedman, B. S., Morizane, R., Lerou, P. H., Valerius, M. T., & Bonventre, J. V. (2014). Rapid and efficient differentiation of human pluripotent stem cells into intermediate mesoderm that forms tubules expressing kidney proximal tubular markers. Journal of the American Society of Nephrology, 25(6), 1211-1225.

Lang RJ, Hashitani H, Tonta MA, Bourke JL, Parkington HC, Suzuki H: Spontaneous electrical and Ca21 signals in the mouse renal pelvis that drive pyeloureteric peristalsis. Clin Exp Pharmacol Physiol 37: 509–515, 2010

Lang, R. J., & Hashitani, H. (2019). Pacemaker mechanisms driving pyeloureteric peristalsis: Modulatory role of interstitial cells. Smooth Muscle Spontaneous Activity, 77-101.

Lang, S. H., Stark, M., Collins, A., Paul, A. B., Stower, M. J., & Maitland, N. J. (2001). Experimental prostate epithelial morphogenesis in response to stroma and three-dimensional matrigel culture. Cell Growth and Differentiation-Publication American Association for Cancer Research, 12(12), 631-640.

Lawrence, M. L., Chang, C. H., & Davies, J. A. (2015). Transport of organic anions and cations in murine embryonic kidney development and in serially-reaggregated engineered kidneys. Scientific reports, 5(1), 1-8.

Lechner, M. S., & Dressler, G. R. (1997). The molecular basis of embryonic kidney development. Mechanisms of development, 62(2), 105-120.

Leube RE, Bader BL, Bosch FX, Zimbelmann R, Achtstaetter T et al. (1988) Molecular characterization and expression of the stratification-related cytokeratins 4 and 15. J Cell Biol 106: 1249-1261. doi: 10.1083/jcb.106.4.1249. PubMed: 2452170.

Leube, R., Bader, B. L., Bosch, F. X., Zimbelmann, R., Achtstaetter, T., & Franke, W. W. (1988). Molecular characterization and expression of the stratification-related cytokeratins 4 and 15. The Journal of cell biology, 106(4), 1249-1261.

Lewis, S. A., & de Moura, J. L. (1982). Incorporation of cytoplasmic vesicles into apical membrane of mammalian urinary bladder epithelium. Nature, 297(5868), 685-688.

Little, M. H., & Combes, A. N. (2019). Kidney organoids: accurate models or fortunate accidents. Genes & development, 33(19-20), 1319-1345.

Little, M. H., & McMahon, A. P. (2012). Mammalian kidney development: principles, progress, and projections. Cold Spring Harbor perspectives in biology, 4(5), a008300.

Little, M. H., Brennan, J., Georgas, K., Davies, J. A., Davidson, D. R., Baldock, R. A., Beverdam, A., Bertram, J. F., Capel, B., Chiu, H. S., Clements, D., Cullen-McEwen, L., Fleming, J., Gilbert, T., Herzlinger, D., Houghton, D., Kaufman, M. H.,

Kleymenova, E., Koopman, P. A., Lewis, A. G., … Yu, J. (2007). A high-resolution anatomical ontology of the developing murine genitourinary tract. Gene expression patterns : GEP, 7(6), 680–699. https://doi.org/10.1016/j.modgep.2007.03.002

Lopez, M. L. S. S., & Gomez, R. A. (2011). Development of the renal arterioles. Journal of the American Society of Nephrology, 22(12), 2156-2165.

Ludwig, K. S., & Landmann, L. (2005). Early development of the human mesonephros. Anatomy and embryology, 209(6), 439-447.

Lye, C. M., Fasano, L., & Woolf, A. S. (2010). Ureter myogenesis: putting Teashirt into context. Journal of the American Society of Nephrology, 21(1), 24-30.

Maddaluno, L., Urwyler, C., & Werner, S. (2017). Fibroblast growth factors: key players in regeneration and tissue repair. Development, 144(22), 4047-4060.

Mae, S. I., Shono, A., Shiota, F., Yasuno, T., Kajiwara, M., Gotoda-Nishimura, N., ... & Osafune, K. (2013). Monitoring and robust induction of nephrogenic intermediate mesoderm from human pluripotent stem cells. Nature communications, 4(1), 1-11.

Maggi, C. A., & Giuliani, S. (1991). The neurotransmitter role of calcitonin gene-related peptide in the rat and guinea-pig ureter: effect of a calcitonin gene-related peptide antagonist and species-related differences in the action of omega conotoxin on calcitonin gene-related peptide release from primary afferents. Neuroscience, 43(1), 261-268.

Marcotte, M., Sharma, R., & Bouchard, M. (2014). Gene regulatory network of renal primordium development. Pediatric nephrology, 29(4), 637-644.

Maretto, S., Cordenonsi, M., Dupont, S., Braghetta, P., Broccoli, V., Hassan, A. B., ... & Piccolo, S. (2003). Mapping Wnt/β-catenin signaling during mouse development and in colorectal tumors. Proceedings of the National Academy of Sciences, 100(6), 3299-3304.

Martin, G. R. (1981). Isolation of a pluripotent cell line from early mouse embryos cultured in medium conditioned by teratocarcinoma stem cells. Proceedings of the National Academy of Sciences, 78(12), 7634-7638.

Mauney JR, Ramachandran A, Yu RN, Daley GQ, Adam RM, Estrada CR. All-trans retinoic acid directs urothelial specification of murine embryonic stem cells via GATA4/6 signaling mechanisms. PloS one. 2010;5:e11513.

Mendelsohn, C., Batourina, E., Fung, S., Gilbert, T., Dodd, J., 1999. Stromal cells mediate retinoid-dependent functions essential for renal development. Devel- opment 126,1139–1148.

Metzger, R., Schuster, T., Till, H., Stehr, M., Franke, F. E., & Dietz, H. G. (2004). Cajal-like cells in the human upper urinary tract. The Journal of urology, 172(2), 769-772.

Michael, L., Sweeney, D. E. and Davies, J. A. (2007). The lectin Dolichos biflorus agglutinin is a sensitive indicator of branching morphogenetic activity in the developing mouse

Michos, O. (2009). Kidney development: from ureteric bud formation to branching morphogenesis. Current opinion in genetics & development, 19(5), 484-490.

Michos, O., Gonçalves, A., Lopez-Rios, J., Tiecke, E., Naillat, F., Beier, K., ... & Zeller, R. (2007). Reduction of BMP4 activity by gremlin 1 enables ureteric bud outgrowth and GDNF/WNT11 feedback signalling during kidney branching morphogenesis. Development, 134(13), 2397-2405.

Mills, C. G., Lawrence, M. L., Munro, D. A., Elhendawi, M., Mullins, J. J., & Davies, J. A. (2017). Asymmetric BMP4 signalling improves the realism of kidney organoids. Scientific Reports, 7(1), 1-8.

Miyazaki, Y., Oshima, K., Fogo, A. and Ichikawa, I. (2003). Evidence that bone morphogenetic protein 4 has multiple biological functions during kidney and urinary tract development. Kidney Int. 63, 835-844.

Miyazaki, Y., Oshima, K., Fogo, A., Hogan, B. L., & Ichikawa, I. (2000). Bone morphogenetic protein 4 regulates the budding site and elongation of the mouse ureter. The Journal of clinical investigation, 105(7), 863-873.

Moffat, D. B. (1975). The mammalian kidney (Vol. 5). CUP Archive.

Moritz, K. M., Bertram, J. F., Black, M. J., Caruana, G., & Wintour-Coghlan, M. (2008). Factors influencing mammalian kidney development: implications for health in adult life (pp. 10-12). Springer.

Morizane R, Lam AQ, Freedman BS, Kishi S, Valerius MT, Bonventre JV. (2015) Nephron organoids derived from human pluripotent stem cells model kidney development and injury. Nat Biotechnol. 33(11):1193-200

Morizane, R., & Bonventre, J. V. (2017). Kidney organoids: a translational journey. Trends in molecular medicine, 23(3), 246-263.

Moscona, A. (1956). Development of heterotypic combinations of dissociated embryonic chick cells. Proceedings of the Society for Experimental Biology and Medicine, 92(2), 410-416.

Mullenders, J., de Jongh, E., Brousali, A., Roosen, M., Blom, J. P., Begthel, H., ... & Clevers, H. C. (2019). Mouse and human urothelial cancer organoids: A tool for bladder cancer research. Proceedings of the National Academy of Sciences, 116(10), 4567-4574.

Munro DAD, Hohenstein P, Davies JA. Cycles of vascular plexus formation within the nephrogenic zone of the developing mouse kidney. Sci Rep. 2017 Jun 12;7(1):3273. doi: 10.1038/s41598-017-03808-4.

Mysorekar, I. U., Mulvey, M. A., Hultgren, S. J., & Gordon, J. I. (2002). Molecular regulation of urothelial renewal and host defenses during infection with uropathogenic Escherichia coli. Journal of Biological Chemistry, 277(9), 7412-7419.

Naganuma, H., & Nishinakamura, R. (2019). From organoids to transplantable artificial kidneys. Transplant International, 32(6), 563-570.

Napoli, J. L. (1999). Interactions of retinoid binding proteins and enzymes in retinoid metabolism. Biochimica et Biophysica Acta (BBA)-Molecular and Cell Biology of Lipids, 1440(2-3), 139-162.

Narath, P. A. (1951). Renal pelvis and ureter. Grune & Stratton.

Ng, J. K. C., & Li, P. K. T. (2018). Chronic kidney disease epidemic: how do we deal with it?. Nephrology, 23, 116-120.

Niederreither, K., Ward, S. J., Dollé, P., & Chambon, P. (1996). Morphological and molecular characterization of retinoic acid-induced limb duplications in mice. Developmental biology, 176(2), 185-198.

Nishinakamura, R. (2019). Human kidney organoids: progress and remaining challenges. Nature Reviews Nephrology, 15(10), 613-624.

Nishinakamura, R., & Sakaguchi, M. (2014). BMP signaling and its modifiers in kidney development. Pediatric nephrology, 29(4), 681-686.

Oliver, G., Wehr, R., Jenkins, N. A., Copeland, N. G., Cheyette, B. N., Hartenstein, V., Zipursky, S. L. and Gruss, P. (1995) 'Homeobox genes and connective tissue patterning.', Development, 121(3), pp. 693–705.

Osborn, S. L., Thangappan, R., Luria, A., Lee, J. H., Nolta, J., & Kurzrock, E. A. (2014). Induction of human embryonic and induced pluripotent stem cells into urothelium. Stem Cells Transl. Med. 3: 610-619

Osman, Y., Shokeir, A., Gabr, M., El-Tabey, N., Mohsen, T., and El-Baz, M. (2004). Canine ureteral replacement with long acellular matrix tube: is it clinically applicable? J. Urol. 172, 1151–1154. doi: 10.1097/01.ju.0000134886.44065.00

Pauli, B. U., Gruber, A. D., & Weinstein, R. S. (1998). Transitional epithelium, bladder, rat. In Urinary System (pp. 323-330). Springer, Berlin, Heidelberg.

Paulie, S., Hansson, Y., Lundblad, M. L., & Perlmann, P. (1983). Lectins as probes for identification of tumor-associated antigens on urothelial and colonic carcinoma cell lines. International journal of cancer, 31(3), 297-303.

Pezzone, M. A., Watkins, S. C., Alber, S. M., King, W. E., de Groat, W. C., Chancellor, M. B., & Fraser, M. O. (2003). Identification of c-kit-positive cells in the mouse ureter: the interstitial cells of Cajal of the urinary tract. American Journal of Physiology-Renal Physiology, 284(5), F925-F929.

Pfeiffer, E. W. (1968). Comparative anatomical observations of the mammalian renal pelvis and medulla. Journal of anatomy, 102(Pt 2), 321.

Pope, B. D., Ryba, T., Dileep, V., Yue, F., Wu, W., Denas, O., ... & Gilbert, D. M. (2014). Topologically associating domains are stable units of replication-timing regulation. *Nature*, *515*(7527), 402-405.

Porter, K.R. & Bonneville, M.A. (1963) Fine Structure of Cells and Tissues, 2nd edn. Lea and Febiger, Philadelphia.

Potter, E. L. (1972). Normal and abnormal development of the kidney. Year Book Medical publishers Inc, Chicago.

Przepiorski, A., Sander, V., Tran, T., Hollywood, J. A., Sorrenson, B., Shih, J. H., ... & Davidson, A. J. (2018). A simple bioreactor-based method to generate kidney organoids from pluripotent stem cells. Stem Cell Reports, 11(2), 470-484.

Qiao J, Bush K.T, Steer D.L, Stuart R.O, Sakurai H, Wachsman W, Nigam S.K. Multiple fibroblast growth factors support growth of the ureteric bud but have different effects on branching morphogenesis. Mech Dev. 2001;109:123–135.

Qiao, J., Sakurai, H., & Nigam, S. K. (1999). Branching morphogenesis independent of mesenchymal–epithelial contact in the developing kidney. Proceedings of the National Academy of Sciences, 96(13), 7330-7335.

Rae, F., Woods, K., Sasmono, T., Campanale, N., Taylor, D., Ovchinnikov, D. A., ... & Little, M. H. (2007). Characterisation and trophic functions of murine embryonic macrophages based upon the use of a Csf1r–EGFP transgene reporter. Developmental biology, 308(1), 232-246.

Redempta Vetter, S. M., & Gibley Jr, C. W. (1966). Morphogenesis and histochemistry of the developing mouse kidney. Journal of morphology, 120(2), 135-155.

Reginensi, A., Clarkson, M., Neirijnck, Y., Lu, B., Ohyama, T., Groves, A. K., ... & Schedl, A. (2011). SOX9 controls epithelial branching by activating RET effector genes during kidney development. Human molecular genetics, 20(6), 1143-1153.

Rosines, E., Sampogna, R. V., Johkura, K., Vaughn, D. A., Choi, Y., Sakurai, H., ... & Nigam, S. K. (2007). Staged in vitro reconstitution and implantation of engineered rat kidney tissue. Proceedings of the National Academy of Sciences, 104(52), 20938-20943.

Rosselot, C., Spraggon, L., Chia, I., Batourina, E., Riccio, P., Lu, B., ... & Mendelsohn, C. (2010). Non-cell-autonomous retinoid signaling is crucial for renal development. Development, 137(2), 283-292.

Ryan, D., Sutherland, M. R., Flores, T. J., Kent, A. L., Dahlstrom, J. E., Puelles, V. G., ... & Black, M. J. (2018). Development of the human fetal kidney from mid to late gestation in male and female infants. EBioMedicine, 27, 275-283.

Sacktor, T. C., Osten, P., Valsamis, H., Jiang, X., Naik, M. U., & Sublette, E. (1993). Persistent activation of the zeta isoform of protein kinase C in the maintenance of long-term potentiation. Proceedings of the National Academy of Sciences, 90(18), 8342-8346

Sagrinati, C., Ronconi, E., Lazzeri, E., Lasagni, L., & Romagnani, P. (2008). Stem-cell approaches for kidney repair: choosing the right cells. Trends in molecular medicine, 14(7), 277-285.

Sainio, K. I. R. S. I., & Raatikainen-Ahokas, A. N. N. E. (2003). Mesonephric kidney--a stem cell factory?. International Journal of Developmental Biology, 43(5), 435-439.

Sainio, K., Suvanto, P., Davies, J., Wartiovaara, J., Wartiovaara, K., Saarma, M., ... & Sariola, H. (1997). Glial-cell-line-derived neurotrophic factor is required for bud initiation from ureteric epithelium. Development, 124(20), 4077-4087.

Sakurai, H., Barros, E. J., Tsukamoto, T., Barasch, J., & Nigam, S. K. (1997). An in vitro tubulogenesis system using cell lines derived from the embryonic kidney shows dependence on multiple soluble growth factors. Proceedings of the National Academy of Sciences, 94(12), 6279-6284.

Santicioli, P., & Maggi, C. A. (2000). Effect of 18β-glycyrrhetinic acid on electromechanical coupling in the guinea-pig renal pelvis and ureter. British journal of pharmacology, 129(1), 163-169.

Sarin, S. K., Sabba, C. and Groszmann, R. J. (1990) 'Splanchnic and systemic hemodynamics in mice using a radioactive microsphere technique', Am.J.Physiol, 258(3 Pt 1), pp. G365–G369

Sariola, H. (2002). Nephron induction revisited: from caps to condensates. Current opinion in nephrology and hypertension, 11(1), 17-21.

Saxén, L. (1987) Organogenesis of the Kidney.pdf. Cambridge: Cambridge University Press.

Saxén, L. and Lehtonen, E. (1987) 'Embryonic kidney in organ culture', Differentiation, 36(1), pp. 2–11.

Saxén, L. and Sariola, H. (1987) 'Early organogenesis of the kidney', Pediatric Nephrology, 1(3), pp. 385–392.

Schedl, A. (2007). Renal abnormalities and their developmental origin. Nature Reviews Genetics, 8(10), 791-802.

Schier, A. F. (2003). Nodal signaling in vertebrate development. Annual review of cell and developmental biology, 19(1), 589-621.

Schmidt-Ott, K. M., Masckauchan, T. N. H., Chen, X., Hirsh, B. J., Sarkar, A., Yang, J., ... & Jagla, B. (2007). β-Catenin/TCF/Lef controls a differentiation-associated transcriptional program in renal epithelial progenitors. Development, 134(17), 3177-3190.

Schuchardt, A., D'Agati, V., Pachnis, V. and Costantini, F. (1996). Renal agenesis and hypodysplasia in ret-k-mutant mice result from defects in ureteric bud development. Development 122, 1919-1929.

Sebinger, D. D. R. et al. A novel, low-volume method for organ culture of embryonic kidneys that allows development of cortico-medullary anatomical organization. PLoS One 5, e10550 (2010).

Sequeira-Lopez, M. L. S., Lin, E. E., Li, M., Hu, Y., Sigmund, C. D., & Gomez, R. A. (2015). The earliest metanephric arteriolar progenitors and their role in kidney vascular

development. American Journal of Physiology-Regulatory, Integrative and Comparative Physiology, 308(2), R138-R149.

Shah, M. M., Sampogna, R. V., Sakurai, H., Bush, K. T., & Nigam, S. K. (2004). Branching morphogenesis and kidney disease. Development, 131(7), 1449-1462.

Shin, H. J., Takeda, M., Enomoto, A., Fujimura, M., Miyazaki, H., Anzai, N., & Endou, H. (2011). Interactions of urate transporter URAT1 in human kidney with uricosuric drugs. Nephrology, 16(2), 156-162.

Shin, K., Lee, J., Guo, N., Kim, J., Lim, A., Qu, L., ... & Beachy, P. A. (2011). Hedgehog/Wnt feedback supports regenerative proliferation of epithelial stem cells in bladder. Nature, 472(7341), 110-114.

Smith, J. (1997). Brachyury and the T-box genes. Current opinion in genetics & development, 7(4), 474-480.

Srinivas, S., Goldberg, M. R., Watanabe, T., D'agati, V., Al-Awqati, Q., & Costantini, F. (1999). Expression of green fluorescent protein in the ureteric bud of transgenic mice: a new tool for the analysis of ureteric bud morphogenesis. Developmental genetics, 24(3-4), 241-251.

Steenkamp, R., Castledine, C., Feest, T., & Fogarty, D. (2011). UK RRT Prevalence in 2009: national and centre-specific analyses. Nephron Clinical Practice, 119(Suppl. 2), c27-c52.

MS, Steinberg . (1963). Reconstruction of tissues by dissociated cells. Some morphogenetic tissue movements and the sorting out of embryonic cells may have a common explanation. Science (New York, NY), 141(3579), 401-408.

Stern, C. D. (1982). Growth and the Development of Pattern. Journal of Anatomy, 135(Pt 3), 663.

Stott, W. T., Dryzga, M. D. and Ramsey, J. C. (1983) 'Blood-flow distribution in the mouse', Journal of Applied Toxicology, 3(6), pp. 310–312.

Sweeney, D., Lindström, N., & Davies, J. A. (2008). Developmental plasticity and regenerative capacity in the renal ureteric bud/collecting duct system. Development, 135(15), 2505-2510.

Taguchi A, Kaku Y, Ohmori T, Sharmin S, Ogawa M, Sasaki H, Nishinakamura R (2014) Redefining the in vivo origin of metanephric nephron progenitors enables generation of complex kidney structures from pluripotent stem cells. Cell Stem Cell 14(1):53–67. https ://doi.org/10.1016/j.stem.2013.11.010

Taguchi A, Nishinakamura R (2017) Higher order kidney organogenesis from pluripotent stem cells. Cell Stem Cell 21:730–746 e736

Taguchi, A., and Nishinakamura, R. (2015). Nephron reconstitution from pluripotent stem cells. Kidney Int. 87, 894–900.

Taguchi, A., Kaku, Y., Ohmori, T., Sharmin, S., Ogawa, M., Sasaki, H., and Nishinakamura, R. (2014). Redefining the in vivo origin of metanephric nephron progenitors enables generation of complex kidney structures from pluripotent stem cells. Cell Stem Cell 14, 53–67.

Tai, G., Ranjzad, P., Marriage, F., Rehman, S., Denley, H., Dixon, J., ... & Woolf, A. S. (2013). Cytokeratin 15 marks basal epithelia in developing ureters and is upregulated in a subset of urothelial cell carcinomas. PLoS One, 8(11), e81167.

Takahashi, K., & Yamanaka, S. (2006). Induction of pluripotent stem cells from mouse embryonic and adult fibroblast cultures by defined factors. cell, 126(4), 663-676.

Takasato, M., Er, P. X., Becroft, M., Vanslambrouck, J. M., Stanley, E. G., Elefanty, A. G., & Little, M. H. (2014). Directing human embryonic stem cell differentiation

towards a renal lineage generates a self-organizing kidney. Nature cell biology, 16(1), 118-126.

Takasato, M., Er, P.X., Chiu, H.S., Maier, B., Baillie, G.J., Ferguson, C., Parton, R.G., Wolvetang, E.J., Roost, M.S., Chuva de Sousa Lopes, S.M., and Little, M.H. (2015). Kidney organoids from human iPS cells contain multiple lineages and model human nephrogenesis. Nature 526, 564–568.

Thomson, J. A. (1998). U.S. Patent No. 5,843,780. Washington, DC: U.S. Patent and Trademark Office.

Torres, M., Gómez-Pardo, E., Dressler, G. R., & Gruss, P. (1995). Pax-2 controls multiple steps of urogenital development. Development, 121(12), 4057-4065.

Trowe MO, Airik R, Weiss AC, Farin HF, Foik AB, Bettenhausen E, Schuster-Gossler K, Taketo MM, Kispert A. (2012) Canonical Wnt signaling regulates smooth muscle precursor development in the mouse ureter. Development. 2012 Sep;139(17):3099-108

Tyritzis, S. I., and Wiklund, N. P. (2015). Ureteral strictures revisited. . . trying to see the light at the end of the tunnel: a comprehensive review. J. Endourol. 29, 124–136. doi: 10.1089/end.2014.0522

Unbekandt, M. & Davies, J. A. Dissociation of embryonic kidneys followed by reaggregation allows the formation of renal tissues. Kidney Int. 77, 407–416 (2010).
Unbekandt, M., & Davies, J. A. (2010). Dissociation of embryonic kidneys followed by reaggregation allows the formation of renal tissues. Kidney international, 77(5), 407-416.

Van den Berg, C. W., Ritsma, L., Avramut, M. C., Wiersma, L. E., van den Berg, B. M., Leuning, D. G., ... & Howden, S. E. (2018). Renal subcapsular transplantation of

PSC-derived kidney organoids induces neo-vasculogenesis and significant glomerular and tubular maturation in vivo. Stem cell reports, 10(3), 751-765.
van Weering, D. H. J., & Bos, J. L. (1998). Signal transduction by the receptor tyrosine kinase Ret. Genes and Environment in Cancer, 271-281.

Velardo JT: Histology of the ureter. In: The ureter, 2nd Ed., edited by Bergman H, New York, Springer-Verlag, 1981

Vize, P. D., Woolf, A. S., & Bard, J. B. (Eds.). (2003). The kidney: from normal development to congenital disease. Elsevier.

Wang, D. Z., & Olson, E. N. (2004). Control of smooth muscle development by the myocardin family of transcriptional coactivators. Current opinion in genetics & development, 14(5), 558-566.

Wang, P. et al. (1993) 'Trauma hemorrhage and resuscitation in the mouse: effects on cardiac output and organ blood flow', The American Journal of Physiology, 264(4 Pt 2), pp. H1166-73.

Weiss, R. M., Guo, S., Shan, A., Shi, H., Romano, R. A., Sinha, S., ... & Guo, J. K. (2013). Brg1 determines urothelial cell fate during ureter development. Journal of the American Society of Nephrology 24: 618-626.

Weiss, R. M., Tamarkin, F. J., & Wheeler, M. A. (2006). Pacemaker activity in the upper urinary tract. Journal of Smooth Muscle Research, 42(4), 103-115.

Wernig, M., Meissner, A., Foreman, R., Brambrink, T., Ku, M., Hochedlinger, K., ... & Jaenisch, R. (2007). In vitro reprogramming of fibroblasts into a pluripotent ES-cell-like state. nature, 448(7151), 318-324.

Whitbread LA, Powell BC (1998) Expression of the intermediate filament keratin gene, K15, in the basal cell layers of epithelia and the hair follicle. Exp Cell Res 244: 448-459. doi: 10.1006/excr.1998.4217. PubMed: 9806795.

Willems, E., & Leyns, L. (2008). Patterning of mouse embryonic stem cell-derived pan-mesoderm by Activin A/Nodal and Bmp4 signaling requires Fibroblast Growth Factor activity. Differentiation, 76(7), 745-759.

Wilson, V., & Beddington, R. (1997). Expression of T protein in the primitive streak is necessary and sufficient for posterior mesoderm movement and somite differentiation. Developmental biology, 192(1), 45-58.

Woolf, A. S., & Davies, J. A. (2013). Cell biology of ureter development. Journal of the American Society of Nephrology, 24(1), 19-25.

Woolf, A. S., Winyard, P. J., Hermanns, M. H., & Welham, S. J. (2003). Maldevelopment of the human kidney and lower urinary tract: an overview. The kidney, 377-393.

Wu, F., Park, F., Cowley Jr, A. W., & Mattson, D. L. (1999). Quantification of nitric oxide synthase activity in microdissected segments of the rat kidney. American Journal of Physiology-Renal Physiology, 276(6), F874-F881.

Wu, X. R., & Sun, T. T. (1993). Molecular cloning of a 47 kDa tissue-specific and differentiation-dependent urothelial cell surface glycoprotein. Journal of cell science, 106(1), 31-43.

Wu, X. R., Kong, X. P., Pellicer, A., Kreibich, G., & Sun, T. T. (2009). Uroplakins in urothelial biology, function, and disease. Kidney international, 75(11), 1153-1165.

Wu, X. R., Lin, J. H., Walz, T., Häner, M., Yu, J., Aebi, U., & Sun, T. T. (1994). Mammalian uroplakins. A group of highly conserved urothelial differentiation-related membrane proteins. Journal of Biological Chemistry, 269(18), 13716-13724.

Wu, X. R., Manabe, M., Yu, J., & Sun, T. T. (1990). Large scale purification and immunolocalization of bovine uroplakins I, II, and III.

Xia, Y., Nivet, E., Sancho-Martinez, I., Gallegos, T., Suzuki, K., Okamura, D., ... & Belmonte, J. C. I. (2013). Directed differentiation of human pluripotent cells to ureteric bud kidney progenitor-like cells. Nature cell biology, 15(12), 1507-1515.

Xie, H., Shaffer, B. S., Wadia, Y., and Gregory, K. W. (2000). Use of reconstructed small intestine submucosa for urinary tract replacement. Asaio J. 46, 268–272. doi: 10.1097/00002480-200005000-00005

Xinaris, C., Benedetti, V., Rizzo, P., Abbate, M., Corna, D., Azzollini, N., ... & Benigni, A. (2012). In vivo maturation of functional renal organoids formed from embryonic cell suspensions. Journal of the American Society of Nephrology, 23(11), 1857-1868.

Xu, C., Chang, A., Hack, B. K., Eadon, M. T., Alper, S. L., & Cunningham, P. N. (2014). TNF-mediated damage to glomerular endothelium is an important determinant of acute kidney injury in sepsis. Kidney international, 85(1), 72-81.

Xue, J.-D., Gao, J., Fu, Q., Feng, C., and Xie, H. (2016). Seeding cell approach for tissue-engineered urethral reconstruction in animal study: a systematic review and meta-analysis. Exp. Biol. Med. 241, 1416–1428. doi: 10.1177/ 1535370216640148

Yue, F., Cheng, Y., Breschi, A., Vierstra, J., Wu, W., Ryba, T., ... & Ren, B. (2014). A comparative encyclopedia of DNA elements in the mouse genome. *Nature*, *515*(7527), 355-364.

Yu J, Manabe M, Wu XR, Xu C, Surya B, Sun TT: Uroplakin I: A 27-kD protein associated with the asymmetric unit membrane of mammalian urothelium. J Cell Biol 111: 1207–1216, 1990

Yu, J., Carroll, T. J., & McMahon, A. P. (2002). Sonic hedgehog regulates proliferation and differentiation of mesenchymal cells in the mouse metanephric kidney. Development, 129(22), 5301-5312.

Yu, J., Lin, J. H., Wu, X. R., & Sun, T. T. (1994). Uroplakins Ia and Ib, two major differentiation products of bladder epithelium, belong to a family of four transmembrane domain (4TM) proteins. The Journal of cell biology, 125(1), 171-182.

Yu, J., McMahon, A. P., & Valerius, M. T. (2004). Recent genetic studies of mouse kidney development. Current opinion in genetics & development, 14(5), 550-557.

8. Papers published from this work

Sallam, M., Palakkan, A. A., Mills, C. G., Tarnick, J., Elhendawi, M., Marson, L., & Davies, J. A. (2020). Differentiation of a Contractile, Ureter-Like Tissue, from Embryonic Stem Cell–Derived Ureteric Bud and Ex Fetu Mesenchyme. Journal of the American Society of Nephrology, 31(10), 2253-2262.

Sallam M, Davies JA (2021) Connection of ES cell-derived collecting ducts and ureter-like structures to host kidneys in culture. Organogenesis in press.

Differentiation of a Contractile, Ureter-Like Tissue, from Embryonic Stem Cell–Derived Ureteric Bud and *Ex Fetu* Mesenchyme

May Sallam,[1,2] Anwar A. Palakkan,[1] Christopher G. Mills,[1] Julia Tarnick,[1] Mona Elhendawi,[1,3] Lorna Marson,[4] and Jamie A. Davies[1]

[1]Deanery of Biomedical Science, University of Edinburgh, Edinburgh, UK
[2]Human Anatomy and Embryology Department, Faculty of Medicine, Mansoura University, Mansoura, Egypt
[3]Clinical Pathology Department, Faculty of Medicine, Mansoura University, Mansoura, Egypt
[4]Edinburgh Transplant Centre, Royal Infirmary of Edinburgh, Edinburgh, UK

ABSTRACT

Background There is intense interest in replacing kidneys from stem cells. It is now possible to produce, from embryonic or induced pluripotent stem cells, kidney organoids that represent immature kidneys and display some physiologic functions. However, current techniques have not yet resulted in renal tissue with a ureter, which would be needed for engineered kidneys to be clinically useful.

Methods We used a published sequence of growth factors and drugs to induce mouse embryonic stem cells to differentiate into ureteric bud tissue. We characterized isolated engineered ureteric buds differentiated from embryonic stem cells in three-dimensional culture and grafted them into *ex fetu* mouse kidney rudiments.

Results Engineered ureteric buds branched in three-dimensional culture and expressed Hoxb7, a transcription factor that is part of a developmental regulatory system and a ureteric bud marker. When grafted into the cortex of *ex fetu* kidney rudiments, engineered ureteric buds branched and induced nephron formation; when grafted into peri-Wolffian mesenchyme, still attached to a kidney rudiment or in isolation, they did not branch but instead differentiated into multilayer ureter-like epithelia displaying robust expression of the urothelial marker uroplakin. This engineered ureteric bud tissue also organized the mesenchyme into smooth muscle that spontaneously contracted, with a period a little slower than that of natural ureteric peristalsis.

Conclusions Mouse embryonic stem cells can be differentiated into ureteric bud cells. Grafting those UB-like structures into peri-Wolffian mesenchyme of cultured kidney rudiments can induce production of urothelium and organize the mesenchyme to produce rhythmically contracting smooth muscle layers. This development may represent a significant step toward the goal of renal regeneration.

JASN 31: 2253–2262, 2020. doi: https://doi.org/10.1681/ASN.2019101075

The past decade has seen significant advances toward the goal of generating kidneys from various types of stem cell. It is now possible to produce renal organoids, representing immature kidneys and showing some physiologic functions, from embryonic and induced pluripotent cells of mouse and human.[1–6] So far, these organoids have not featured a ureter. This report describes a technique for differentiating mouse embryonic stem (ES) cells into urothelium that can organize fetal peri-Wolffian mesenchyme around it to produce contractile muscle layers.

Our experiments rest on two bodies of prior work. One is an effort to explore the self-organizing properties of cells, specifically renogenic stem cells from young fetal mouse kidney rudiments. It was shown in 2010 that these cells, disaggregated then reaggregated, could interact to produce what have since come to be called renal organoids, containing small collecting duct trees and immature nephrons.[7] A series of technical advances,[8–10] most of which break the symmetry of the system to create large-scale order, have improved the realism of the tissues produced, resulting in organoids with nephrons arranged around a single collecting duct tree with a single urothelial end.[10]

Received October 18, 2019. Accepted June 11, 2020.

Published online ahead of print. Publication date available at www.jasn.org.

Correspondence: Dr. May Sallam, Deanery of Biomedical Science, University of Edinburgh Medical School, Hugh Robson Building 15, George Square, Edinburgh, Scotland, UK, EH8 9XD. Email: s1688924@sms.ed.ac.uk

The other body of work aimed to produce kidneys from human induced pluripotent stem (iPS) cells.[11,12] From early application of sequences of signaling molecules to differentiate mouse ES cells into renal epithelia that could integrate into developing kidneys,[13] methods were established to produce complete renal organoids from human iPS and ES cells[4–6] that are able to connect with host blood systems.[14] Like the 2010 *ex fetu* mouse organoids, they lack proper large-scale anatomic organization. This issue has been partly addressed by Taguchi and Nishinakamura in 2017,[4] who generated the first anatomically organized kidney organoid derived mainly from mouse ES cells, with some *ex fetu* material included. The organoids had a single collecting duct tree, but no ureter.

Here, we report the results of combining the Taguchi and Nishinakamura differentiation techniques[4] with grafting into *ex fetu* peri-Wolffian mesenchyme to produce urothelial structures surrounded by smooth muscle coats showing spontaneous contractions.

Significance Statement

There is intense interest in engineering new kidneys from embryonic stem cells and induced pluripotent stem cells as research models, and perhaps eventually for clinical transplant. Although protocols exist for producing renal organoids from stem cells, these organoids lack an essential component, the ureter. The authors describe the production of ureter-like tissue consisting of embryonic stem cell–derived ureteric buds that organize *ex fetu* mesenchyme around it to form smooth muscle layers. These muscles spontaneously contract with a periodicity that is a little slower than that of peristalsis in natural ureters. This work represents a step toward developing organoids with a ureter, although inducing the tissue to elongate into a tube and connect it to the kidney is a remaining challenge.

METHODS

Animals

Mice mated overnight, and the morning of vaginal plug discovery was considered embryonic day (E) 0.25. Pregnant mice were euthanized at E11.5 by trained UK Home Office license holders, by methods listed in Schedule One of the UK Animals (Scientific Procedures) Act. Embryos were decapitated and dissected to obtain "nephrogenic areas" (the metanephros, ureter, nearby Wolffian duct, and mesenchyme), or isolated metanephroi, according to the experiment.

Induction of Ureteric Bud Differentiation from Mesenchymal ES Cells

A Hoxb7-GFP mouse ES cell line was a gift from Professor Ryuichi Nishinakamura's laboratory (Kumamoto University, Kumamoto, Japan). Cells were maintained in GMEM (G5154; Sigma) supplemented with 10% FBS, GlutaMAX (1×, Gibco), MEM-NEAA (1×, Gibco), sodium pyruvate (1 mM, Gibco), β-mercaptoethanol (0.1 mM), and leukemia inhibitory factor (sc-4989, LIF, 1 U/μl; Santa Cruz Biotechnology). The mouse embryonic stem (mES) cell line was differentiated into ureteric bud (UB) cells using a slight modification of a method previously described by Taguchi and Nishinakamura.[4] Briefly, at 0 hours cells were dissociated with Accutase (Gibco); reaggregated at 2000 cells/aggregate in 96-well, U-bottomed, low cell–binding plates (650970; Greiner); and cultured to form embryonic bodies (EBs). At 48 hours, the medium was replaced by "base medium," comprising 75% Iscove modified Dulbecco medium (12440–046; Gibco) and 25% Ham F12 (11765–054; Gibco), with 0.5× N2 (17502–048; Gibco), 0.5× B27 (12587–010; Gibco), 0.5× penicillin/streptomycin, 0.05% BSA (Sigma), 2 mM L-glutamine (Life Technologies), 0.5 mM ascorbic acid (Sigma), 450 μM 1-thioglycerol (Sigma), with the addition of 10 ng/ml human Activin A (338-AC; R&D Systems) as step 1. At 72 hours (all times are from 0 hours), the medium was changed for base medium containing 0.3 ng/ml human BMP4 (314-BP; R&D Systems) and 10 μM CHIR99021 (TOCRIS 4423) as step 2. At 108 hours, the medium was changed for base medium containing 0.1 μM retinoic acid (R-2625, RA; Sigma), 100 ng/ml human FGF9 (273-F9; R&D Systems), and 10 μM SB431542 (TOCRIS 1614) as step 3. At 132 hours, the medium was changed for base medium containing 0.1 μM RA, 100 ng/ml human FGF9, and 5 μM CHIR99021 as step 4. At 156 hours, the medium was changed for base medium containing 10 μM Y27632 (72302; Stem Cell Technologies), 0.1 μM RA, 1 μM CHIR99021, 5 ng/ml human FGF9, and 10% growth factor–reduced Matrigel (354230; Corning) as step 5. At 180 hours, 3 μm CHIR99021 and 1 ng/ml GDNF (212-GD; R&D Systems) were added to a fresh change of the medium used from 156 hours, as step 6. At 204 hours, this was changed to the same medium with 2 ng/ml GDNF and without FGF9, as step 7. After 24 hours of step 7, the EBs developed numerous ES cell–derived UB-like radiating tubules, which we refer to as engineered uteric buds (eUBs) in this report.

For culture in Matrigel,[4] projecting eUB tubules were isolated by manual dissection from EBs produced using the method described above, and were suspended in 20% Matrigel in DMEM/F12 medium containing 10% FBS, 0.1 μM RA, 100 ng/ml human Rspondin1 (4645-RS; R&D Systems), 2 ng/ml human GDNF (212-GD; R&D Systems), and 100 ng/ml mouse FGF1 (450–33A; Pepro Tech) in U-bottomed, low cell–binding plates.

Grafting of eUBs into Cultured Kidney Rudiments

E11.5 kidneys were isolated from CD1 mouse embryos, and the rudiments were cultured on 24-mm, 0.4-μm-pore membranes (3450, Transwells; Corning) in kidney culture medium (KCM) comprising Minimum Eagle Medium with Earle salts (M5650, MEM; Sigma) with 10% FBS. Hoxb7-GFP eUBs were isolated manually from day 10 (approximately 230 hours) EBs using sharpened tungsten needles, and grafted into either the metanephric mesenchyme (Figure 1A) or the peri-Wolffian mesenchyme (Figure 3A) of E11.5 embryonic kidneys in culture as above. The kidneys and grafts were cultured

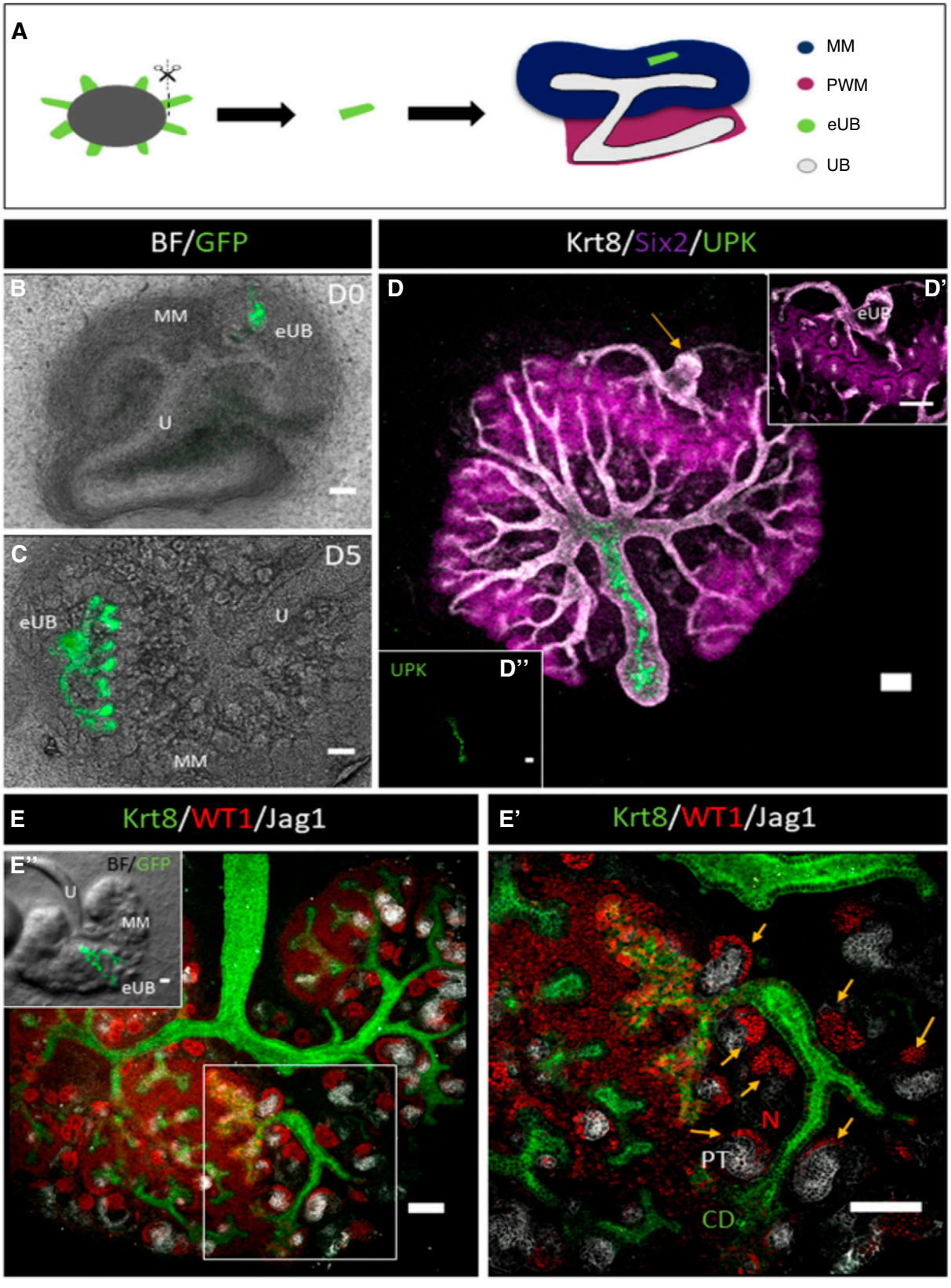

Figure 1. eUB branches and induced nephrogenesis in renal metanephric mesenchyme. (A) Steps of grafting eUB into MM. (B and C) Combined bright-field and GFP fluorescence image of a HoxB7-GFP mES cell–derived eUB grafted into the MM of an E11.5 kidney at (B) 0, and (C) 5 days of culture. (D) Immunofluorescence of (C); the grafted eUB is indicated by the arrow (the sample has been rotated by 90° because of the differences between microscopes); (D') region of (D) showing the eUB tips surrounded by $SIX2^{+}$ nephron progenitor cells,

for 5 or 9 days in KCM, with the medium being changed every 2 days.

Combination of eUB with Peri-Wolffian Mesenchyme or Metanephric Mesenchyme

Peri-Wolffian mesenchyme was isolated by manual dissection from E11.5 nephrogenic areas using sharp tungsten needles, and dispersed by incubation in 1× trypsin/EDTA (T4174; Sigma) at 37°C for 2 minutes. Around 150,000 cells were suspended in 150 μl KCM, and centrifugation (3 minutes at 3000×*g*) was used to obtain a cell pellet. Pellets were transferred to wells in 96-well, low cell–binding, U-bottom plates. The eUBs were dissected from day 10 organoids, added to the mesenchymal cell pellet at 1 eUB per well, and incubated at 37°C and 5% CO_2. After 24 hours, the combination had formed a compact spheroid, which was transferred to a 24-mm, 0.4 μm-pore Transwell membrane (3450) in a well containing 1.5 ml KCM (Figure 4A). The same method was used to combine eUB with isolated metanephric mesenchyme (Figure 2A), with the spheroids being cultured in KCM for 5 days, with the addition of 50 μl KCM containing 10% Matrigel on top.

Immunofluorescence

Samples were fixed by immersion in cold methanol, and the immersed samples were allowed to warm to room temperature (19°C±5°C) over 30 minutes. They were washed with PBS and blocked in staining buffer, comprising 5% BSA in PBS, overnight at 4°C. For Krt15 and NP63 staining, samples were fixed in 4% PFA in PBS and blocked using 5% BSA and 0.2% Triton X-100 (Sigma) in PBS. After blocking, primary antibodies (Supplemental Table 1) diluted in staining buffer were applied to samples at 4°C for 24 hours. Unbound primary antibody was washed off in PBS (3×5 minutes), and secondary antibodies (Supplemental Table 1) in staining buffer were applied overnight at 4°C. Samples were washed (3×15 minutes PBS) and mounted onto a slide using Vectashield (H-1000; Vector Laboratories).

Paraffin Wax–Embedded Tissue Sectioning

Samples were fixed in methanol as above, and were then placed in an automatic wax processing machine (Sakura VIP E300; Sakura). Wax-infused samples were embedded in paraffin wax blocks, and 6-μm sections were cut using a Leica RM2245 microtome. Sections were floated out before mounting on slides (Superfrost plus; Thermo Fisher Scientific) and dried in a 37°C oven. Samples were dewaxed in xylene (30 minutes), rehydrated in an ethanol series (100%, 90%, 70%, for 5 minutes each), and then placed under running water. Antigen retrieval was carried out by microwaving the dewaxed slides in sodium citrate buffer (10 mM sodium citrate, 0.05% Tween 20, pH 6.0) for 3×15 minutes. Immunohistochemical staining was carried out as described above.

Statistical Analyses

For categorical (feature present/absent) data, 95% confidence intervals (95% CIs) were calculated using the binomial normal approximation interval, corrected for small sample sizes, as $\pm 1.96\,[\sqrt{(p(1-p)/n)}]+1/2n$.[15]

RESULTS AND DISCUSSION

Engineering of GFP-Labeled UBs from mES Cells

We differentiated HoxB7-GFP mESC[4,16] to UB cells using the method of Taguchi and Nishinakamura.[4] In agreement with their findings, by day 2, mES cells formed Hoxb7-GFP$^-$ EBs (Supplemental Figure 1, A and B). By day 10, they developed numerous epithelial projections (Supplemental Figure 1C) expressing the UB marker HoxB7-GFP (Supplemental Figure 1D: six runs, at least six EBs in each, all showing these features). When isolated and cultured in three-dimensional Matrigel supplemented with GDNF, R-Spondin1, FGF1, and retinoic acid,[4] the epithelial projections branched in a manner similar to natural UBs in gel culture (Supplemental Figure 1, F and G; three runs, four samples in each, all branching).[17] Expression of HoxB7-GFP was maintained (Supplemental Figure 1H), suggesting retention of UB character, and the UB markers Calbindin D_{28k}, pan-cytokeratin, Krt8, E-cadherin (Cdh1), Gata3, and Pax2 were present in all three samples tested (Supplemental Figure 1, I–L). Furthermore, the epithelia expressed the GNDF receptor c-Ret (Supplemental Figure 2, A–D; all five samples) and the "tip" marker Sox9 (Supplemental Figure 2, E and F; all six samples). They did not, however, bind the "stalk" maker *Dolichos biflorus* agglutinin[18] (Supplemental Figure 2, G and H; zero out of three samples). Therefore, the whole structure had the character of ureteric tip, with no evidence of differentiation to stalk. We refer to tubular structures as eUBs.

eUBs Differentiate into Collecting Duct-Like Epithelial Trees in a Metanephric Mesenchymal Environment

Building on previous work,[19–21] Mills and colleagues grafted isolated tips or stalks of natural UBs into either the metanephric mesenchyme or the peri-Wolffian mesenchyme of cultured kidney rudiments. They found that differentiation of the UB fragments was controlled by the identity of surrounding mesenchyme.

like those of the natural UB. (D″) Image (D) with only the UPK channel, showing UPK expression in the host ureter but not the eUB graft. (E) Immunofluorescence image of an eUB graft in MM showing eUB branching and induction of JAG1$^+$ early nephrons. (E′) Magnified image of the boxed area in (E) showing the early nephrons (arrows) associated with the eUB. (E″) Combined bright-field and GFP image of (E) showing the location of the GFP-eUB graft. Scale bar for all images, 100 μm. CD, collecting duct; MM, metanephric mesenchyme; N, nephron; PT, proximal tubule; U, natural ureter.

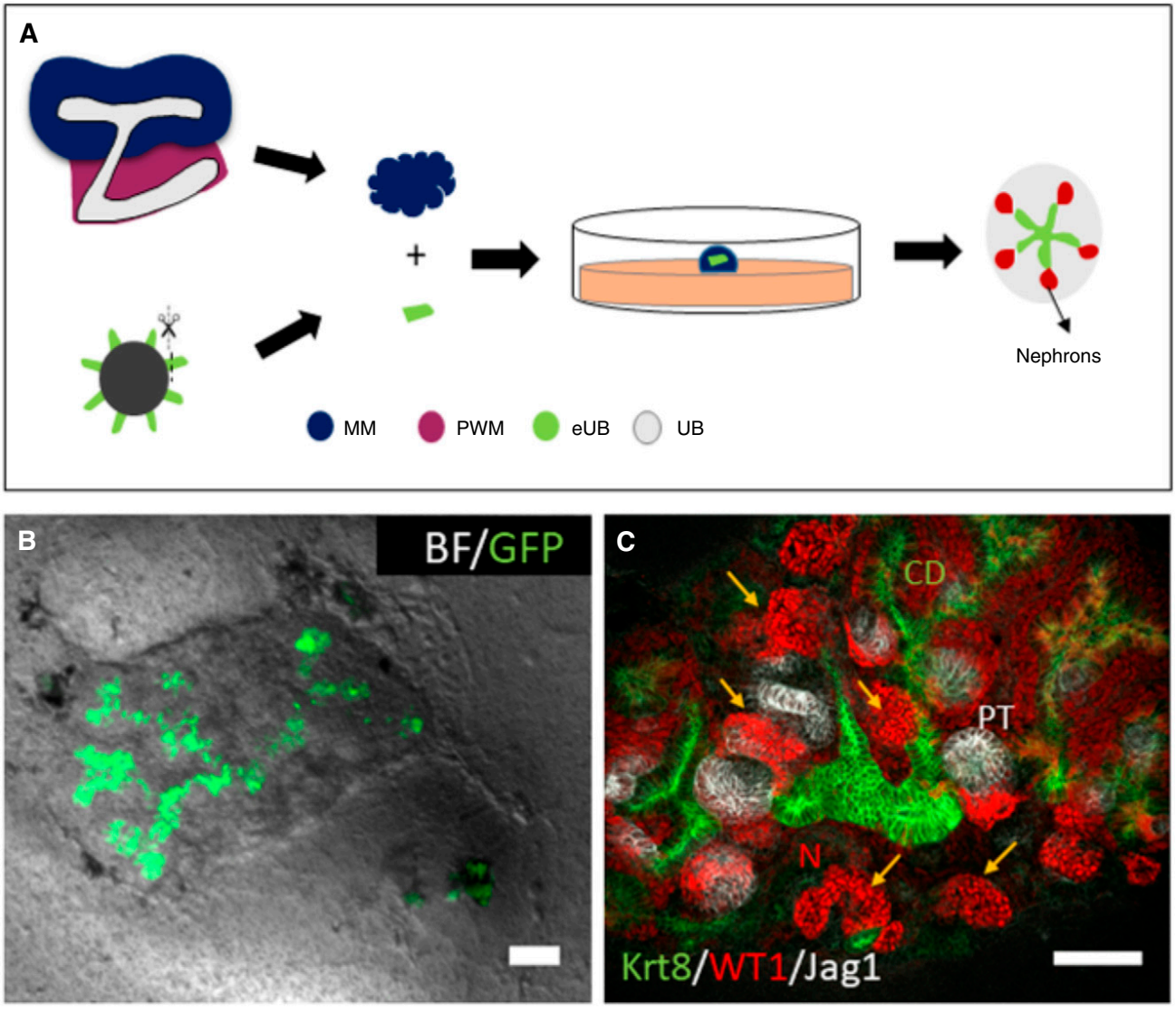

Figure 2. eUBs branch and induce nephrons when placed into isolated metanephric mesenchyme. (A) Steps of recombination of eUB with isolated MM cells. (B) Combined bright-field (BF) and GFP image of Hoxb7-GFP eUB recombined with MM, showing branching of the eUB, survival of the MM, and induction of nephron differentiation. (C) Immunofluorescence showing the eUB epithelial branching (KRT8 expression), nephrogenic condensates (indicated by arrows and WT1 expression), and early nephrons expressing strong WT1 at their glomerular poles and the proximal tubule marker JAG1, connecting to the eUB. Scale bar for all images, 100 μm. MM, metanephric mesenchyme; PWM, peri-Wolffian mesenchyme.

Importantly for our study, they found that ureteric tips grafted into the peri-Wolffian mesenchyme expressed the urothelial marker, Uroplakin (UPK).[10]

We tested whether eUBs showed the same plasticity, beginning with grafting to the metanephric mesenchyme (Figure 1A). Grafted eUBs (Figure 1B) grew and branched to produce a tree (Figure 1C: all ten branched; 100%, 95% CI, 95% to 100%). As well as expressing Hoxb7-GFP (Figure 1C) and KRT8 (Figure 1D), they organized a nephrogenic response in the host metanephric mesenchyme. Their tips became surrounded by $SIX2^+$ cap mesenchyme cells (Figure 1D; all three samples tested, 100%, 95% CI, 83% to 100%). Early-stage nephrons, with $WT1^+$ glomerular poles and $JAG1^+$ proximal tubules, formed near the grafted eUBs and eventually connected to them (Figure 1, E and E'; all eight samples tested 100%, 95% CI, 94% to 100%). All but one graft into metanephric mesenchyme were UPK^-, with the UPK^+ host ureter acting as a positive staining control (Figure 1D; five out of six tested). The exception was in a damaged host kidney that had lost its own ureter and had a torn mesenchyme. Across these experiments, UPK expression rate was therefore 17% (95% CI, 0% to 56%).

The host UB is not necessary for this response. When eUBs were grafted into isolated metanephric mesenchyme (Figure 2A), they still branched (Figure 2B) and induced the differentiation of nephrons with

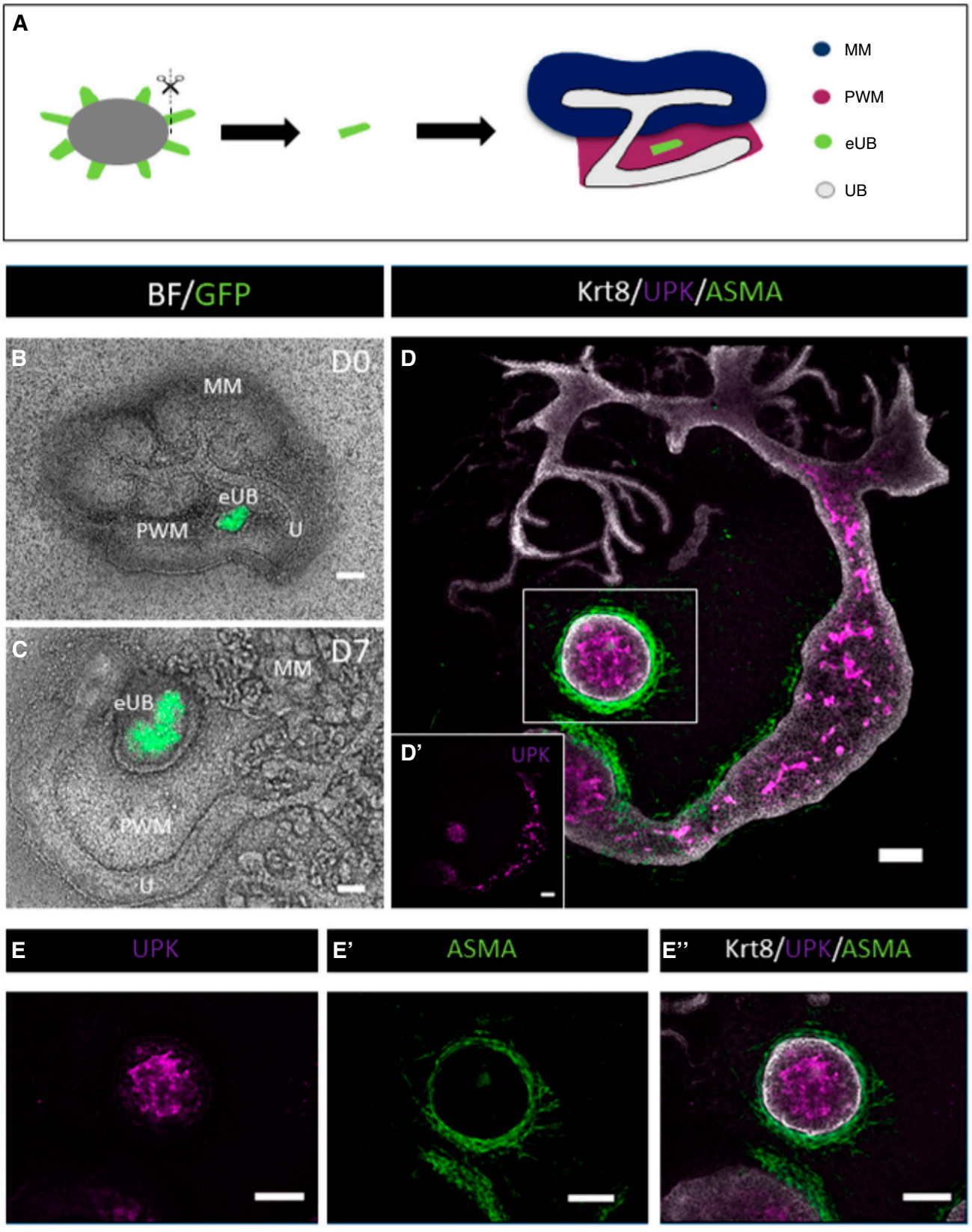

Figure 3. mES cell–derived eUBs differentiate into ureter tissue when grafted into peri-Wolffian mesenchyme. (A) Steps of grafting eUB into peri-Wolffian mesenchyme (PWM). (B) A combined bright-field (BF) and GFP image of a Hoxb7-GFP eUB grafted into PWM cells at the time of grafting, and (C) 7 days later. (D) Immunofluorescence stain of an eUB grafted into PWM showing expression of UPK in the

WT1$^+$ glomerular poles and Jagged-1$^+$ proximal tubules (Figure 2C; all three samples tested, 100%, 95% CI, 83% to 100%). Again, this observation confirms the prior work of Taguchi and colleagues.

eUBs Differentiate into Ureter-Like Epithelia in a Peri-Wolffian Mesenchyme Environment

When grafted instead into the peri-Wolffian mesenchyme of *ex fetu* kidney rudiments (Figure 3A), eUBs did not branch and did not induce nephrons, although they retained Hoxb7-GFP expression (Figure 3, B and C). They now showed robust expression of UPK (Figure 3D; all 12 samples examined; 100%; 95% CI, 96% to 100%, a range that does not overlap the 95% CI of grafts into metanephric mesenchyme described in the previous paragraph). In addition to expressing UPK, they acquired a smooth muscle layer expressing α-smooth muscle actin (Figure 3, D and E).

It is known that the ureteric stalk epithelium and the mesenchyme that surrounds it collaborate to produce a ureter *via* reciprocal inductive signaling. There is strong evidence that epithelium-derived SHH signaling to the mesenchyme is necessary for the mesenchyme to express BMP4 as a result of an internal FOXF1-dependent pathway and to become competent to differentiate into muscle.[22] BMP4 from the mesenchyme signals to the epithelium to drive urothelial differentiation,[10] whereas the epithelium signals to the mesenchyme to drive smooth muscle differentiation. This urothelium-to-mesenchyme communication involves β-catenin–mediated WNT signaling, probably by WNT7B and/or WNT9B, both present in the epithelium.[23] In addition, retinoic acid signaling is required for a correct balance of differentiation in both compartments.[24] Are local paracrine signals such as these sufficient to drive urothelial eUB differentiation, or are influences from the kidney or natural ureter needed? Testing this by combination of eUBs with isolated *ex fetu* peri-Wolffian mesenchyme (Figure 4A) again resulted in the eUBs remaining unbranched (Figure 4B), activating UPK expression and gaining a smooth muscle layer (Figure 4C; all three cases examined, 100%, 95% CI, 83% to 100%). This argues that local interactions between peri-Wolffian mesenchyme and the eUB are sufficient to induce differentiation.

When in the peri-Wolffian mesenchyme, either in the kidney or isolated, the form of these grafts was fully or oblately spherical, with no evidence of elongation into a tube. Within the structures, the eUB-derived urothelium differentiated to form the layered structure similar to a natural ureter. At the core were cells showing strong expression of UPK (Figure 4, C and D), a classic superficial ("S") cell marker (UPKIII).[25] In some samples, there was evidence of a lumen, albeit somewhat collapsed rather than inflated (Figure 4D). Between the superficial cells and the basement membrane were cells showing strong expression of KRT5 (Figure 4D; all three samples), a classic basal ("B") cell marker.[25–27] Within the B cell zone were occasional cells expressing KRT15 (Figure 4E; all five samples), as in natural ureter.[28] In some places along the least-basal parts of the zone dominated by B cells were cells expressing no KRT5 and only very weak UPK (Figure 4D), and expressing strong NP63 (Figure 4F; all four samples), a pattern characteristic of intermediate ("I") cells.[25]

Ureter-Like Tissues Made by Combination of eUBs with Peri-Wolffian Mesenchyme Show Spontaneous Contractions

By 7 days after combination, the ureter-like tissues formed by grafting eUBs into peri-Wolffian mesenchyme of host kidneys started to show rhythmic contractions. These became stronger and more frequent by day 9 and were detectable in all three of the samples filmed under time lapse (100%, 95% CI, 83% to 100%; Supplemental Video 1). To assess whether contractions of the graft were synchronized with those of the host ureter, this video was analyzed frame by frame and the times of peak contraction (minimum diameter) of the graft and host were recorded separately. Times of individual contractions are shown in Supplemental Figure 3. The period of contraction of the natural ureter, averaged over eight intervals between nine contractions in the recording, was 12 seconds (SEM 0.8 seconds), comparable with that *in vivo*[29]; the period of the graft, averaged over seven intervals between its eight contractions, was slightly slower at 15 seconds (SEM 0.6 seconds). There was no obvious relationship between the timings, the graft sometimes leading and sometimes lagging the host (Supplemental Figure 3). No contractility was detected in any eUB grafted in the metanephric mesenchyme.

The asynchronous contraction of graft and host implies that the contractions of the muscles formed around the graft are spontaneous and independent of activity in the nearby natural ureter. To verify this, we filmed combinations of eUBs and pure peri-Wolffian mesenchyme with no host ureter present. These still showed large spontaneous rhythmic contractions (Supplemental Figure 4, Supplemental Video 2), of period 11 seconds (SEM 0.8 seconds) in one video and 20 seconds (SEM 0.7 seconds) in another. This indicates not only that the muscles are functional, but that at least some have the "pacemaker" activity usually ascribed to atypical muscle cells normally found at the proximal end of the ureter or renal pelvis.[30] Careful observation showed that, between these large contractions, there were very small

epithelium, KRT8 in the epithelial layers, and smooth muscle actin (ASMA) around the epithelium. (D′) Separate UPK channel of D, for clarity. (E-E″) Shows a magnification of the boxed area in D, individual UPK channel in E. ASMA channel in (E′). (E″) Shows the combined channels UPK, ASMA, and Krt8. MM, metanephric mesenchyme.

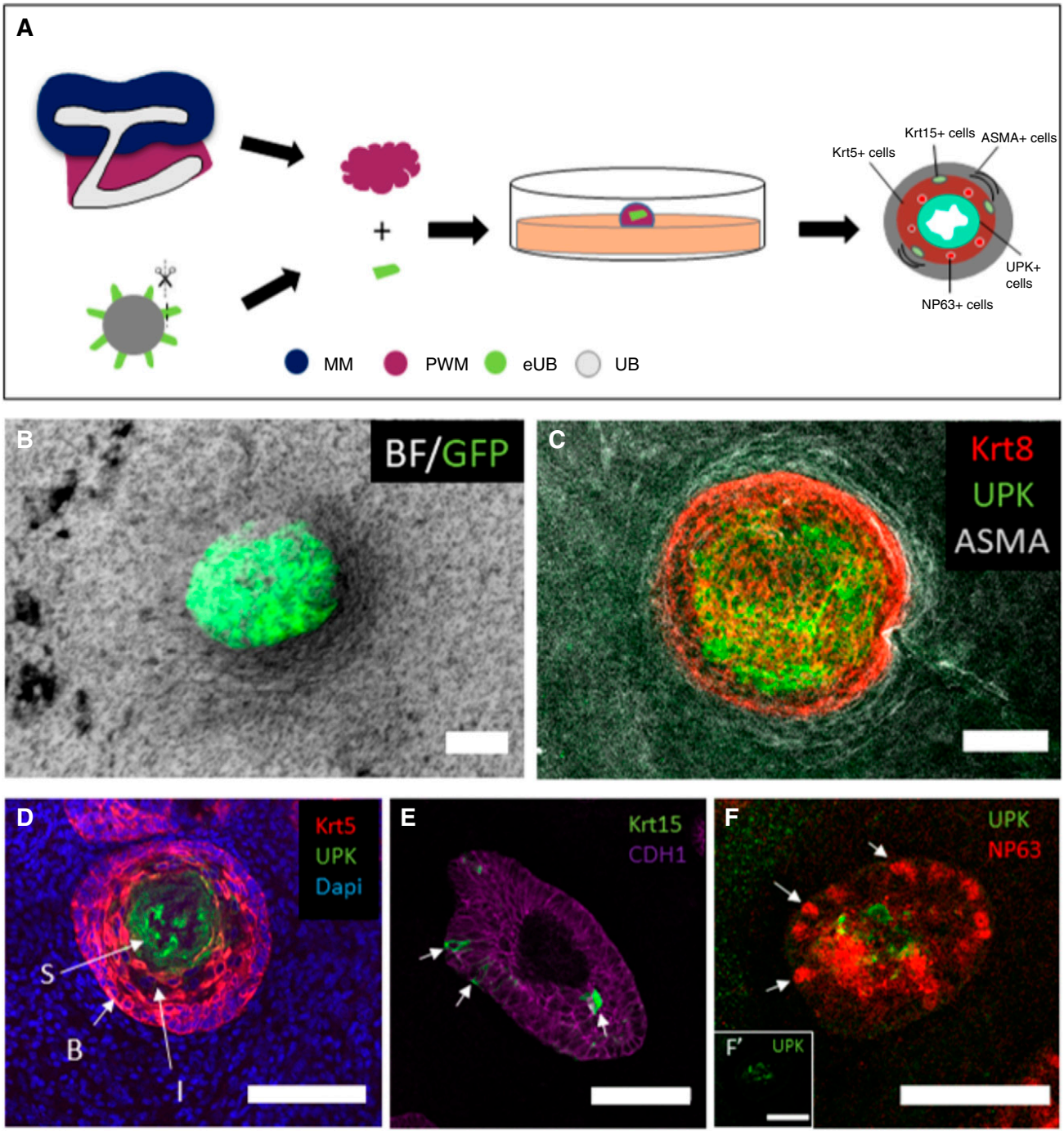

Figure 4. Urothelial differentiation in pure peri-Wolffian mesenchyme. (A) Steps of recombination of Hoxb7-GFP-eUB with PWM cells. (B) A combined bright-field (BF) and GFP image of a Hoxb7-GFP eUB recombined with PWM cells. (C) Immunofluorescence stain of an eUB recombined with PWM cells showing expression of UPK in the adluminal epithelium, KRT8 in the urothelium as a whole, and smooth muscle actin (ASMA) around the epithelium. (D) A 6-μm section of an eUB combined with PWM shows UPKIII expression in superficial ("S") cells, KRT5 in basal ("B") cells, and also the presence of KRT5- intermediate ("I") cells in the less basal zone of the area otherwise dominated by B cells. (E) Krt15 is expressed by occasional cells in the B cell layer; the counterstain E-cadherin (Cdh1) marks all epithelial cells of the eUB graft. (F) Cells expressing the intermediate cell marker NP63 (arrows) and others expressing UPK; the insert (F') shows the UPK channel alone, for clarity. MM, metanephric mesenchyme; PWM, peri-Wolffian mesenchyme.

contractions that, with the large contractions, formed a steady sequence with periods 6.4 seconds (SEM 0.4 seconds) and 7.5 seconds (SEM 0.5 seconds) in the same two videos. It is already known from electrical measurements that pacemaker activity in ureter smooth muscle cells runs at two to four times the frequency of gross peristaltic

contraction because of the mechanism of muscle contraction having a refractory period[29]; the small contractions we observed between large ones may reflect this underlying clock. We did not observe small contractions in either host or grafted UBs in the whole-kidney samples described in the previous paragraph, perhaps because the more closely packed stroma in these prevented visible small movements.

This is not the first report of differentiation of ES and iPS cells into urothelial cells, but previous examples[31] lacked three-dimensional structure, and both these and those of Santos *et al.*[32] lacked smooth muscle. A recent publication by Mullenders *et al.*[33] described ureter organoids made from bladder cancers and from adult human tissue. They adopted a cyst-like shape with a lumen, but with no organization of mesenchymal components or muscle and no evidence of contraction. Our approach is distinct in combining ES-derived ureters with *ex fetu* mesenchymal cells to generate multiple epithelial layers and smooth muscle coat that contract spontaneously. Important future goals are to develop techniques for differentiating peri-Wolffian mesenchyme from ES cells, and inducing the engineered tissue to elongate into a proper tube.

DISCLOSURES

All authors have nothing to disclose.

FUNDING

Work in this report was funded by Medical Research Council grant MR/R026483/1 (to J.A. Davies) and Kidney Research UK grants RP_002_20160223 and ST_001_20161116 (to J.A. Davies). M. Sallam is funded by a scholarship from Newton-Mosharafa program between the Egyptian Cultural and Educational Bureau and the British Council in Egypt.

ACKNOWLEDGMENTS

We thank Prof. Tung-Tien Sun (New York University) for the uroplakin antibody and Prof. Ryuichi Nishinakamura (Kumamato University) for the HoxB7-GFP cell line.

Dr. May Sallam conducted experiments and led manuscript writing. Dr. Anwar Palakkan helped in data analysis and paper editing, Dr. Christopher G. Mills helped in grafting experiments. Ms. Julia Tarnick helped in time-lapse video recording and paper editing. Dr. Mona Elhendawi assisted with thoughtful discussions. Prof. Lorna Marson co-supervised Dr. May Sallam's work and made suggestions about the strategy for experiment. Prof. Jamie A. Davies is primary supervisor of Dr. May Sallam's work, participated in overall project design and detailed experimental design, advised about methods of analysis, analyzed timing of contractions, and participated in writing the manuscript. All authors approved the final version of the manuscript.

SUPPLEMENTAL MATERIAL

This article contains the following supplemental material online at http://jasn.asnjournals.org/looSkup/suppl/doi:10.1681/ASN.2019101075/-/DCSupplemental.

Supplemental Table 1. Antibodies used for immunofluorescence analysis.

Supplemental Video 1. A GFP-expressing eUB grafted into the peri-Wolffian mesenchyme of an intact nephrogenic zone, showing regular smooth muscle contractions.

Supplemental Video 2. An eUB combined with peri-Wolffian mesenchyme in the absence of an associated kidney, also showing regular smooth muscle contractions.

Supplemental Figure 1. Production of eUBs from Hoxb7-GFP mES cells.

Supplemental Figure 2. ES cell–derived eUBs show tip markers.

Supplemental Figure 3. Contraction in grafted eUB-derived ureter-like tissue and in the natural ureter.

Supplemental Figure 4. Contraction in eUB-derived ureter-like tissue in isolated peri-Wolffian mesenchyme.

REFERENCES

1. Morizane R, Miyoshi T, Bonventre JV: Concise review: Kidney generation with human pluripotent stem cells. *Stem Cells* 35: 2209–2217, 2017
2. Morizane R, Bonventre JV: Kidney organoids: A translational journey. *Trends Mol Med* 23: 246–263, 2017
3. Davies JA, Chang CH, Lawrence ML, Mills CG, Mullins JJ: Engineered kidneys: Principles, progress, and prospects. *Adv Regen Biol* 1: 24990, 2014
4. Taguchi A, Nishinakamura R: Higher-order kidney organogenesis from pluripotent stem cells. *Cell Stem Cell* 21: 730–746.e6, 2017
5. Morizane R, Lam AQ, Freedman BS, Kishi S, Valerius MT, Bonventre JV: Nephron organoids derived from human pluripotent stem cells model kidney development and injury. *Nat Biotechnol* 33: 1193–1200, 2015
6. Takasato M, Er PX, Chiu HS, Maier B, Baillie GJ, Ferguson C, et al: Kidney organoids from human iPS cells contain multiple lineages and model human nephrogenesis. *Nature* 526: 564–568, 2015
7. Unbekandt M, Davies JA: Dissociation of embryonic kidneys followed by reaggregation allows the formation of renal tissues. *Kidney Int* 77: 407–416, 2010
8. Ganeva V, Unbekandt M, Davies JA: An improved kidney dissociation and reaggregation culture system results in nephrons arranged organotypically around a single collecting duct system. *Organogenesis* 7: 83–87, 2011
9. Davies JA, Chang CH: Engineering kidneys from simple cell suspensions: An exercise in self-organization. *Pediatr Nephrol* 29: 519–524, 2014
10. Mills CG, Lawrence ML, Munro DAD, Elhendawi M, Mullins JJ, Davies JA: Asymmetric BMP4 signalling improves the realism of kidney organoids. *Sci Rep* 7: 14824, 2017
11. Taguchi A, Kaku Y, Ohmori T, Sharmin S, Ogawa M, Sasaki H, et al: Redefining the *in vivo* origin of metanephric nephron progenitors enables generation of complex kidney structures from pluripotent stem cells. *Cell Stem Cell* 14: 53–67, 2014
12. Takasato M, Er PX, Becroft M, Vanslambrouck JM, Stanley EG, Elefanty AG, et al: Directing human embryonic stem cell differentiation towards a renal lineage generates a self-organizing kidney. *Nat Cell Biol* 16: 118–126, 2014
13. Kim D, Dressler GR: Nephrogenic factors promote differentiation of mouse embryonic stem cells into renal epithelia. *J Am Soc Nephrol* 16: 3527–3534, 2005
14. van den Berg CW, Ritsma L, Avramut MC, Wiersma LE, van den Berg BM, Leuning DG, et al: Renal subcapsular transplantation of PSC-derived kidney organoids induces neovasculogenesis and significant glomerular and tubular maturation *in vivo*. *Stem Cell Reports* 10: 751–765, 2018
15. Bremer M, Doerge RW: *Statistics at the Bench*, NY, Cold Spring Harbor Laboratory Press, 2010
16. Srinivas S, Goldberg MR, Watanabe T, D'Agati V, al-Awqati Q, Costantini F: Expression of green fluorescent protein in the ureteric bud of transgenic mice: A new tool for the analysis of ureteric bud morphogenesis. *Dev Genet* 24: 241–251, 1999
17. Qiao J, Sakurai H, Nigam SK: Branching morphogenesis independent of mesenchymal-epithelial contact in the developing kidney. *Proc Natl Acad Sci U S A* 96: 7330–7335, 1999
18. Michael L, Sweeney DE, Davies JA: The lectin Dolichos biflorus agglutinin is a sensitive indicator of branching morphogenetic activity in the developing mouse metanephric collecting duct system. *J Anat* 210: 89–97, 2007

19. Michos O, Gonçalves A, Lopez-Rios J, Tiecke E, Naillat F, Beier K, et al: Reduction of BMP4 activity by gremlin 1 enables ureteric bud outgrowth and GDNF/WNT11 feedback signalling during kidney branching morphogenesis. *Development* 134: 2397–2405, 2007
20. Sweeney D, Lindström N, Davies JA: Developmental plasticity and regenerative capacity in the renal ureteric bud/collecting duct system. *Development* 135: 2505–2510, 2008
21. Bohnenpoll T, Bettenhausen E, Weiss AC, Foik AB, Trowe MO, Blank P, et al: Tbx18 expression demarcates multipotent precursor populations in the developing urogenital system but is exclusively required within the ureteric mesenchymal lineage to suppress a renal stromal fate. *Dev Biol* 380: 25–36, 2013
22. Bohnenpoll T, Wittern AB, Mamo TM, Weiss AC, Rudat C, Kleppa MJ, et al: A SHH-FOXF1-BMP4 signaling axis regulating growth and differentiation of epithelial and mesenchymal tissues in ureter development. *PLoS Genet* 13: e1006951, 2017
23. Trowe MO, Airik R, Weiss AC, Farin HF, Foik AB, Bettenhausen E, et al: Canonical Wnt signaling regulates smooth muscle precursor development in the mouse ureter. *Development* 139: 3099–3108, 2012
24. Bohnenpoll T, Weiss AC, Labuhn M, Lüdtke TH, Trowe MO, Kispert A: Retinoic acid signaling maintains epithelial and mesenchymal progenitors in the developing mouse ureter. *Sci Rep* 7: 14803, 2017
25. Bohnenpoll T, Feraric S, Nattkemper M, Weiss AC, Rudat C, Meuser M, et al: Diversification of cell lineages in ureter development. *J Am Soc Nephrol* 28: 1792–1801, 2017
26. Mysorekar IU, Mulvey MA, Hultgren SJ, Gordon JI: Molecular regulation of urothelial renewal and host defenses during infection with uropathogenic *Escherichia coli*. *J Biol Chem* 277: 7412–7419, 2002
27. Wu XR, Manabe M, Yu J, Sun TT: Large scale purification and immunolocalization of bovine uroplakins I, II, and III. Molecular markers of urothelial differentiation. *J Biol Chem* 265: 19170–19179, 1990
28. Tai G, Ranjzad P, Marriage F, Rehman S, Denley H, Dixon J, et al: Cytokeratin 15 marks basal epithelia in developing ureters and is upregulated in a subset of urothelial cell carcinomas. *PLoS One* 8: e81167, 2013
29. Lang RJ, Hashitani H, Tonta MA, Bourke JL, Parkington HC, Suzuki H: Spontaneous electrical and Ca2+ signals in the mouse renal pelvis that drive pyeloureteric peristalsis. *Clin Exp Pharmacol Physiol* 37: 509–515, 2010
30. Lang RJ, Hashitani H: Pacemaker mechanisms driving pyeloureteric peristalsis: Modulatory role of interstitial cells. *Adv Exp Med Biol* 1124: 77–101, 2019
31. Osborn SL, Thangappan R, Luria A, Lee JH, Nolta J, Kurzrock EA: Induction of human embryonic and induced pluripotent stem cells into urothelium. *Stem Cells Transl Med* 3: 610–619, 2014
32. Santos CP, Lapi E, de Villarreal JM, Álvaro-Espinosa L, Fernández-Barral A, Barbáchano A, et al: Urothelial organoids originating from Cd49f high mouse stem cells display Notch-dependent differentiation capacity. *Nat Commun* 10: 4407, 2019
33. Mullenders J, de Jongh E, Brousali A, Roosen M, Blom JPA, Begthel H, et al: Mouse and human urothelial cancer organoids: A tool for bladder cancer research. *Proc Natl Acad Sci U S A* 116: 4567–4574, 2019

See related editorial, "Patterning a Ureter Is All in the Stroma," on pages 2231–2232.

Supplementary Information

Table 1S	Antibodies used for immunofluorescence analysis.
Video 1S	A GFP-expressing eUB grafted into the peri-Wolffian mesenchyme of an intact nephrogenic zone, showing regular smooth muscle contractions.
Video 2S	An eUB combined with peri-Wolffian mesenchyme in the absence of an associated kidney, also showing regular smooth muscle contractions.
Figure 1S	Production of eUBs from Hoxb7-GFP mESC.
Figure 2S	ES-cell derived eUBs show tip markers.
Figure 3S	Contraction in grafted eUB-derived ureter-like tissue and in the natural ureter.

Table 1S: antibodies and lectins used in this study.

Antibody	**Host Species**	**Supplier & catalogue number**	**Working dilution**
Alpha-Smooth Muscle (FITC conjugate)	Mouse	Sigma 3777	1/100
Alpha-Smooth muscle actin	Goat	Novus nb300-978	1/100
Calbindin D28k	Mouse	Sigma C9848	1/100
Dolicous biflourus agglutinin (fluoresceinated)	Conjugated	Vector FL-1031	1/50
E-cadherin	Mouse	BD biosciences 610182	1/100
GATA3	Goat	R&D AF2605	1/100
Jagged 1	Goat	R&D AF599	1/100
Krt5	Rabbit	Abcam ab24647	1/100
Krt8	Rat	DSBH repository TROMA-1	1/100
Krt15	Rabbit	Abcam Ab52816	1/100
NP63	Rat	Biolegend 699501	1/100
Pax2	Rabbit	Biolegend PRB-276P-200	1/100
RET	Rabbit	Santa cruz SC-167	1/50
Sox9	Rabbit	Sigma AB5535	1/100
Uroplakin	Rabbit	Gift from Tung-Tien Sun, New York University	1/500
Uroplakin III	Goat	Santa Cruz sc15180	1/100
WT1	Rabbit	Abcam ab89901	1/100
Anti-Rabbit 594	Donkey	Invitrogen 21207	1/100
Anti-Rabbit 488	Donkey	Invitrogen 21206	1/100
Anti-Rabbit 647	Donkey	Invitrogen A-31573	1/100
Anti-Goat 488	Donkey	Invitrogen A-11055	1/100
Anti-Goat 594	Donkey	Invitrogen A-11058	1/100
Anti-Goat 647	Donkey	Invitrogen A-21447	1/100
Anti-mouse 488	Donkey	Invitrogen 21202	1/100
Anti-mouse 594	Donkey	Invitrogen 21203	1/100
Anti-Rat 594	Chicken	Invitrogen A-21471	1/100
Anti-Rat 488	Donkey	Abcam Ab150153	1/100

Figure 1S

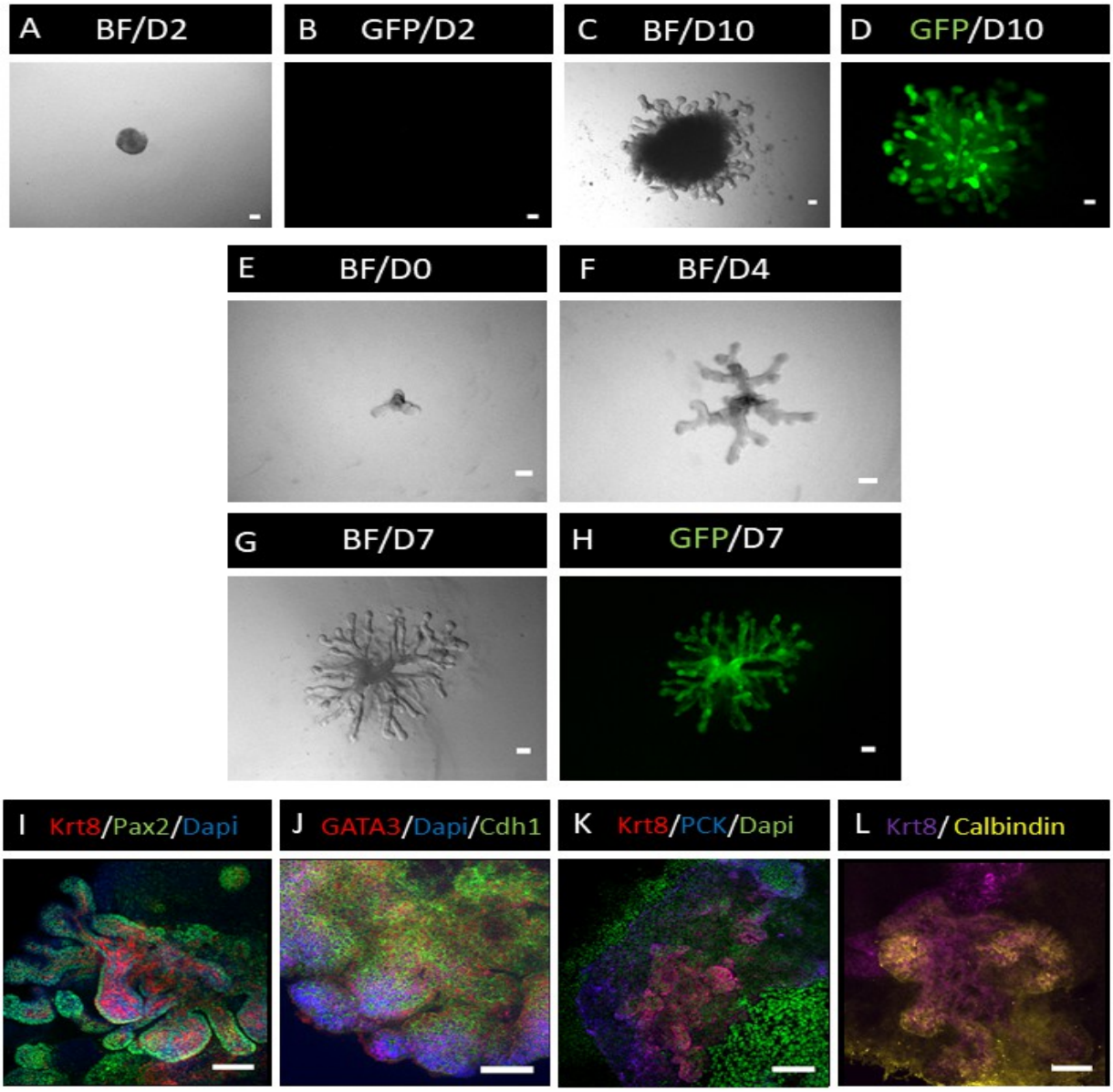

Figure 1S legend Production of eUBs from Hoxb7-GFP mESC. (A) Bright field image showing an embryoid body (EB), on day 2 of the HoxB7-GFP mESC differentiation; (B) it expresses no GFP.
(C) Bright field image of an EBs 10 days after induction of differentiation, showing UB-like projections, and (D) expressing HoxB7-GFP. (E-H) A single eUB bud isolated on day 10 and cultured in 3D gel with ramogenic mixture at days (E) 0, (F) 4, and (G) 7; it branches and (H) continues to express GFP. (I-L) Immunofluorescence images of day 10 EBs expressing the UB markers Calbindin-D28k, pan-cytokeratin (PCK), E-cadherin (Cdh1), Cytokeratin 8 (Krt8), GATA3 and Pax2; DAPI is used as a nuclear stain. Scale bar = 100µm.

Figure 2S

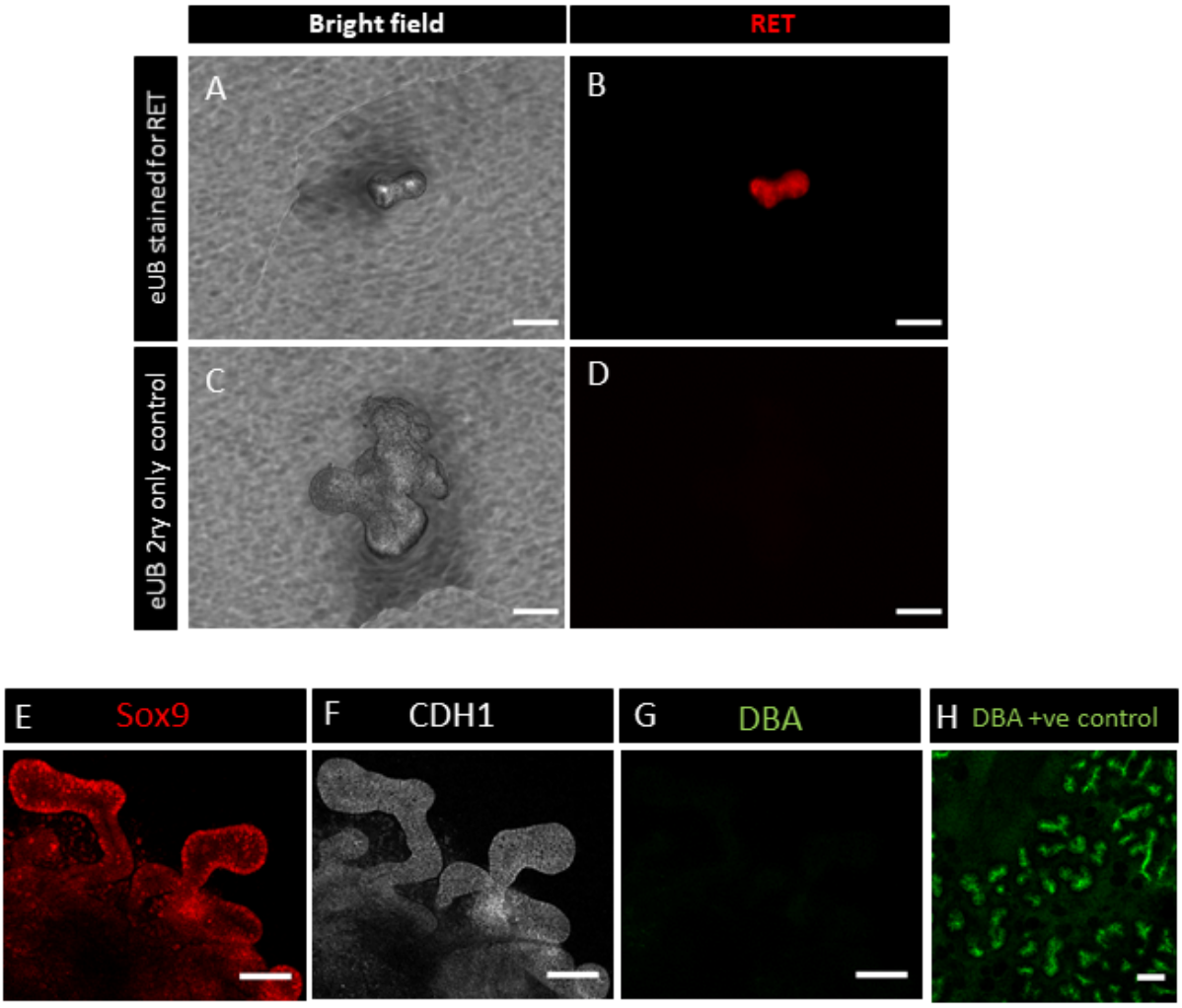

Figure 2S legend: ES-cell derived eUBs express UB tip markers. (A, B) Show both bright field and immunfluorescence images of an eUB stained for RET showing positive expression; . (C, D) are the corresponding secondary-only control. (E-H) show day 10 eUBs stained for Sox9 (E), CDH1 (F), and with DBA (G); H is a cultured embryonic kidney stained with DBA as a positive staining control.

Figure 3S: Contraction in grafted eUB-derived ureter-like tissue and in the natural ureter.

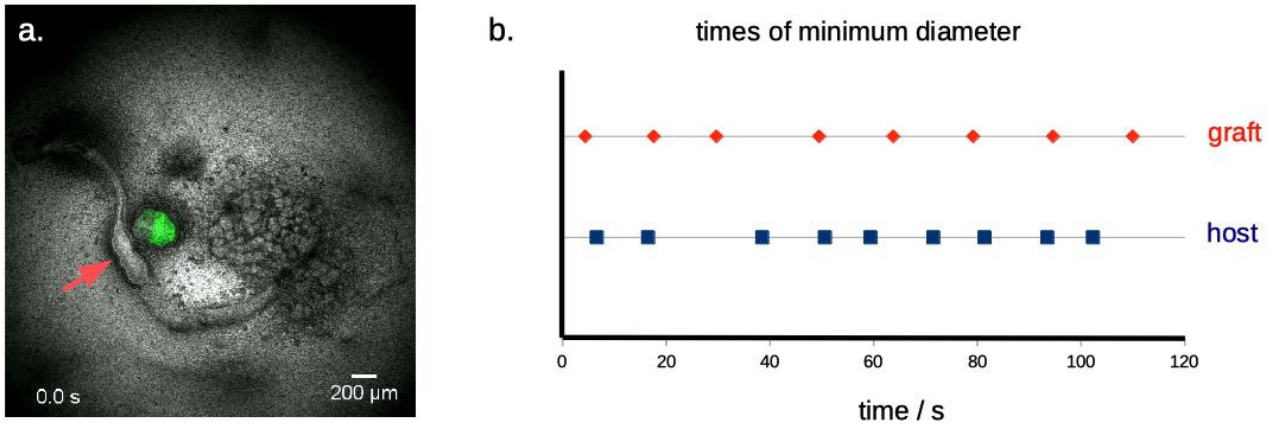

Figure 3S legend: Contraction in grafted eUB-derived ureter-like tissue and in the natural ureter. (a) shows a starting frame of the video recording (video 1S); the graft is identifiable by the GFP fluorescence in its ES-derived urothelial tissues, and the arrow indicates the place at which contractions in the nearby natural ureter were timed (they passed this point as waves from kidney to distal ureter). (b) shows the timings at which contractions occurred, depicted as dots on the same time-scale. The time-stamps on the recording incremented at intervals of 1.1s, which sets a lower limit of resolution of the timings shown on the graph. Timings for the host were 6.6, 16.5, 38.5, 50.6, 59.4, 71.5, 81.4, 93.5 and 102.3s, and for the graft, 4.4, 17.6, 29.7, 49.5, 63.8, 79.2, 94.6 and 110s.

Figure 4S: Contraction in eUB-derived ureter-like tissue grafted into isolated peri-Wollffian mesenchyme

a.

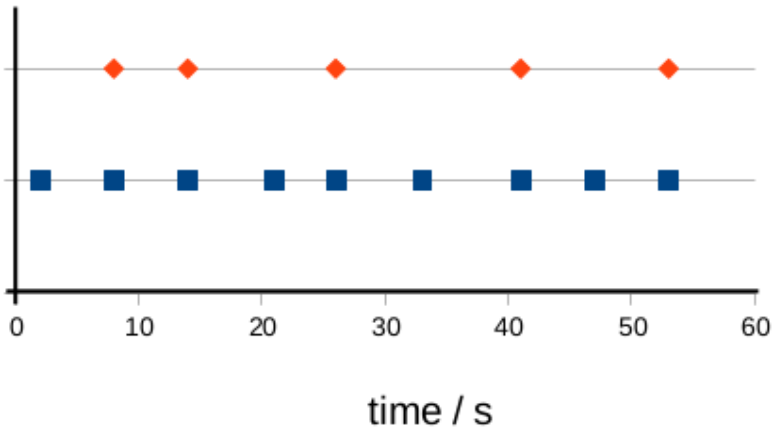

b.

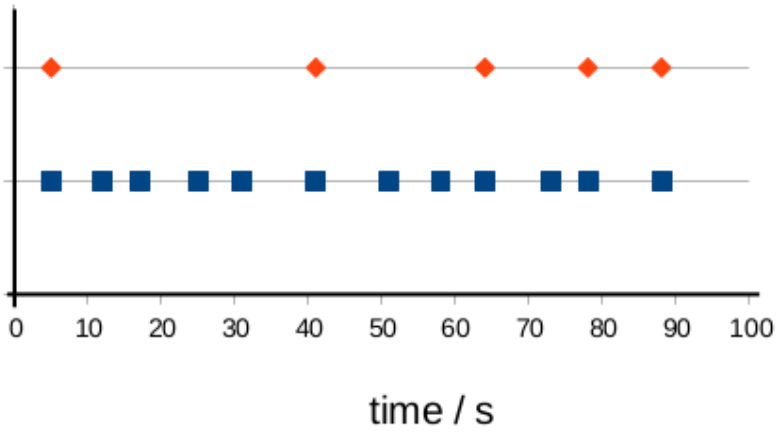

Figure 4S legend: Contraction in eUB-derived ureter-like tissue in isolated peri-Wolffian mesenchyme. (a) and (b) show the timing of very small contractions (blue), and of large contractions (red, these large contractions being comparable to those in Fig 3S), in two different examples. In (a), timings of contractions were 2, 8, 14, 21, 26, 33, 41, 47 and 52s and in (b) they were 5, 12, 17, 25, 31, 41, 51, 58, 64, 73, 78, 88s (colour code as in the charts).